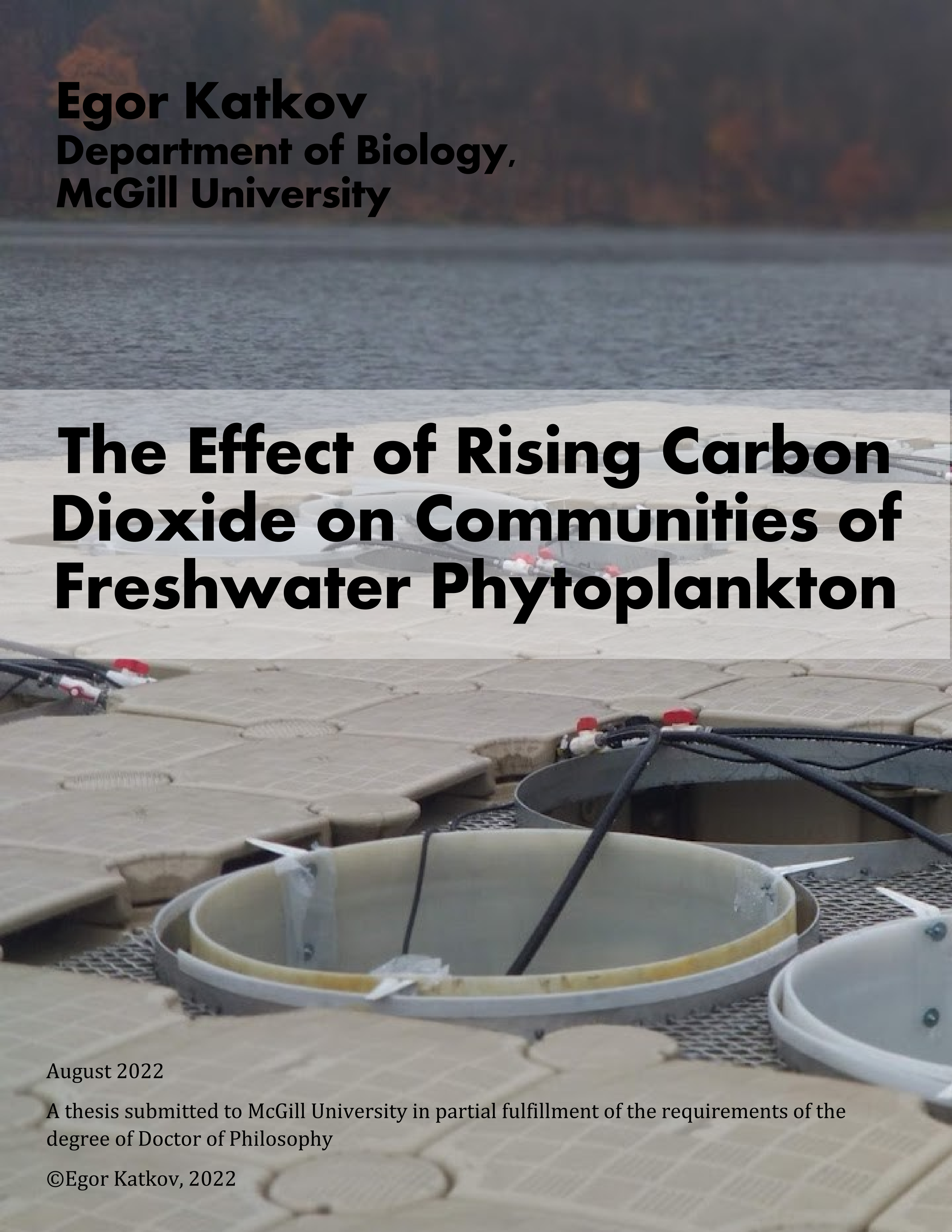

Egor Katkov

Department of Biology,
McGill University

The Effect of Rising Carbon Dioxide on Communities of Freshwater Phytoplankton

August 2022

A thesis submitted to McGill University in partial fulfillment of the requirements of the degree of Doctor of Philosophy

Table of Contents

Introduction

0.1 Thesis Abstract

Human activities, such as carbon dioxide (CO_2) emissions are altering aquatic ecosystems in ways that are not fully understood. Because phytoplankton are essential organisms, forming the base of pelagic aquatic food webs, I focus on this group to help us understand how lake ecosystems respond to anthropogenic change. Specifically, I focus on the response of total phytoplankton biomass and community composition to increasing pCO_2 in concert with (1) nutrient enrichment, (2) increasing temperatures, and (3) organismal evolution.

In the first chapter, I investigated whether CO_2 can act as a co-limiting resource that can promote phytoplankton growth and alter community composition (at a coarse, 4-group level) across different times of the year in a semi-natural environment. I conducted experiments that used 1200 L mesocosms suspended in a mesotrophic (having a moderate amount of dissolved nutrients) lake near Montreal, Quebec, Canada, and were designed to evaluate the interactive effects of nitrogen, phosphorus, and CO_2 enrichment in the months of July, August, October, April and June. I found that, in some seasons, CO_2 acted as a co-limiting factor with phosphorus when nitrogen was also added. The phytoplankton community was affected by all three resources in diverse ways at different times of the year. I concluded that CO_2 can affect the community composition and be a co-limiting factor for freshwater phytoplankton communities, especially when other resources such as P and N are abundant, as is typical in eutrophic lakes.

In chapter two, I investigated the interactive effect of CO_2 and temperature on phytoplankton and zooplankton communities, two highly inter-related factors in the context of climate change. In the same lake as Chapter 1, I ran a single mesocom experiment in late Fall over four weeks. I did not detect an interactive effect between CO_2 and temperature, although both factors had independent and sometimes additive effects on the phytoplankton community, and temperature altered zooplankton community composition. Through time, I found that CO_2 had opposing effects on different phytoplankton groups over the course of the experiment, highlighting the complexity of the role of CO_2 in this community. Additionally, CO_2 altered the stoichiometry of the seston, which has been shown in other

studies to affect zooplankton food quality. I concluded that, although no evidence for interactive effects was found, both CO_2 and temperature can have independent and additive effects across and multiple trophic levels in freshwater ecosystems.

The third chapter deals with the evolutionary potential of phytoplankton species responding to changing atmospheric CO_2 concentrations. I developed an eco-evolutionary model where phytoplankton growth depends on the influx of atmospheric CO_2 and where the population's affinity for carbon uptake can evolve to trade off rapid maximum carbon flux for high affinity. Analysing the equilibrium conditions, I found that populations adapted by optimizing carbon uptake to environmental conditions, which, in modelled monocultures, allowed populations to reach higher biomass, and in multi-species communities, allowed certain species to gain an unexpected advantage over others. The biomass increases depended on the species-specific parameters and concentrations of atmospheric CO_2 and initial HCO_3^-. I conclude that although more complex trade-offs may be at play in natural systems, evolution in the context of changing pCO_2 can affect population's R^*s, thereby altering community composition and generate greater biomass increases than expected from CO_2 co-limitation alone.

In sum, I found that freshwater phytoplankton communities can be affected by increases in pCO_2 at the level of total biomass and community composition, via co-limiting mechanisms, potentially in concert with associated factors such as temperature changes, and evolution. One important observation and conclusion across all chapters of this thesis is that I rarely found dramatic effects of CO_2. On the contrary, the ecological and evolutionary effects of CO_2 are generally small (compared to, for instance, those usually associated with severe eutrophication) and may be involved in complex interactions. These small effect sizes, combined with the logistical difficulties of working with a gas, may seem to make it unnecessary to study the effects of enriched CO_2. However, the fact that pCO_2 concentrations are increasing around the world, that even a small but large-scale effect can be significant, and that freshwaters are fragile but essential ecosystems that are at the mercy of countless potentially interacting human activities emphasizes the interest and importance of understanding the impact of increased pCO_2 on freshwater communities.

0.2 Résumé de la Thèse

Les activités humaines, telles que les émissions de dioxyde de carbone (CO_2), modifient les écosystèmes aquatiques d'une manière qui n'est pas entièrement comprise. Parce que le phytoplancton est un organisme essentiel, formant la base de nombreux réseaux trophiques aquatiques, je me concentre sur ce groupe pour nous aider à comprendre comment la réponse des écosystèmes lacustres aux changements anthropiques. Plus précisément, je me concentre sur la réponse de la biomasse totale du phytoplancton et de la composition de la communauté à l'augmentation de pCO_2 de concert avec (1) l'enrichissement en nutriments, (2) l'augmentation des températures et (3) l'évolution de l'organisme.

Dans le premier chapitre, j'ai investigué si le CO_2 peut agir comme une ressource co-limitante qui peut favoriser la croissance du phytoplancton et modifier la composition de la communauté (à un niveau grossier de 4 groupes) à différents moments de l'année dans un environnement semi-naturel. J'ai mené des expériences qui ont utilisé des mésocosmes de 1200 L en suspension dans un lac mésotrophe (ayant une quantité modérée de nutriments dissous) près de Montréal, Québec, Canada, et ont été conçues pour évaluer les effets interactifs de l'enrichissement en azote, phosphore et CO_2 au mois de juillet, août, octobre, avril et juin. J'ai découvert qu'à certaines saisons, le CO_2 agissait comme un facteur co-limitant avec le phosphore lorsque de l'azote était également ajouté. La communauté de phytoplancton a été affectée par les trois ressources de diverses manières à différents moments de l'année. Je conclus que le CO_2 peut affecter la composition de la communauté et être un facteur co-limitant pour les communautés de phytoplancton d'eau douce, en particulier lorsque d'autres ressources telles que P et N sont abondantes, comme cela est typique dans les lacs eutrophes.

Dans le chapitre deux, j'ai étudié l'effet interactif du CO_2 et de la température sur les communautés de phytoplancton et de zooplancton, deux facteurs étroitement liés dans le contexte du changement climatique. Dans le même lac que le chapitre 1, j'ai mené une seule expérience en mésocosme à la fin de l'automne pendant quatre semaines. Je n'ai pas détecté d'effet interactif entre le CO_2 et la température, bien que les deux facteurs aient des effets indépendants et parfois additifs sur la communauté de phytoplancton et que la température

modifie la composition de la communauté de zooplancton. Au fil du temps, nous avons constaté que le CO_2 avait des effets opposés sur différents groupes de phytoplancton au cours de l'expérience, soulignant la complexité du rôle du CO_2 dans cette communauté. De plus, le CO_2 altérait la stoechiométrie du seston, ce qui a été démontré dans d'autres études comme affectant la qualité de la nourriture du zooplancton. J'ai conclu que, bien qu'aucune preuve d'effets interactifs n'ait été trouvée, le CO_2 et la température peuvent avoir des effets indépendants et additifs sur plusieurs niveaux trophiques dans les écosystèmes d'eau douce.

Le troisième chapitre traite du potentiel évolutif des espèces de phytoplancton répondant aux variations des concentrations atmosphériques de CO_2. J'ai développé un modèle éco-évolutif où la croissance du phytoplancton dépend de l'afflux de CO_2 atmosphérique et où l'affinité de la population pour l'absorption de carbone peut évoluer pour échanger un flux de carbone maximum rapide contre une affinité élevée. En analysant les conditions d'équilibre, j'ai constaté que les populations s'adaptaient en optimisant l'absorption de carbone aux conditions environnementales, ce qui, en monoculture modélisée, a permis aux populations d'atteindre une biomasse plus élevée, et dans les communautés multi-espèces, a permis à certaines espèces d'acquérir un avantage inattendu sur d'autres. Les augmentations de la biomasse dépendaient des paramètres spécifiques à l'espèce et des concentrations de CO_2 atmosphérique et de HCO_3^- initial. Je conclus que bien que des compromis plus complexes puissent être en jeu dans les systèmes naturels, l'évolution dans le contexte de l'évolution du pCO_2 peut affecter les R^*s de la population, modifiant ainsi la composition de la communauté et pouvant générer de plus grandes augmentations de la biomasse que prévu à partir du CO_2 co-limitation seule.

En somme, j'ai trouvé que les communautés de phytoplancton d'eau douce peuvent être affectés par l'augmentation du pCO_2 au niveau de la biomasse totale et de la composition des communautés, via des mécanismes de co-limitation, potentiellement en concret avec des facteurs associés tels que les changements de température, et d'évolution. Une observation et une conclusion importantes dans tous les chapitres de cette thèse est que j'ai rarement trouvé des effets dramatiques du CO_2. Au contraire, les effets écologiques et évolutifs du CO_2 sont généralement faibles (par rapport, par exemple, à ceux généralement associés à une eutrophisation sévère) et peuvent être impliqués dans des interactions complexes. Ces faibles tailles d'effet, combinées aux difficultés logistiques de travailler avec un gaz, peuvent sembler de rendre inutile l'étude des effets du CO_2 enrichi. Pourtant, le fait que les concentrations de pCO_2 augmentent à travers la planète, que même un petit effet à grande échelle peut être important, et que les eaux douces sont des écosystèmes fragiles mais essentiels qui sont à la merci d'innombrables activités humaines potentiellement interactives souligne l'intérêt et l'importance de comprendre l'impact de l'augmentation de la pCO_2 sur les communautés d'eau douce.

0.3 Acknowledgements

This thesis would have been impossible to complete without a bloom of people, which I will try to enumerate here, in no particular order. Although each chapter contains a separate Acknowledgements section, here I list contributions that are outside the scope of a single chapter.

I would like to thank my supervisor, Gregor Fussmann for providing helpful and constructive feedback on nearly all of my written work, for allowing me to experiment with different methodologies, whether it be designing chemostats in the lab, purchasing 165 gallon barrels for more environmentally-friendly mesocosm experiments, or writing my thesis using RMarkdown, and for his understanding, kindness and great sense of humour even when things did not work out as planned.

I also thank my co-supervisor, Étienne Low-Décarie for agreeing to co-supervise me, despite being an ocean away at a time before everyone knew what Zoom was, for remaining on my supervisory committee despite moving away from academia, and for providing swathes of helpful feedback and discussions.

I thank my supervisory committee, composed of Irene Gregory-Eaves, Frédéric Guichard and Anthony Ricciardi for providing insightful and helpful feedback throughout my graduate education. In particular, I thank Irene Gregory-Eaves and her lab for sharing equipment with me, in particular the FluoroProbe, without which my first chapter would not have been possible. I also thank Frédéric Guichard for providing the opportunity to attend his lab's meetings, allowing me to better understand how theoretical models can allow us to make scientific progress (which came in helpful for Chapter 3). I thank Neil Price for many helpful suggestions during my qualifying exam and beyond. I thank Andrew Gonzalez for allowing me to use the FluoroProbe, the facilities at the LEAP lab and in his lab space at McGill.

I thank my lab members, and the greater student community for providing constructive feedback, exchanging ideas, and providing an amazing network of helpful, fun-loving people. In the lab, Marie-Pier Hébert, Christina Tadiri, and Sebastien Portalier provided great feedback and informative discussions. At the Gault Nature Reserve, Marie-Pier Hébert, Vincent Fugère, and several others had some great conversations. I thank Alexandre Baud, Alex Crew, Michelle Gros, Genviève D'Avignion and others involved in limnological studies at McGill for their ideas and feedback, but also helping find materials for experimentation. In particular I thank Justin Marleau, Ridouan Bani, Russell Milne, Julien Massé Jodoin and Tianna Peller for helpful feedback and discussions related to theoretical ecology. I thank Mary-Rose Bradley-Gill, Logan Smith, Michelle Gros, Melissa Wong, and all the other Biology Graduate Student Association (BGSA) presidents and other people occupying the positions that allowed the BGSA to function, and provide treasured opportunities to interact with other students, professors and staff in the department. I also thank all the undergraduate students that helped me with sampling and setting up experiments: Melissa Langley, Marie-Claire Chiasson, Aurélie Hawes, Ashley Cameron and Andrea Cherry.

I would like to thank the university staff at the Biology Department which contributed to making my experiments happen and to making my graduate experience pleasant when dealing with bureaucratic procedures a breeze. In particular, I thank Ancil Gittens for helping me navigate the yearly requirements for graduate school, funding applications, and the requirements for graduation. I also thank Frank Scopelleti for helping me get some hard to find to tools that he had accumulated over the years in his workshop. I thank Joseph Dent and Guy L'Heureux in making sure that I get all my packages on time. I thank Carole Smith for making getting access to the different rooms around the department a breeze. I thank Dino Bisanti and the custodial team of Stewart Biology for letting me into where I needed to go on the multiple occasions I had forgotten my keys or been locked out. I thank Drenusha Myha and Luisa Sabaz for ensuring that I got my stipends on time. I thank Mark Romer and Mahnaz Mansoori for accommodating my experiment in the McGill Phytotron.

I would like to thank the staff at the Gault Nature Reserve who provided essential on-site support for Chapters 1 & 2. I thank Charles Normandin for his interest in the scientific process, for ensuring that the mesocosm dock was ready to use, for giving me advice on electrical components of the mesocosm experiments and for setting up an electrical switching system which allowed me to conduct three CO_2 treatments with a single gas pump. I thank David Maneli for being a kind and reassuring voice, for trusting my ideas, and for putting in a good word for me which allowed me to work on my thesis in the first place. I thank Sonia Tétrault and Christian Côté for helping me sample when no one else could. I thank Julie Tremblay, Carole Lemieux, Theresa Ramundo-Liberta, Jean Deslauriers, Martin Duval and Marc-André Langlois for helping me with administrative and other miscellaneous tasks.

I would like to thank all the people involved in making the EcoLac program happen. In particular, Marie-Andrée Fallu and Pierre-Olivier Benoit oversaw all the activities which made this program a great success. I also thank all the other students that were part of the program for sharing their knowledge and exchanging ideas about aquatic ecosystems. I thank all the speakers that came, of which the most marked for me was Jérôme Marty, who covered career opportunities for aquatic ecologists.

I thank Jolanda Verspagen and Jef Huisman for allowing me to visit the Institute for Biodiversity and Ecosystem Dynamics department of Freshwater & Marine Ecology at the University of Amsterdam for several months to work with their world-class chemostat setup. I thank Merijn Schuurmans, Bas van Beusekom, Pieter Slot and the other support staff who helped make my time in the lab smooth and enjoyable. I thank all the other students and professors at the department who welcomed me with open arms.

Finally, I thank my parents, Natalia Levina and Pavel Katkov for believing in my abilities to perform in graduate school and staying interested in what I did for seven years. I thank my wonderful finacée, Hilal Pilavci who provided support, both moral, and physical, when came the time to undertake a field experiment at the peak of COVID. I thank my brother, Daniil Katkov, for his interest and help with my experiments. I also thank my cat, Dim Dim, for trying his best to help me type both code as well as text.

0.3.1 Funding

I thank Gregor Fussmann for obtaining the Natural Sciences and Engineering Research Council (NSERC) grants, themselves funded by the people of Canada, and grants from McGill University, which supported a large part of my graduate student career. I thank the people of the Groupe de recherche interuniversitaire en limnologie (GRIL) for obtaining the NSERC CREATE grant which also funded part of my graduate experience, including a scholarship for my internship at the University of Amsterdam.

0.4 Contributions to Original Knowledge

All three chapters contain contributions to original knowledge. I list, to the best of my knowledge, the contributions from each of the three thesis chapters.

0.4.1 Chapter 1

This is the first study to:

- examine the seasonal effects of CO_2 enrichment in concert with nutrient enrichment in a freshwater system,
- examine the seasonal effects of CO_2 enrichment in a mesotrophic lake,
- examine the effects of CO_2 enrichment paired with well-defined nitrogen and phosphorus additions in freshater systems,
- explain the intra-annual variability of the interactive effects of nitrogen and phosphorus enrichment on the concentration of chlorophyll *a* using an array of environmental factors (in this case, total nitrogen to total phosphorus ratios, water temperature and mean daily insolation) in a freshwater system,
- find evidence of independent co-imitation of a natural phytoplankton community by CO_2 and a nutrient (here, phosphorus).

0.4.2 Chapter 2

This is the first study to:

- examine the interactive effect of CO_2 and temperature on a semi-natural freshwater community (phytoplankton & zooplankton),
- use rigid, submerged mesocosms (repurposed 165 gallon barrels) in North America, a more eco-friendly approach compared to thin, flexible, single-use plastic which is prone to tear, resulting in plastic pollution in the lake,

- test the cascading effect of CO_2 on zooplankton food quality in a freshwater system.

0.4.3 Chapter 3

This is the first study to:

- integrate the evolution of carbon uptake kinetics within a resource competition model,
- investigate the effect of evolution of carbon uptake kinetics on competitive outcomes within a phytoplankton community,
- make numeric predictions about the effects of increasing atmospheric pCO_2 on the evolution of populations of phytoplankton.

0.5 Author Contributions

0.5.1 Chapter 1

This chapter was co-authored by me, Étienne Low-Décarie, and Gregor Fussmann. I contributed to the experimental design, gathered the materials, determined the methodology, conducted the experiments (with help from research assistants and volunteers), performed the bulk of the data analysis and wrote the first draft of the manuscript. Étienne Low-Décarie and Gregor Fussmann both helped with supervision, the experimental design and statistical analyses, drafted pieces of the manuscript and provided comments. All authors contributed to the editing and provided final approval of the complete manuscript.

0.5.2 Chapter 2

This chapter was co-authored by me and Gregor Fussmann. I contributed to the experimental design, secured the necessary materials, determined the methodology, set up the experiment, collected and analysed the data, generated the visualizations, wrote the original draft, and helped with the review and editing. Gregor Fussmann conceptualized the general idea for this project, contributed to the experimental design, provided supervision, performed administrative tasks, acquired funding, and helped with the review and editing of the text.

0.5.3 Chapter 3

This chapter was co-authored by me, Gregor Fussmann, Jef Huisman, and Jolanda Verspagen, with all three authors contributed to the conceptualization, the methodology and the review and editing. I helped with data curation, did the bulk of the formal and exploratory analysis, acquired parts of the funding, performed the bulk of the investigation, helped secure computational resources, wrote the bulk of the software, performed validations, generated visualizations, and wrote the original draft. Gregor Fussmann secured the rest of the funding, helped with project administration, acquiring computational resources and supervision. Jef Huisman helped with the project administration and made contributions to the formal analysis. Jolanda Verspagen did a large part of the data curation, helped with the project administration, contributed code, supervision, and validation of the results.

0.6 Literature Review

Carbon-based molecules are the building blocks of life, they are essential for energy storage, providing structure to the cells, and every other necessary life function. However, most carbon on Earth is in inorganic form, such as atmospheric CO_2, and needs to be converted to an organic form, via photosynthesis, for it to be useful. Primary producers, such as plants and phytoplankton perform this essential function, and provide energy for the rest of life on Earth. As a result, it is important to study how changes in inorganic carbon concentrations might affect primary producers. Here, I focus on the effects of inorganic carbon (primarily CO_2) on phytoplankton in freshwater lakes. Freshwaters, while they form a small percentage of water on Earth, harbor a vast number of species, and support vast ecosystems, including many land mammals such as humans. I also include information about the effects of CO_2 on phytoplankton in marine environments in cases where freshwater studies are lacking. After explaining the basic chemistry of dissolved inorganic carbon (DIC), I address the ecological, evolutionary, and interactive roles of CO_2 in shaping phytoplankton communities.

0.6.1 The Carbonate System

When atmospheric CO_2 dissolves in water, it enters a dynamic equilibrium between three chemical compounds: carbon dioxide (CO_2), bicarbonate (HCO_3^-), and carbonate (CO_3^{2-}). Together, these compounds form DIC. The ratios between the different compounds are primarily controlled by pH, and to a lesser extent, temperature, and salinity. At more acidic pH, CO_2 is the dominant form, at pH around 6-9, HCO_3^- dominates, and at higher pH, CO_3^{2-} is the most common form (Emerson & Hedges, 2008). Interestingly, CO_2 itself is acidic, meaning that aquatic systems that experience increases in CO_2, for example due to increased net respiration, or increasing atmospheric CO_2 concentrations, will have further CO_2 increases due to decreasing pH (Cole & Prairie, 2009). On the other hand, HCO_3^-, CO_3^{2-}, and other chemical compounds which tend to increase water hardness and alkalinity, act as buffers, meaning that systems with high pH are less prone to pH fluctuations, resulting in more stable carbonate systems (Wolf-Gladrow *et al.*, 2007). Warm temperatures and high salinities also reduce the ability of water to dissolve CO_2, which pushes the equilibrium toward HCO_3^- and CO_3^{2-}.

In contrast to seawater, which generally has a pH between 7.6 and 8.2 (Emerson & Hedges, 2008), lakes are much more variable. For example, the 2007 national lake assessment in the US recorded lakes with a pH as low as 3.3 and as high as 10.9 (Figure 1a). Similarly, the partial pressure of CO_2 (pCO_2) in lakes around the world is also highly variable (Figure 1b), whereas the world's oceans are generally near equilibrium with the atmosphere. Eutrophic lakes with high levels of primary production are more likely to be undersaturated, in contrast to oligotrophic lakes, which are frequently over-saturated, as they can be hotspots for decomposition of organic matter (Cole *et al.*, 1994; Balmer & Downing, 2011) or for the conversion of weathered carbonate rock to CO_2 (Marce *et al.*, 2015). However, the distinction is not general, as supersaturated eutrophic lakes also exist, and can produce and emit carbon at much higher rates than oligo- or mesotrophic lakes (Morales-Williams *et al.*, 2021).

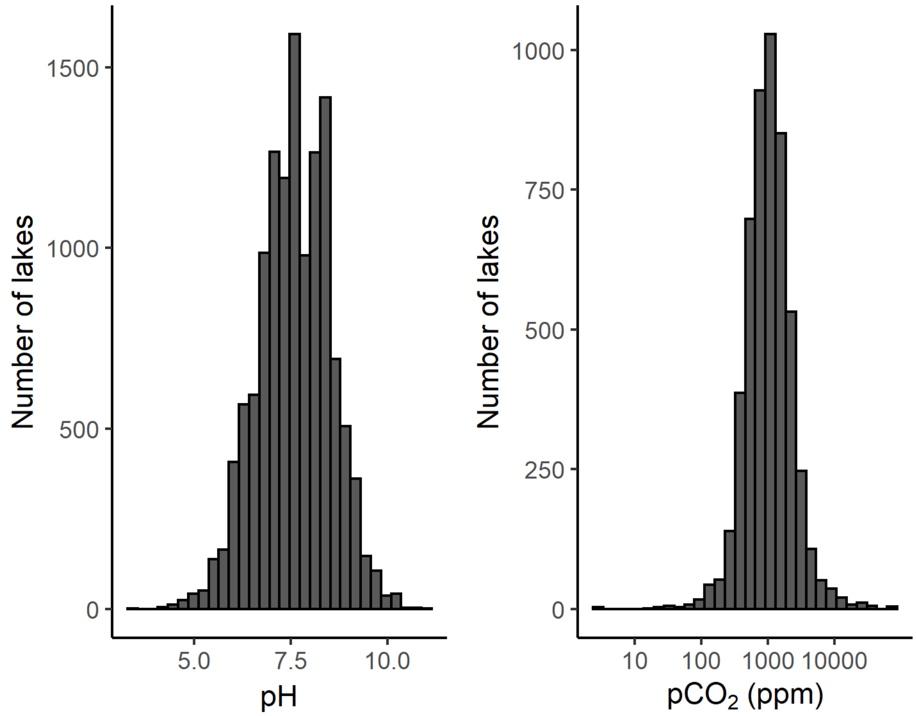

Figure 1: Histogram of (a) the pH across US lakes as measured by the US National Lake Assessment of 2007 (USEPA (US Environmental Protection Agency), 2009) (b) the pCO_2 in 5190 lakes across the world (data compiled by Marotta *et al.* (2009)).

0.6.2 Anthropogenic Effects on DIC

A defining feature of the Anthropocene Epoch is the greenhouse gas emissions related to human activities, characterized by the rapidly increasing atmospheric pCO_2 (Ruddiman, 2013). Whereas the physical impact of increasing atmospheric pCO_2 on aquatic ecosystems is relatively well-studied in terms of ocean acidification (Doney *et al.*, 2009), the same cannot be said about freshwaters. Unlike the ocean, lakes and rivers are often far from equilibrium with atmospheric pCO_2 (Figure 1b). Nevertheless, according to Fick's first law of diffusion (Cole & Prairie, 2009) we can still expect that an increase in the atmospheric pCO_2 will increase influx of CO_2 to undersaturated water bodies and decrease the efflux of CO_2 from supersaturated water bodies. This means that, at least on average, increasing atmospheric pCO_2 should also lead to increases in freshwater pCO_2.

Other anthropogenic effects may also lead to changes in the DIC of freshwater bodies. For example, in a process called brownification of lakes, increases in coloured dissolved organic matter in lakes have been observed (Touchart *et al.*, 2012). This process is thought to be caused by several anthropogenic factors, including changes in climate and land cover of the surrounding landscape. Dissolved organic matter offers substrate for bacteria, which, through the process of respiration produce CO_2. Furthermore, the process of agricultural liming, where carbonate powders are spread across the soil to decrease acidity, can result in run-off that is rich in HCO_3^- and CO_3^{2-}, leading to increased DIC in surrounding water bodies (Zeng, Liu & Groves, 2022).

0.6.3 CO_2 (Co-)Limitation

The first theory of resource limitation (known to us) was Liebig's Law of the Minimum. The Law of the Minimum was used to explain why agricultural fields became infertile after several consecutive years of fruitful yields, stating that as the plants grow, one resource can reach sufficiently low values to stop further growth (von Liebig, 1855; de Baar, 1994). The concept is fundamental to our understanding of resource limitation of phytoplankton in aquatic systems and is still being referenced and tested to this day (Tang & Riley, 2021). For example, the idea that phosphorus was the limiting resource for lake phytoplankton led several countries to adopt legislation that limited the input of phosphorus into freshwater ecosystems, which helped curb eutrophication (Schindler *et al.*, 2016). However, a review of 653 freshwater mesocosm experiments found that N and P limitation are equally prevalent in communities of freshwater primary producers (Elser *et al.*, 2007). Furthermore, communities were found to display a range of responses, such as simultaneous limitation by both N and P, independent co-limitation by either N or P, or no limitation by either resource alone or in combination (Harpole *et al.* (2011); Figure 2a). Instances of independent co-limitation could also be classified as additive, where the sum of the single-nutrient effects is equal to the multiple nutrient enrichment effect, or synergistic, where the sum of the single-nutrient effects is less than the multiple nutrient enrichment effect (Figure 2b). This is similar to ecotoxicology, where a synergistic effect means that the combined additions of two toxins can cause greater mortality than one would expect from additions of each toxin individually. This was a clear demonstration that in numerous cases, the Law of the Minimum is insufficient to fully understand the resource limitation of primary producer communities. Due to the possibility of interaction between multiple limiting factors, it seems clear that additional resources must be considered if a more complete understanding of aquatic communities is to be attained.

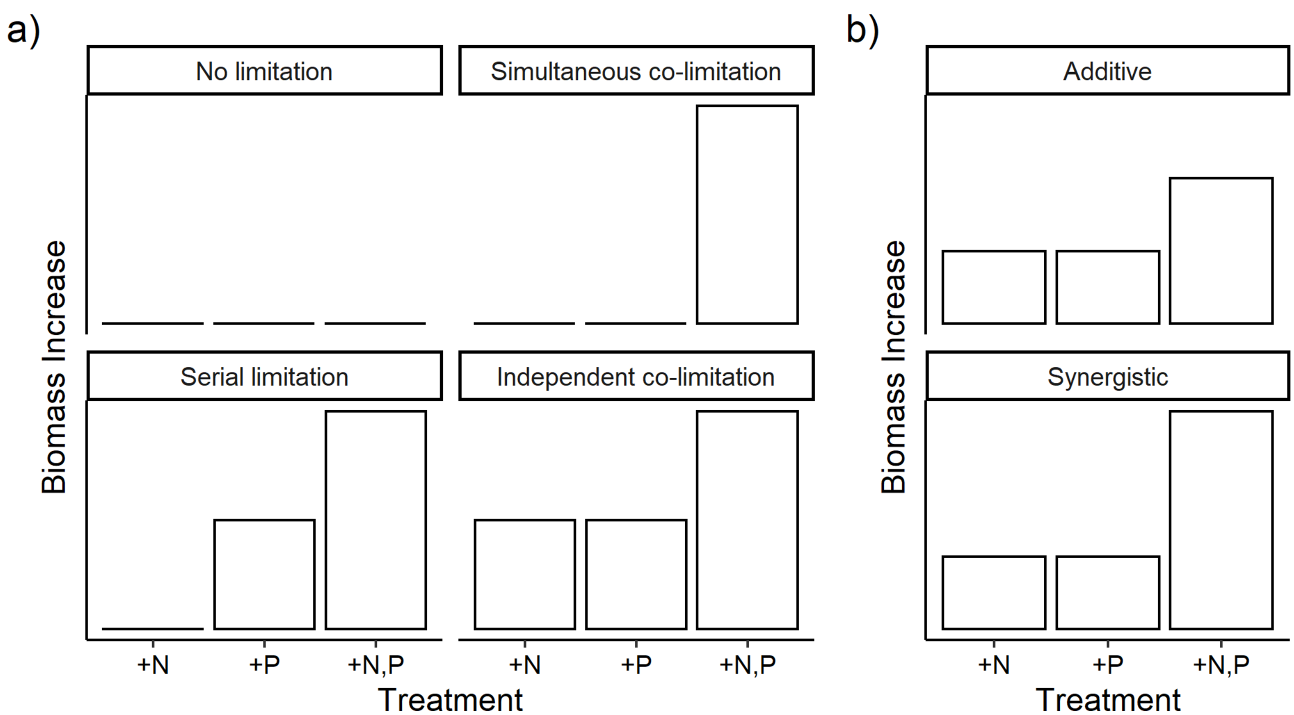

Figure 2: Examples of several types of limitation (facets) observed in mesocosm experiments. The community biomass (y-axis) responds differently to different combinations of additions of N and P (x-axis).

Prior to the publication of Harpole *et al.*'s (2011) meta-analysis, CO_2, despite being an essential resource, had not received nearly as much attention as N or P in terms of resource limitation experiments. In the experimental lakes area, researchers discovered that by midday, DIC concentrations in lakes fertilized with phosphorus and nitrogen decreased to such low levels that primary production became carbon-limited (Schindler & Fee, 1973). Four years later, in his review on the impact of anthropogenic CO_2 emissions on the earth's biota, Daniel Botkin writes that "although CO_2-enrichment is not the cause of algal blooms symptomatic of eutrophication, it could potentially increase the frequency and duration of such blooms in fertilized lakes" (Botkin, 1977). However, it was not until 20 years later that CO_2 limitation in freshwaters was addressed again (Shapiro, 1997).

Whole-lake experiments in a eutrophic Wisconsin lake (USA) found that cyanobacteria were not limited by CO_2, and typically had superior CO_2 kinetic compared to other species (Shapiro, 1997). In contrast, bottle experiments with water from Scandinavian supersaturated lakes showed that primary production was reduced in bottles where pCO_2 was equilibrated with atmospheric concentrations (Jansson, Karlsson & Jonsson, 2012). Furthermore, the same study found that together with nutrients, pCO_2 explained most variation in primary production across 70 subarctic lakes, suggesting that CO_2 and nutrients may co-limit phytoplankton communities (Jansson *et al.*, 2012). A series of subsequent publications from mesotrophic and eutrophic lakes around the world found that CO_2 enrichment displayed interactions with nutrient enrichment (Low-Décarie, Bell & Fussmann, 2015; Katkov, Low-Décarie & Fussmann, 2020), seasonal variation (Shi *et al.*, 2015), and direct effects on phytoplankton biomass (Kragh & Sand-Jensen, 2018; Hammer, Kragh & Sand-Jensen, 2019). Additionally, a laboratory study showed that the green alga *Chlamydomonas acidophilia* was co-limited by CO_2 and phosphorus (Spijkerman, Castro & Gaedke, 2011). Taken together, these studies suggest that phytoplankton populations and communities can be co-limited by carbon and other nutrients (see Low-Décarie, Fussmann & Bell (2014) for further discussion on how CO_2 fits in with the co-limitation concept).

0.6.4 Effect of Changing pCO_2 on Community Composition

Although there have been much fewer carbon enrichment experiments relative to phosphorus and nitrogen enrichment experiments, physiological research on photosynthesis, for which phytoplankton provide an ideal study system have allowed us to gain important insights about the competition for carbon. One important finding was that many phytoplankton species have “carbon concentration mechanisms,” a general term that encompasses several molecular mechanisms which allow cells to maximize the uptake rates of inorganic carbon (Raven & Beardall, 2003; Giordano, Beardall & Raven, 2005). The photosynthetic enzyme Rubisco, responsible for carbon fixation, has also evolved in response to changing atmospheric CO_2 concentrations (Young *et al.*, 2012). In addition to providing evidence for the importance of carbon (co-)limitation, the large diversity of carbon concentration mechanisms and Rubisco efficiencies among different taxa provide a strong physiological basis for differences in competitive ability among taxa. Indeed, many species of cyanobacteria have carbon concentration mechanisms that allow them to thrive at very low concentration of inorganic carbon, leading to the prediction that increasing atmospheric CO_2 concentrations may benefit species, such as green algae, which typically require higher levels of inorganic carbon (Shapiro, 1997; Tortell, 2000; Low-Décarie *et al.*, 2014). However, this hypothesis has received limited empirical support (Shapiro, 1997; Low-Décarie, Fussmann & Bell, 2011; Low-Décarie *et al.*, 2015; Katkov *et al.*, 2020). Other studies suggest that cyanobacteria may simply benefit from the added carbon supply (Ji *et al.*, 2017, 2020; Huisman *et al.*, 2018). In marine systems, where rising CO_2 is framed in terms of ocean acidification, diatoms are often found to benefit from high pCO_2 (Dutkiewicz *et al.*, 2015; Feng *et al.*, 2021). I suggest that more freshwater studies are needed to understand how competition for carbon can affect natural phytoplankton communities at a finer taxonomic or molecular level. For example, one study found that a strain of the cyanobacterium *Microcystis aeruginosa* with high affinity for inorganic carbon was favoured when CO_2 levels in a eutrophic lake were low, and the low affinity strain of the same species was favoured when CO_2 levels were high (Sandrini *et al.*, 2016).

0.6.5 Interaction of CO_2 and Temperature

In addition to the direct effects of increasing pCO_2 on primary producers, the warming generated by anthropogenic carbon emissions can also affect aquatic ecosystems. Although variability among lakes is large, on average, surface temperatures of lakes worldwide rose by 0.34°C decade^{-1} between 1985 and 2009 (O'Reilly *et al.*, 2015). Because the population growth rates of phytoplankton taxa are generally temperature-dependent, increasing temperature can allow for increased proliferation for many types of phytoplankton, such as cyanobacteria which typically require higher temperatures than heterokonts (Paerl & Otten, 2013). However, despite temperature and pCO_2 being inter-related, and having potential consequences on aquatic ecosystems, only a few studies have addressed the interaction of these two factors.

The best studied aspect of the ecological interaction of temperature with CO_2 relates to the effect of food quality on zooplankton species. When growing in high pCO_2 environments, phytoplankton cells typically contain higher proportions of carbon compared to other resources than in low pCO_2 environments (Verspagen *et al.*, 2014). This shift in stoichiometry has been found to have a negative effect on the nutritional quality of the food plankton, which can cascade up to their zooplanktonic predators (Urabe, Togari & Elser, 2003; Rossoll *et al.*, 2012; Schoo *et al.*, 2013; Meunier *et al.*, 2016). This effect was found to be modulated by temperature, though the mechanism and the direction of the effect seems to vary with different zooplankton species (Persson *et al.*, 2010; Malzahn, Doerfler & Boersma, 2016; Garzke, Sommer & Ismar-Rebitz, 2020).

Several other studies have investigated the interactive effects of temperature and CO_2 in marine phytoplankton species and have been summarised by Raven & Beardall (2021). However, most of these studies consider a multitude of factors, such that the explicit interaction of CO_2 and temperature is rarely tested (*e.g.*, Boyd *et al.* (2015)). Nevertheless, a meta-analysis of multiple driver experiments revealed how primary production in different areas of the ocean and how growth rates of different species are likely to respond to climate change (Seifert *et al.*, 2020). In freshwaters, however, it remains difficult to draw any simple conclusions from the available studies, even when taken together, beyond the importance of studying the interactive effects of multiple factors.

0.6.6 Phenotypic Plasticity of Phytoplankton in Varying DIC Environments

Phenotypic plasticity refers to an organism's ability to change certain traits in response to changing environmental conditions, without any changes to the organism's genetic code. "Carbon uptake kinetics," which regulate the rate of carbon uptake depending on the DIC concentrations outside of the cell, are a group of physiological traits of phytoplankton cells that exhibit phenotypic plasticity (Ji *et al.*, 2020). Ji *et al.* (2020) have found that changing pCO_2 concentrations can affect CO_2 and HCO_3^- uptake kinetics in several phytoplankton species. Changes in alkalinity were also found to affect CO_2 and HCO_3^- uptake kinetics across multiple species (Spijkerman, Maberly & Coesel, 2005). These studies suggest that carbon concentration mechanisms, the most likely candidates for regulating carbon uptake kinetics, exhibit phenotypic plasticity in response to changing DIC. Other traits can also be affected by changing pCO_2 concentrations. For example, one study found that several physiological traits, including growth rate, of the marine diatom *Phaeodactylum tricornutum* had different responses to elevated pCO_2 depending on the time of exposure - 20 versus 1800 generations (Li *et al.*, 2016). A literature analysis study found a "universal reaction norm," which describes the phenotypic plasticity of phytoplankton growth rates in response to changing pCO_2 (Paul & Bach, 2020). For an updated list of studies on the phenotypic effects of CO_2 on growth rate, see Collins, Whittaker & Thomas (2022). Another study found that marine picoplankters exhibit plastic growth rates, which depend on their "social milieu," *i.e.*, the other species strains growing in the same environment, an effect which is enhanced by increasing pCO_2 (Collins & Schaum, 2021). Taken together, these studies suggest that environmental DIC can play in important role in the expression of a variety of traits, including carbon concentration mechanisms, in a range of phytoplankton species.

0.6.7 Evolutionary Response to Changing pCO_2

The diversity of carbon concentration mechanisms, together with the observed phenotypic plasticity related to carbon uptake highlights the possibility of a future evolutionary response to anthropogenic changes in CO_2 concentrations. Studies on this topic demonstrate a variety of species-specific responses. Several studies found that various phytoplankton species showed no specific adaptations in response to increasing pCO_2 (Collins & Bell, 2004; Collins & Bell, 2005; Collins, Sultemeyer & Bell, 2006; Low-Décarie *et al.*, 2013). In some cases, however, conditionally neutral mutations accumulated in lines exposed to high pCO_2, causing them to grow less effectively at low pCO_2 (Collins & Bell, 2004; Collins *et al.*, 2006; Low-Décarie *et al.*, 2013). By measuring CO_2 and HCO_3^- uptake kinetics in these lines, it was discovered that they lost the plastic response to low pCO_2, which normally results in increased affinity for carbon (Collins *et al.*, 2006). Finally, an evolutionary response to elevated pCO_2 was detected in the green alga *Chlamydomonas reinhardtii*, in conjunction with the finding that competition limited this adaptive response (Collins, 2010).

The process of phytoplankton cell calcification, thought to be important for protection from viruses and predation, is slowed by increasing acidity, which itself is caused by increasing pCO_2 concentrations. For this reason, the responses of calcifying marine phytoplankton, coccolithophores, to increasing pCO_2 and ocean acidification has garnered significant interest (Rost, Zondervan & Wolf-Gladrow, 2008; Brownlee, Langer & Wheeler, 2021). Evolutionary adaptation to increasing pCO_2 was found in the most prominent marine calcifier, the coccolithophore *Emiliania huxleyi* grown *in vitro* (Lohbeck, Riebesell & Reusch, 2012). A follow-up study found that the adaptation of *E. huxleyi* to increasing pCO_2 can involve (depending on the growth environment) strong pleiotropic effects, meaning that several different genes can be responsible for the genetic adoption to high pCO_2 (Lohbeck *et al.*, 2013). Laboratory experiments with the coccolithophore *Gephyrocapsa oceanica* showed that elevated pCO_2 selected for reduced rates of calcification. Together, these studies point to the fact that although evolution may help calcifying coccolithophores adapt to increasing pCO_2, calcification rates are still likely to suffer in many species.

Examples of evolutionary responses to increasing pCO_2 also exist for other groups of phytoplankton. The evolutionary responses of different strains of the marine green alga *Ostreococcus* grown in the laboratory under increased pCO_2 were found to correlate with the phenotypic plasticity measured in terms of growth rates (Schaum & Collins, 2014). Experiments with the marine cyanobactria *Trichodesmium erythraeum* found that cell lines exposed to elevated pCO_2 for 850 generations adapted by irreversibly increasing the rate of nitrogen fixation (Hutchins *et al.*, 2015). Several laboratory experiments with marine diatoms showed varying levels of adaptation to elevated pCO_2 (Crawfurd *et al.*, 2011; Tatters *et al.*, 2013; Li *et al.*, 2016) These findings accentuate the fact that different groups, species and even strains may have quite different responses to increasing pCO_2.

Most of the studies focusing on the evolutionary responses to high pCO_2 focus on marine phytoplankton. The ecological effects of high pCO_2 are better understood in marine systems, and, unlike lakes, oceanic pCO_2 is typically in close equilibrium with the atmosphere (Emerson & Hedges, 2008), which provides evolutionary studies with clear expectations and treatments. Nevertheless, a freshwater study, replicated in chemostats and in a eutrophic lake, found evidence for selection for different genotypes (associated with different carbon uptake rates) of the cyanobacterium *Microcystis sp.* depending on ambient pCO_2 levels (Sandrini *et al.*, 2016). This study underlines the possibility of taking advantage of temporal variation of pCO_2 in the freshwater lake to assess the role of natural selection *in situ*. Long-term mesocosm experiments can also provide opportunities to assess evolutionary responses to increasing pCO_2 in both marine and freshwater environments (*e.g.* Scheinin *et al.* (2015)).

0.6.8 Investigative Approaches

The studies mentioned in this review employ a number of investigative approaches, which help provide complementary information and, together, can generate a holistic understanding of the impacts of climate change on aquatic ecosystems. Observational studies are essential in forming a solid foundation for how processes of interest play out in nature. Such studies rely on using naturally-occurring variability for comparative purposes (*e.g.*, Sandrini *et al.* (2016) compare genotypes of a cyanobacteria population during periods of high and low pCO_2 in a eutrophic lake). However, it is difficult to infer causation from observations in natural systems because a large number of parameters are changing among systems. A variety of experimental approaches can help address this gap. For single species, small communities or ecosystems, chemostat and microcosm experiments can be performed in the laboratory. Microcosms are logistically simple to set up - flasks filled with growth medium and inoculated with the organisms of interest (*e.g*,, Jansson *et al.* (2012) filled flasks with lake water and either bubbled them with air, or left them in their naturally super-saturated state to measure the effect of pCO_2 on primary production). As a result, many microcosms, or, in experimental terms, "experimental units" can be studied simultaneously. Chemostats are more logistically complex, but can provide valuable data about steady state conditions, which are essential for certain measurements (*e.g.*, Ji *et al.* (2020)). To study communities or more complex ecosystems using an experimental approach, researchers employ mesocosm experiments. Mesocosms enclose parts of the environment that are much bigger than would be feasible in a controlled laboratory environment (*e.g.*, Low-Décarie *et al.* (2015) used 2500 L impermeable enclosures in a lake to study the effect of pCO_2 on phytoplankton community composition). However, mesocosm experiments are often more costly and logistically complex than laboratory studies, which often translates to fewer experimental units.

Across all experimental approaches, it is of utmost importance to learn as much as possible from a limited number of experimental units. It is often interesting to study the effects of a factor at many levels, particularly in the case of pCO_2, which is present at many different concentrations in different lakes and at different times. In reality, there are often multiple factors at play, and studying the interactive effects between them is often relevant. Finally, replication is essential for decreasing the statistical error. Boyd *et al.* (2018) provide an overview over experimental design for studying global ocean change, and suggest focusing on fewer factors by combining several factors into one where possible. Collins *et al.* (2022) suggest focusing on multiple levels, at the expense of replication, to better understand the general trends, or "response curves" (in the case of a single factor), or "responses surfaces" (in the case of multiple factors). Understanding such general trends allows for better synthesis work, in the form of modelling studies, or meta-analyses to combine information, form a new understanding, ask new questions and emit new hypotheses.

0.6.9 Conclusion

Taken together, it seems plausible that CO_2 can affect aquatic primary producers, playing an ecological role as a co-limiting factor and an evolutionary role by affecting carbon uptake kinetics and other traits. Additionally, cascading effects to higher trophic levels, and interactive effects with temperature are also possible. Nevertheless, there is a large variability among studies, possibly due to different focal species, or environments, which suggests that a lot remains to be explored when it comes to understanding the contexts under which the effects of changing pCO_2 will be most impactful. Thus, this thesis aims to contribute to our understanding of how anthropogenic changes, particularly increasing pCO_2, will affect freshwater aquatic ecosystems. Our main investigative approach is to use mesocosm experiments with multiple factors, to study the interactive effects, and a theoretical modelling approach to understand the evolutionary role of pCO_2.

0.6.10 References

Balmer M.B. & Downing J.A. (2011). Carbon dioxide concentrations in eutrophic lakes: Undersaturation implies atmospheric uptake. *Inland Waters* **1**, 125–132. https://doi.org/10.5268/iw-1.2.366

Botkin D.B. (1977). Forests, lakes, and the anthropogenic production of carbon dioxide. *BioScience* **27**, 325–331. https://doi.org/10.2307/1297631

Boyd P. W., Dillingham P. W., McGraw C. M., Armstrong E. A., Cornwall C. E., Feng Y.-y., *et al.* (2015). Physiological responses of a Southern Ocean diatom to complex future ocean conditions. *Nature Climate Change* **6**, 207–213. https://doi.org/10.1038/nclimate2811

Boyd P.W., Collins S., Dupont S., Fabricius K., Gattuso J.-P., Havenhand J., *et al.* (2018). Experimental strategies to assess the biological ramifications of multiple drivers of global ocean change-A review. *Global Change Biology* **24**, 2239–2261. https://doi.org/10.1111/gcb.14102

Brownlee C., Langer G. & Wheeler G.L. (2021). *Coccolithophore* calcification: Changing paradigms in changing oceans. *Acta Biomaterialia* **120**, 4–11. https://doi.org/10.1016/j.actbio.2020.07.050

Cole J.J., Caraco N.F., Kling G.W. & Kratz T.K. (1994). Carbon dioxide supersaturation in the surface waters of lakes. *Science* **265**, 1568

Cole J.J. & Prairie Y.T. (2009). Dissolved CO_2. Oxford: Elsevier.

Collins S. (2010). Competition limits adaptation and productivity in a photosynthetic alga at elevated CO_2. *Proceedings of the Royal Society B: Biological Sciences* **278**, 247–255. https://doi.org/10.1098/rspb.2010.1173

Collins S. & Bell G. (2005). Evolution of natural algal populations at elevated CO_2. *Ecology Letters* **9**, 129–135. https://doi.org/10.1111/j.1461-0248.2005.00854.x

Collins S. & Bell G. (2004). Phenotypic consequences of 1,000 generations of selection at elevated CO_2 in a green alga. *Nature* **431**, 566–569. https://doi.org/10.1038/nature02945

Collins S. & Schaum C.E. (2021). Growth strategies of a model picoplankter depend on social milieu and $p$$CO_2$. *Proceedings of the Royal Society B: Biological Sciences* **288**, 20211154. https://doi.org/10.1098/rspb.2021.1154

Collins S., Sultemeyer D. & Bell G. (2006). Changes in C uptake in populations of *Chlamydomonas reinhardtii* selected at high CO_2. *Plant, Cell and Environment* **29**, 1812–1819. https://doi.org/10.1111/j.1365-3040.2006.01559.x

Collins S., Whittaker H. & Thomas M.K. (2022). The need for unrealistic experiments in global change biology. *Current Opinion in Microbiology* **68**, 102151. https://doi.org/10.1016/j.mib.2022.102151

Crawfurd K.J., Raven J.A., Wheeler G.L., Baxter E.J. & Joint I. (2011). The Response of *Thalassiosira pseudonana* to Long-Term Exposure to Increased CO_2 and Decreased pH. *PLoS ONE* **6**, e26695. https://doi.org/10.1371/journal.pone.0026695

de Baar H.J.W. (1994). Von liebig's law of the minimum and plankton ecology (18991991). *Progress in Oceanography* **33**, 347–386. https://doi.org/10.1016/0079-6611(94)90022-1

Doney S.C., Fabry V.J., Feely R.A. & Kleypas J.A. (2009). Ocean Acidification: The Other CO_2 Problem. *Annual Review of Marine Science* **1**, 169–192. https://doi.org/10.1146/annurev.marine.010908.163834

Dutkiewicz S., Morris J.J., Follows M.J., Scott J., Levitan O., Dyhrman S.T., *et al.* (2015). Impact of ocean acidification on the structure of future phytoplankton communities. *Nature Climate Change* **5**, 1002–1006. https://doi.org/10.1038/nclimate2722

Elser J.J., Bracken M.E.S., Cleland E.E., Gruner D.S., Harpole W.S., Hillebrand H., *et al.* (2007). Global Analysis of Nitrogen and Phosphorus Limitation of Primary Producers in Freshwater, Marine and Terrestrial Ecosystems. *Ecology Letters* **10**, 1135–1142. https://doi.org/10.1111/j.1461-0248.2007.01113.x

Emerson S. & Hedges J. (2008). Carbonate chemistry. pp. 101–133. Cambridge University Press.

Feng Y., Chai F., Wells M.L., Liao Y., Li P., Cai T., *et al.* (2021). The combined effects of increased pCO2 and warming on a coastal phytoplankton assemblage: From species composition to sinking rate. *Frontiers in Marine Science* **8**. https://doi.org/10.3389/fmars.2021.622319

Garzke J., Sommer U. & Ismar-Rebitz S.M.H. (2020). Zooplankton growth and survival differentially respond to interactive warming and acidification effects. *Journal of Plankton Research* **42**, 189–202. https://doi.org/10.1093/plankt/fbaa005

Giordano M., Beardall J. & Raven J.A. (2005). CO_2 concentrating mechanisms in algae: Mechanisms, environmental modulation, and evolution. *Annual Review of Plant Biology* **56**, 99–131. https://doi.org/10.1146/annurev.arplant.56.032604.144052

Hammer K.J., Kragh T. & Sand-Jensen K. (2019). Inorganic carbon promotes photosynthesis, growth, and maximum biomass of phytoplankton in eutrophic water bodies. *Freshwater Biology* **64**, 1956–1970. https://doi.org/10.1111/fwb.13385

Harpole W.S., Ngai J.T., Cleland E.E., Seabloom E.W., Borer E.T., Bracken M.E.S., *et al.* (2011). Nutrient co-limitation of primary producer communities. *Ecology Letters* **14**, 852–862. https://doi.org/10.1111/j.1461-0248.2011.01651.x

Huisman J., Codd G.A., Paerl H.W., Ibelings B.W., Verspagen J.M.H. & Visser P.M. (2018). Cyanobacterial Blooms. *Nature Reviews Microbiology* **16**, 471–483. https://doi.org/10.1038/s41579-018-0040-1

Hutchins D.A., Walworth N.G., Webb E.A., Saito M.A., Moran D., McIlvin M.R., *et al.* (2015). Irreversibly increased nitrogen fixation in *Trichodesmium* experimentally adapted to elevated carbon dioxide. *Nature Communications* **6**. https://doi.org/10.1038/ncomms9155

Jansson M., Karlsson J. & Jonsson A. (2012). Carbon dioxide supersaturation promotes primary production in lakes. *Ecology Letters* **15**, 527–532. https://doi.org/10.1111/j.1461-0248.2012.01762.x

Ji X., Verspagen J.M.H., Stomp M. & Huisman J. (2017). Competition between cyanobacteria and green algae at low versus elevated CO_2: Who will win, and why? *Journal of experimental botany* **68**, 3815–3828. https://doi.org/10.1093/jxb/erx027

Ji X., Verspagen J.M.H., Van de Waal D.B., Rost B. & Huisman J. (2020). Phenotypic plasticity of carbon fixation stimulates cyanobacterial blooms at elevated CO_2. *Science Advances* **6**, eaax2926. https://doi.org/10.1126/sciadv.aax2926

Katkov E., Low-Décarie É. & Fussmann G.F. (2020). Intra-annual variation of phytoplankton community responses to factorial N, P, and CO_2 enrichment in a temperate mesotrophic lake. *Freshwater Biology* **65**, 960–970. https://doi.org/10.1111/fwb.13482

Kragh T. & Sand-Jensen K. (2018). Carbon limitation of lake productivity. *Proceedings of the Royal Society B: Biological Sciences* **285**, 20181415. https://doi.org/10.1098/rspb.2018.1415

Li F., Beardall J., Collins S. & Gao K. (2016). Decreased Photosynthesis and Growth with Reduced Respiration in the Model Diatom *Phaeodactylum tricornutum* Grown Under elevated CO_2 over 1800 Generations. *Global Change Biology* **23**, 127–137. https://doi.org/10.1111/gcb.13501

Lohbeck K.T., Riebesell U., Collins S. & Reusch T.B.H. (2013). Functional genetic divergence in high CO_2 adapted *emiliania huxleyi* populations. *Evolution* **67**, 1892–1900. https://doi.org/10.1111/j.1558-5646.2012.01812.x

Lohbeck K.T., Riebesell U. & Reusch T.B.H. (2012). Adaptive evolution of a key phytoplankton species to ocean acidification. *Nature Geoscience* **5**, 346–351. https://doi.org/10.1038/ngeo1441

Low-Décarie E., Bell G. & Fussmann G.F. (2015). CO_2 alters community composition and response to nutrient enrichment of freshwater phytoplankton. *Oecologia* **177**, 875–883

Low-Décarie E., Fussmann G.F. & Bell G. (2014). Aquatic primary production in a high-CO_2 world. *Trends in ecology & evolution* **29**, 223–232

Low-Décarie E., Fussmann G.F. & Bell G. (2011). The effect of elevated CO_2 on growth and competition in experimental phytoplankton communities. *Global Change Biology* **17**, 2525–2535. https://doi.org/10.1111/j.1365-2486.2011.02402.x

Low-Décarie E., Jewell M.D., Fussmann G.F. & Bell G. (2013). Long-term culture at elevated atmospheric CO_2 fails to evoke specific adaptation in seven freshwater phytoplankton species. *Proceedings of the Royal Society B: Biological Sciences* **280**. https://doi.org/10.1098/rspb.2012.2598

Malzahn A.M., Doerfler D. & Boersma M. (2016). Junk food gets healthier when it's warm. *Limnology and Oceanography* **61**, 1677–1685. https://doi.org/10.1002/lno.10330

Marce R., Obrador B., Morgui J.-A., Lluis Riera J., Lopez P. & Armengol J. (2015). Carbonate weathering as a driver of CO_2 supersaturation in lakes. *Nature Geosci* **8**, 107–111. https://doi.org/10.1038/ngeo2341

Marotta H., Duarte C.M., Sobek S. & Enrich-Prast A. (2009). Large CO_2 Disequilibria in Tropical Lakes. *Global Biogeochemical Cycles* **23**. https://doi.org/10.1029/2008gb003434

Meunier C.L., Algueró-Muñiz M., Horn H.G., Lange J.A.F. & Boersma M. (2016). Direct and indirect effects of near-future pCO_2 levels on zooplankton dynamics. *Marine and Freshwater Research* **68**, 373–380. https://doi.org/10.1071/MF15296

Morales-Williams A.M., Wanamaker A.D., Williams C.J. & Downing J.A. (2021). Eutrophication drives extreme seasonal CO_2 flux in lake ecosystems. *Ecosystems* **24**, 434–450. https://doi.org/10.1007/s10021-020-00527-2

O'Reilly C.M., Sharma S., Gray D.K., Hampton S.E., Read J.S., Rowley R.J., *et al.* (2015). Rapid and highly variable warming of lake surface waters around the globe. *Geophysical Research Letters* **42**. https://doi.org/10.1002/2015gl066235

Paerl H.W. & Otten T.G. (2013). Harmful Cyanobacterial Blooms: Causes, Consequences, and Controls. *Microbial Ecology* **65**, 995–1010. https://doi.org/10.1007/s00248-012-0159-y

Paul A.J. & Bach L.T. (2020). Universal response pattern of phytoplankton growth rates to increasing CO_2. *New Phytologist* **228**, 1710–1716. https://doi.org/10.1111/nph.16806

Persson J., Wojewodzic M.W., Hessen D.O. & Andersen T. (2010). Increased risk of phosphorus limitation at higher temperatures for *Daphnia magna*. *Oecologia* **165**, 123–129. https://doi.org/10.1007/s00442-010-1756-4

Raven J.A. & Beardall J. (2003). Carbon acquisition mechanisms of algae: Carbon dioxide diffusion and carbon dioxide concentrating mechanisms. (Eds A.W.D. Larkum, S.E. Douglas & J.A. Raven), pp. 225–244. Springer Netherlands, Dordrecht.

Raven J.A. & Beardall J. (2021). Influence of Global Environmental Change on Plankton. *Journal of Plankton Research* **43**, 779–800. https://doi.org/10.1093/plankt/fbab075

Rossoll D., Bermúdez R., Hauss H., Schulz K.G., Riebesell U., Sommer U., *et al.* (2012). Ocean acidification-induced food quality deterioration constrains trophic transfer. *PLOS ONE* **7**, e34737. https://doi.org/10.1371/journal.pone.0034737

Rost B., Zondervan I. & Wolf-Gladrow D. (2008). Sensitivity of phytoplankton to future changes in ocean carbonate chemistry: current knowledge, contradictions and research directions. *Marine Ecology Progress Series* **373**, 227–237. https://doi.org/10.3354/meps07776

Ruddiman W.F. (2013). The Anthropocene. *Annual Review of Earth and Planetary Sciences* **41**, 45–68. https://doi.org/10.1146/annurev-earth-050212-123944

Sandrini G., Ji X., Verspagen J.M.H., Tann R.P., Slot P.C., Luimstra V.M., *et al.* (2016). Rapid adaptation of harmful cyanobacteria to rising CO_2. *Proceedings of the National Academy of Sciences* **113**, 9315–9320. https://doi.org/10.1073/pnas.1602435113

Schaum C.E. & Collins S. (2014). Plasticity Predicts Evolution in a Marine Alga. *Proceedings of the Royal Society B: Biological Sciences* **281**, 20141486. https://doi.org/10.1098/rspb.2014.1486

Scheinin M., Riebesell U., Rynearson T.A., Lohbeck K.T. & Collins S. (2015). Experimental evolution gone wild. *Journal of The Royal Society Interface* **12**, 20150056. https://doi.org/10.1098/rsif.2015.0056

Schindler D.W., Carpenter S.R., Chapra S.C., Hecky R.E. & Orihel D.M. (2016). Reducing phosphorus to curb lake eutrophication is a success. *Environmental Science & Technology* **50**, 8923–8929. https://doi.org/10.1021/acs.est.6b02204

Schindler D.W. & Fee E.J. (1973). Diurnal variation of dissolved inorganic carbon and its use in estimating primary production and CO_2 invasion in lake 227. *Journal of the Fisheries Research Board of Canada* **30**, 1501–1510. https://doi.org/10.1139/f73-240

Schoo K.L., Malzahn A.M., Krause E. & Boersma M. (2013). Increased carbon dioxide availability alters phytoplankton stoichiometry and affects carbon cycling and growth of a marine planktonic herbivore. *Marine Biology* **160**, 2145–2155. https://doi.org/10.1007/s00227-012-2121-4

Seifert M., Rost B., Trimborn S. & Hauck J. (2020). Meta-analysis of multiple driver effects on marine phytoplankton highlights modulating role of *p* CO ₂. *Global Change Biology* **26**, 6787–6804. https://doi.org/10.1111/gcb.15341

Shapiro J. (1997). The role of carbon dioxide in the initiation and maintenance of blue-green dominance in lakes. *Freshwater Biology* **37**, 307–323. https://doi.org/10.1046/j.1365-2427.1997.00164.x

Shi X., Zhao X., Zhang M., Yang Z., Xu P. & Kong F. (2015). The responses of phytoplankton communities to elevated CO_2 show seasonal variations in the highly eutrophic lake taihu. *Canadian Journal of Fisheries and Aquatic Sciences* **73**, 727–736. https://doi.org/10.1139/cjfas-2015-0151

Sommer U., Gliwicz Z.M., Lampert W. & Duncan A. (1986). The PEG-model of seasonal succession of planktonic events in fresh waters. *Arch. Hydrobiol* **106**, 433–471

Spijkerman E., Castro F. de & Gaedke U. (2011). Independent co-limitation for carbon dioxide and inorganic phosphorus. *PLOS ONE* **6**, e28219. https://doi.org/10.1371/journal.pone.0028219

Spijkerman E., Maberly S.C. & Coesel P.F. (2005). Carbon acquisition mechanisms by planktonic desmids and their link to ecological distribution. *Canadian journal of botany* **83**, 850–858

Tang J. & Riley W.J. (2021). Finding Liebig's Law of the Minimum. *Ecological Applications*. https://doi.org/10.1002/eap.2458

Tatters A.O., Roleda M.Y., Schnetzer A., Fu F., Hurd C.L., Boyd P.W., *et al.* (2013). Short- and long-term conditioning of a temperate marine diatom community to acidification and warming. *Philosophical Transactions of the Royal Society B: Biological Sciences* **368**, 20120437. https://doi.org/10.1098/rstb.2012.0437

Tortell P.D. (2000). Evolutionary and ecological perspectives on carbon acquisition in phytoplankton. *Limnology and Oceanography* **45**, 744–750. https://doi.org/10.4319/lo.2000.45.3.0744

Touchart L., Józsa J., Rákóczi L., Krámer T., Andrén T., Bouffard D., *et al.* (2012). Brownification of lakes. pp. 117–119. Springer Netherlands.

Urabe J., Togari J.U.N. & Elser J.J. (2003). Stoichiometric impacts of increased carbon dioxide on a planktonic herbivore. *Global Change Biology* **9**, 818–825. https://doi.org/10.1046/j.1365-2486.2003.00634.x

USEPA (US Environmental Protection Agency) (2009). *National lakes assessment: A collaborative survey of the nation's lakes*. USEPA Office of Water Washington.

Verspagen J.M.H., Van de Waal D.B., Finke J.F., Visser P.M. & Huisman J. (2014). Contrasting effects of rising CO_2 on primary production and ecological stoichiometry at different nutrient levels. *Ecology Letters* **17**, 951–960. https://doi.org/10.1111/ele.12298

von Liebig J.F. (1855). *Principles of agricultural chemistry: With special reference to the late researches made in England*. Walton & Maberly.

Wolf-Gladrow D.A., Zeebe R.E., Klaas C., Körtzinger A. & Dickson A.G. (2007). Total Alkalinity: The explicit conservative expression and its application to biogeochemical processes. *Marine Chemistry* **106**, 287–300. https://doi.org/10.1016/j.marchem.2007.01.006

Young J.N., Rickaby R.E.M., Kapralov M.V. & Filatov D.A. (2012). Adaptive Signals in Algal Rubisco Reveal a History of Ancient Atmospheric Carbon Dioxide. *Philosophical Transactions of the Royal Society B: Biological Sciences* **367**, 483–492. https://doi.org/10.1098/rstb.2011.0145

Zeng S., Liu Z. & Groves C. (2022). Large-scale CO_2 removal by enhanced carbonate weathering from changes in land-use practices. *Earth-Science Reviews* **225**, 103915. https://doi.org/10.1016/j.earscirev.2021.103915

1 Chapter 1: Intra-annual variation of phytoplankton community responses to factorial N, P and CO_2 enrichment in a temperate mesotrophic lake

Egor Katkov[1], Étienne Low-Décarie[2,3] & Gregor F. Fussmann[1]

[1] Department of Biology, McGill University, Montreal, Quebec, Canada H3A 1B1

[2] School of Biological Sciences, University of Essex, Colchester CO4 3SQ, UK

[3] Present address: Canadian Space Agency, 6767 Route de l'Aéroport, Saint-Hubert, QC J3Y 8Y9

1.1 Preamble

This chapter has been published in the journal *Freshwater Biology* (Katkov *et al.*, 2020). It features a series of five replicate experiments that took place at different times of the year, each focused on investigating the interactive effects of nitrogen, phosphorus and CO_2. As a result, the phytoplankton community and, more generally, ecosystem dynamics, were different in each of the five experiments. The natural differences in the community can be explained using the plankton ecology group (PEG) model (Sommer *et al.*, 1986). In summary, the model states that in the spring, a dimictic, temperate lake is in a mixed state, which promotes nutrient distribution throughout the water column and abundance of heterokonts. Next, the lake stratifies, the phytoplankton community shifts to green algae, and zooplankton begin to develop and graze the phytoplankton until the lake reaches a "clear-water" state. As the summer progresses, nutrient concentrations in the upper layer decrease and a number of community shifts occur; most significantly, by the end of the summer, non-edible species of phytoplankton begin to dominate the community. Eventually, the cold of the Fall causes the lake to mix again, leading to another resurgence of heterokonts, and a second zooplankton bloom.

Furthermore, the number of potentially interacting factors in this study is high: Experiment (*i.e.* time of year), and ambient or enriched nitrogen, phosphorus and CO_2 concentrations. Although four-way interactions are notoriously difficult to interpret, in this case, it is straightforward. When reading the analysis of variance (ANOVA) output table, we need only consider the highest-order interactions that are significant and that are not sub-sets of each other (*e.g.*, Experiment:Nitrogen:Phosphorus and Nitrogen:CO_2). If Experiment is involved in an interaction, this means that the effects of the remaining terms vary among the different experiments. An interaction between two resources suggests that there is a synergistic (or antagonistic) effect when these resources are added in combination. A synergistic effect means that the addition of both resources together produces an effect that is greater than the sum of the effects when each resource is added individually. To determine the type of limitation or co-limitation (serial, simultaneous, independent; see Section 0.6.3), a post-hoc test is required.

1.2 Summary

1. Across primary producer communities in different lakes, nitrogen (N) and phosphorus (P) can exhibit many different patterns of limitation across different lakes. Here, we look at the intra-annual variability of these patterns in a single lake. Furthermore, we investigate whether a third resource, carbon dioxide (CO_2) can have significant effects on phytoplankton biomass and community composition.

2. We performed five *in situ* lacustrine mesocosm experiments at different times of the year. In each experiment, we had a factorial design with two levels of N, P and CO_2 enrichment (no enrichment or double lake concentrations for N and P and atmospheric (400 ppm) and ~1000 ppm for CO_2) resulting in a total of eight treatments. Mesocosms of ~1600 L were suspended in a temperate, mesotrophic lake (Lac Hertel, Canada). Each experiment lasted two weeks and chlorophyll *a* biomass, coarse chemotaxonomic community composition (measured using fluorometry) and several environmental variables were recorded at a minimum of four timepoints.

3. We found that the limiting, synergistic and community composition effects of N and P varied between experiments. TN:TP ratios explained, in part, some of this variability, along with insolation and water temperature.

4. Despite relatively high levels of CO_2 in the control mesocosms, we found a constant synergistic effect of CO_2 with N. In combination with the synergistic effect of P with N found in some experiments, this provides support for CO_2 as one of the multiple limiting resources in nutrient-rich systems. This finding could have implications for eutrophic lakes exposed to increasing concentrations of CO_2.

5. We also found that the effects of CO_2 on community composition varied intra-annually. Thus, we conclude that generalized predictions about the effect of CO_2 on community composition at a coarse chemotaxonomic scale are unlikely to hold, but predictions specific to season and system are likely to hold.

1.3 Introduction

Phytoplankton dominate the base of most freshwater food webs. Phytoplankton blooms, especially cyanobacterial blooms, have major environmental and economic impacts (Smith 2009). Eutrophication is the process by which the increased concentration of resources in aquatic ecosystems, from anthropogenic or, to a lesser degree, natural sources result in the appearance, increased intensity and duration of blooms (Smith, 1998). Phosphorus (P) has received a great deal of attention due to its key role in eutrophication management (Schindler et al., 2016). However, Elser *et al.* (2007) demonstrated that nitrogen (N) and P are equally common limiting resources with similar effect sizes on biomass. N and P were also found to be frequently co-limiting, meaning that each resource can have an independent effect on community biomass. Harpole *et al.* (2011) also showed that when N and P are added together, synergistic effects, which can increase biomass beyond what might be expected from additions of each resource alone are common in freshwater ecosystems.

In temperate, dimictic lakes, phytoplankton are generally expected to become resource-limited during the summer months, some time after stratification sets in and available nutrients in the epilimnion become scarce. In the classic PEG model, each resource becomes limiting one at a time as the summer progresses (Sommer et al., 1986). However, nutrient enrichment experiments have demonstrated that N and P limitation rarely follow such a simple pattern (Bukaveckas & Crain, 2002; Nydick et al., 2004; Nydick et al., 2003). Scientists also devised rules for determining limitation for certain categories of lakes, based on stoichiometric ratios of nitrogen and phosphorus (Dzialowski et al., 2005; Maberly et al., 2002). However, we are not aware of studies focused on determining weather stoichiometric ratios affected the seasonal changes in limitation regimes.

In the past decade, several researchers have begun to investigate the possibility of carbon limitation in freshwaters. In the context of a single-resource limitation framework, often called Liebig limitation (de Baar, 1994; Monod, 1950), CO_2, like N, was largely disregarded as a limiting factor for freshwater algae, in favor of P (Schindler, 1977; Schindler et al., 1972). Later, research on the mechanisms of algal photosynthesis revealed that most algal groups invested heavily in carbon concentration mechanisms in order to compensate for the high intra-cellular concentrations of CO_2 required for photosynthesis to proceed (Badger et al., 1998; Badger et al., 1980; Tortell, 2000). Next, bottle and mesocosm experiments provided evidence that CO_2 can limit primary productivity (Jansson et al., 2012) and influence community composition (Low-Décarie et al., 2015). Further experimentation showed that phytoplankton in soft waters are more prone to carbon limitation due to the smaller bicarbonate pool compared to hard waters and due to the chemically enhanced uptake rates of CO_2 in alkaline water (Hammer et al., 2019; Kragh & Sand-Jensen, 2018).

Although mesocosm experiments (Low-Décarie et al., 2015) and mathematical models (Verspagen, et al. 2014a; Verspagen, et al., 2014b) suggest that carbon limitation is more likely in eutrophic waters, other studies suggest otherwise. A survey of boreal oligotrophic lakes found that CO_2 concentrations of surface waters influenced phytoplankton production in supersaturated lakes (Vogt et al., 2017). Jansson et al. (2012) also conducted their experiments in Scandinavian oligotrophic lakes, supersaturated with CO_2 and found that primary production was reduced 10-fold when bottles were aerated with ambient air.

The idea that pCO_2 can affect phytoplankton competition is not new (Raven & Johnston, 1991) but it is still unclear to what extent CO_2 might affect the community composition of lakes. Several studies were able to correctly predict competitive outcomes based on population growth rates in monoculture at different levels of pCO_2 (Ji et al., 2017; Low-Décarie et al., 2011; Verschoor et al., 2013). However, these studies make contrasting predictions about the effects of CO_2 enrichment on phytoplankton communities in general. Furthermore, a survey of boreal lakes found no relationship between pCO_2 and community composition (Vogt et al., 2017). Thus, it seems likely that there is no generalizable trend in terms of the effect of CO_2 on community composition. However, it is still possible that specific communities have predictable responses to CO_2 enrichment. For instance, in Lac Hertel, the relative biomass of chlorophytes increased in response to CO_2 enrichment in two consecutive experiments in September and October of 2012 (Low-Décarie et al., 2015).

We analyzed the effects of N and P enrichment, combined with pCO_2 manipulation on phytoplankton biomass (as chlorophyll *a*) and community composition across an annual cycle (June 2015 to May 2016) by conducting five *in situ* factorial mesocosm experiments in a temperate mesotrophic lake. The goal of the experiments was to determine how resource limitation, synergistic effects, and the response of the phytoplankton community varied throughout the seasons. We hypothesized that: (1) the effects of N, P and CO_2 addition would vary across the five experiments, such that different resources, or combinations of resources, would be limiting at different times of the year and that this variability would correlate with CO_2:TN:TP ratios in the control mesocosms; (2) the effect of CO_2 on biomass would consist of synergistic responses with other limiting factors; (3) even if CO_2 did not affect biomass, it would still promote changes in community composition, particularly a shift from cyanobacteria to chlorophytes whenever these species would be present, as seen in previous experiments at the study site (Low-Décarie et al., 2015). Additionally, we explored the effects of N and P enrichment treatments on chlorophytes, heterokonts (diatoms, dinoflagelates, chrysophytes), cyanobacteria, cryptophytes and the intensity of these treatment effects compared to those of seasonal change.

1.4 Methods

1.4.1 Study Site

The experiments were conducted on a platform floating on Lac Hertel in McGill University's Gault Nature Reserve, Mont-Saint-Hilaire, Quebec, Canada. Lac Hertel is a small, dimictic lake with a maximum depth of 8 m, a mean depth of 4.7 m and a surface area of 0.31 km^2 surrounded by forested hills (Rooney & Kalff, 2003). The lake is mesotrophic, with a mean total N concentration (TN) of 271 μg/L and total P concentration (TP) of 18 μg/L and is known to exhibit summer cyanobacterial blooms. The lake can be qualified as soft water, bordering on hard water, with summer alkalinity ranging from 0.48 to 0.66 meq/L (Hem, 1985; Kalff, 1972). We found comparable values by estimating ANC from pCO_2, pH and water temperature (Cole & Prairie, 2009).

1.4.2 Seasonal timing of experiments

In order to capture intra-annual variability in phytoplankton community responses, we conducted five separate experiments at different times of the year. This allowed us to prevent complications associated with running a year-long mesocosm experiment without compromising our ability to capture intra-annual variability. We associated each experiment with a step on the plankton ecology group model which describes seasonal succession of phytoplankton and zooplankton in temperate lakes (Sommer et al., 2012; Sommer et al., 1986). The July 2015 experiment was linked with mid-summer succession and started on July 6, 2015. The August 2015 experiment was associated with late summer succession typically characterized by cyanobacterial blooms and started on July 31, 2015. The October 2015 experiment started after the water column had mixed, an event typically associated with the onset of diatom dominance, on October 3, 2015. The April 2016 experiment started as soon as ice on the lake had melted around the dock, an event associated with the start of the phytoplankton spring bloom, on April 25, 2016. The June 2016 experiment, associated with the clear-water phase characterized by strong grazing started on May 26, 2016.

1.4.3 Mesocosms

The floating dock was located 30 m offshore, near the deepest part of the lake. For each experiment, twenty-four 2.0 m deep, ~1600 L mesocosms constructed from 0.15-mm-thick polyethylene tubes were sealed with a heat gun at one end and attached to 1 m wide metal rings fixed to the dock. The mesocosms were filled with unfiltered lake water via two electric centrifugal pumps submerged to a depth of 1 m one or two days prior to the start of each experiment. Locations of treatments across the array of mesocosms were randomized in each experiment. Previous experiments conducted on the mesocosm platform of Lac Hertel have been published by Thibodeau et al. (2015) and Low-Décarie et al. (2015).

1.4.4 Experiments

For each experiment, a full factorial design across two levels of N, P and CO_2 concentrations with three replicates was established (a total 24 mesocosms). Whereas controls for N and P enrichment remained at natural TN and TP concentrations, treatments were administered with pulses at the start of each experiment with the goal of increasing TN by 300 μg/L and TP by 20 μg/L. These values correspond approximately to a doubling of the mean TN and TP concentrations in the epilimnion of Lac Hertel and were deemed consistent with the magnitude of cultural eutrophication observed in natural systems. To enrich nitrogen, 3.401 g of KNO_3 was added to each mesocosm while controls each received 2.508 g of KCl to account for the addition of potassium (K) as it could potentially act as a limiting nutrient

(Talling, 2010). Note that the concentration of Cl added in the controls represents approximately 0.75mg/L (or 0.04 mmol/L), which is unlikely to significantly affect freshwater phytoplankton (Chakraborty et al., 2011; Reynoso & de Gamboa, 1982), nor their zooplanktonic predators (Gonçalves et al., 2007; Martínez-Jerónimo & Martínez-Jerónimo, 2007). To enrich phosphorus while maintaining a stable pH, 0.069 g of H_2KPO_4 and 0.088 g of HK_2PO_4 were added to each mesocosm while controls each received 0.113 g KCl. For CO_2, on the other hand, we opted to apply a press treatment, with the goal of keeping control mesocosms at current atmospheric levels, approximately 400 ppm (ESRL, 2005) and high-CO_2 mesocosms at expected atmospheric concentrations levels for the end of the century, around 1000 ppm (IPCC, 2013). Following the method described by (Low-Décarie et al., 2015), mesocosms were bubbled for 15 minutes every 1.5 hours with ambient air in controls and air enriched to a concentration of 4500 ppm CO_2 in treatments (Figure A1.1). This design allowed us to avoid any limiting effects of CO_2 drawdown by phytoplankton and instead focus on growth conditions of CO_2 at equilibrium with the atmosphere.

1.4.5 Measurements

Samples from each mesocosm and the surrounding lake were taken from surface waters in the mornings, between 8:30 and 11:00 am, two to three times a week. Bubbling was turned off for this period to prevent changes in water chemistry within a single sampling session. pCO_2 was measured using the headspace method (Cole & Prairie, 2009). In a 60 mL syringe, a 30 mL water sample was mixed with 30 mL of ambient air pulled in through Sofonolime (Molecular Products), which removes pCO_2. The air sample was then injected into an Infrared Gas Analyzer (IRGA, PP Systems). Aqueous pCO_2 was calculated from the equilibrated air sample, accounting for temperature and salinity. Physical measurements, including temperature, conductivity, and pH were measured using a YSI probe at 0.5 m depth. Total phosphorus (TP) and total nitrogen (TN) were taken from a depth of 0.5 to 1 m using a Kemmerer sampler with a valve. In under 5 hours, acid-washed test tubes were rinsed, filled with sample water, placed in a cooler with ice-packs, taken to a laboratory and stored in a 4°C refrigerator or in a -20°C freezer before they could be processed within the next 16 days or 75 days respectively. Following digestion with potassium persulfate and the addition of an ammonium molybdate solution, TP concentrations were measured using colorimetric detection with a spectrophotometer at 890 nm (Wetzel & Likens, 2000). TN concentrations were measured using a continuous flow analyzer (ALPKEM Flow Solution IV, OI Analytical, College Station, Texas, USA) using an alkaline persulfate digestion method, coupled with a cadmium reactor (Patton & Kryskalla, 2003). To characterize the phytoplankton community, reusable semi-transparent plastic 100 mL bottles were rinsed directly in the mesocosms, submerged upside-down and flipped underwater to be filled from a depth of ~0.3 m. Samples were immediately placed in a cooler to avoid direct sunlight exposure and, in the same day, transported to a laboratory and analyzed using a bench-top Fluoroprobe (bbe Moldaenke, GmbH) under default parameter settings, which are sufficient for estimating relative changes in biomass and community composition (Catherine et al., 2012). We use the term "chemotaxonomic" for this type of fluorometric identification, which relies on the presence of characteristic pigments (chemicals). Daily insolation data for Lac Hertel were obtained from the NASA Langley Research Center (LaRC) POWER Project funded through the NASA Earth Science/Applied Science Program.

1.4.6 Analysis

Values averaged across the two-week experimental period were analyzed because standing biomass, rather than changes in growth rates were the focus of these experiments and because chlorophyll concentration and taxonomic frequency did not change linearly (or monotonically) with time. In August 2015, all three replicates of the phosphorus and CO_2 treatment were removed from the analysis due to nitrogen contamination from an unknown source. Eleven other mesocosms, from a total of 120, were removed from the analysis after the discovery of holes in the polyethylene material (Table A1.1).

Chlorophyll *a* (Chl *a*) measurements were modeled as linear responses to responses to levels of nitrogen (two levels), phosphorus (two levels), CO_2 (two levels) and experiment (five levels) and all possible interactions. Chl *a* was log-transformed to stabilize the variance. The model was analyzed using Type II analysis of variance (ANOVA from car R package; Fox & Weisberg, 2011) which are unbiased by unbalanced data resulting from broken mesocosm bags. Interactions that were found to be significant at the $p<0.05$ level were analyzed further. We contrasted single-resource addition treatments with controls to determine if the resource was limiting at the $p<0.05$ level using the estimated marginal means from the model (emmean R package (Lenth, 2018)). Using the same package, synergistic effects (Eqn. 1.1) were calculated by first summing the effects of two resources added individually on the response scale and second, contrasting the result with the effect of combined resource addition on a log-scale in order to extract the percent difference. In Eqn. 1.1, R_i is the mean Chl *a* concentration in the treatment where resource *i* was added and C is the Chl *a* concentration in the control. We report effect size means and 95% confidence intervals (95% CI) calculated by assuming normality of log-transformed data.

$$Synergy = \frac{(R_{12} - C)}{(R_1 - C) + (R_2 - C)} \tag{1.1}$$

In order to determine if resource ratios could explain intra-annual differences in resource limitation, we modified the model described in the above paragraph. First, we removed the factor that distinguished between the five experiments. Next, we added three co-variates: the TN:TP ratio, insolation and water temperature. Initially, we had also considered the pCO2:TN ratio, but removed it from the model because the biomass response to CO2 addition did not vary between experiments (see Results – Chl a Responses). Each co-variate could interact with N, P and CO2 enrichment, but not with another co-variate. Then, we tested the statistical significance of each co-variate and its interactions using a Type II ANCOVA (Fox & Weisberg, 2011). Finally, we analyzed the slopes of the co-variates using the emmeans R package to understand how they controlled biomass responses (Lenth, 2018).

A similar strategy was used to assess the response of chlorophytes, although no log-transformation was needed. The effects of co-variates were not explored since we did not make any hypotheses to their regard. Instead of synergistic effects, pairwise contrasts were used to interpret significant simple effects and interactions found in the model (Lenth, 2018). The responses of chlorophytes, heterokonts, cyanobacteria and cryptophytes were then explored using a Type II multivariate analysis of variance (MANOVA) with the Roy statistic (Fox & Weisberg, 2011) and estimated marginal means (Lenth, 2018). We were forced to remove the August 2015 experiment from this analysis due to missing values mentioned above.

Additionally, to quantify the relative importance of resource availability compared to other factors governing seasonal succession, the Mann-Whitney U test was used to detect significant differences between two groups: 1) absolute differences between the mean of each treatment and its control (for each experiment and taxonomic group) and 2) absolute differences between the control means of each pair of successive experiments. Effect sizes and ranges were also reported for each group.

1.5 Results

1.5.1 Treatment Effectiveness

All our treatments achieved the expected changes in nutrients, including CO_2 concentration, between control and treatment mesocosms, although these changes varied between experiments (Figure 1.1a-c). We found that N-enrichment resulted in a mean total N increase of 213 ± 6 μg/L (± Std. Error; Figure 1.1a), P-enrichment in a mean total P increase of 17.4 ± 0.9 μg/L (Figure 1.1b), CO_2-enrichment in a mean CO_2 partial pressure increase of 1083 ± 41 ppm (Figure 1.1c) and a mean pH decrease of 0.39 ± 0.02 (Figure 1.1d). Additionally, we found that pCO_2 was drawn down to 50 ± 121 in July 2015, and to 86 ± 121 in August 2015, an aspect of CO_2 dynamics that was not reflected in our experimental approach (Figure 1.1c).

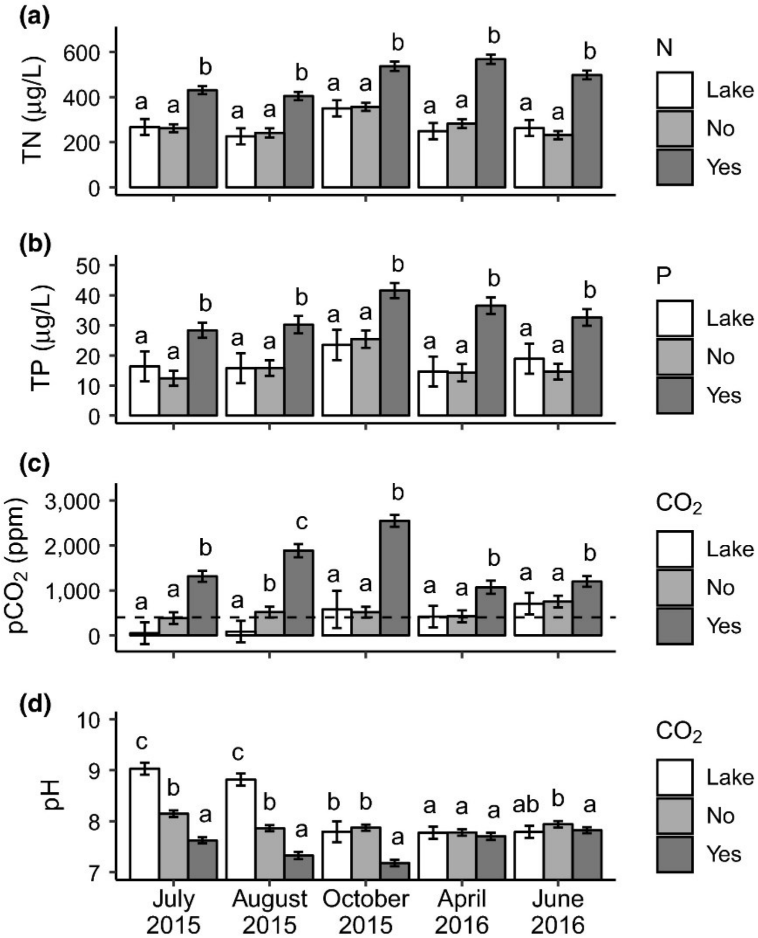

Figure 1.1: Treatment effects (shaded) in each replicate experiment compared to the control treatments (white) for a) P enrichment, b) N enrichment, c) CO_2 enrichment and d) the effect of CO_2 enrichment on pH. The dotted horizontal line in c) represents an average atmospheric pCO_2 of 400 ppm. Error bars represent 95% confidence limits around the estimated marginal means. For total phosphorus (TP) and total nitrogen (TN) enrichment, we had a goal of doubling lake concentrations. For CO_2, we had the goal of keeping controls at 400 ppm and treatments at 1000 ppm by intermittently bubbling with atmospheric air and atmospheric air enriched up to 4500 ppm respectively. Technical problems resulted in higher than expected pCO_2 in August and October 2015.

1.5.2 Chl a Responses

First, we found that the four-way interaction between the four independent variables was not significant (ANOVA: $F_{3,77}$=0.3, p=0.858). However, a significant three-way interaction between N, P and experiment was found (ANOVA: $F_{4,77}$=3.8, p=0.007), suggesting that the biomass responses to additions of N, P, and N with P varied between experiments (Figure

1.2). We did not find evidence of co-limitation by N and P in any of the experiments because N and P did not have independent effects on biomass (sensu essential interactive resources; Sperfeld et al 2016). Instead, we found N-limitation in July 2015, N-limitation with a synergistic effect of P in August 2015, no limitation in October 2015 and simultaneous limitation by N and P in April and June 2016 (Table 1.1).

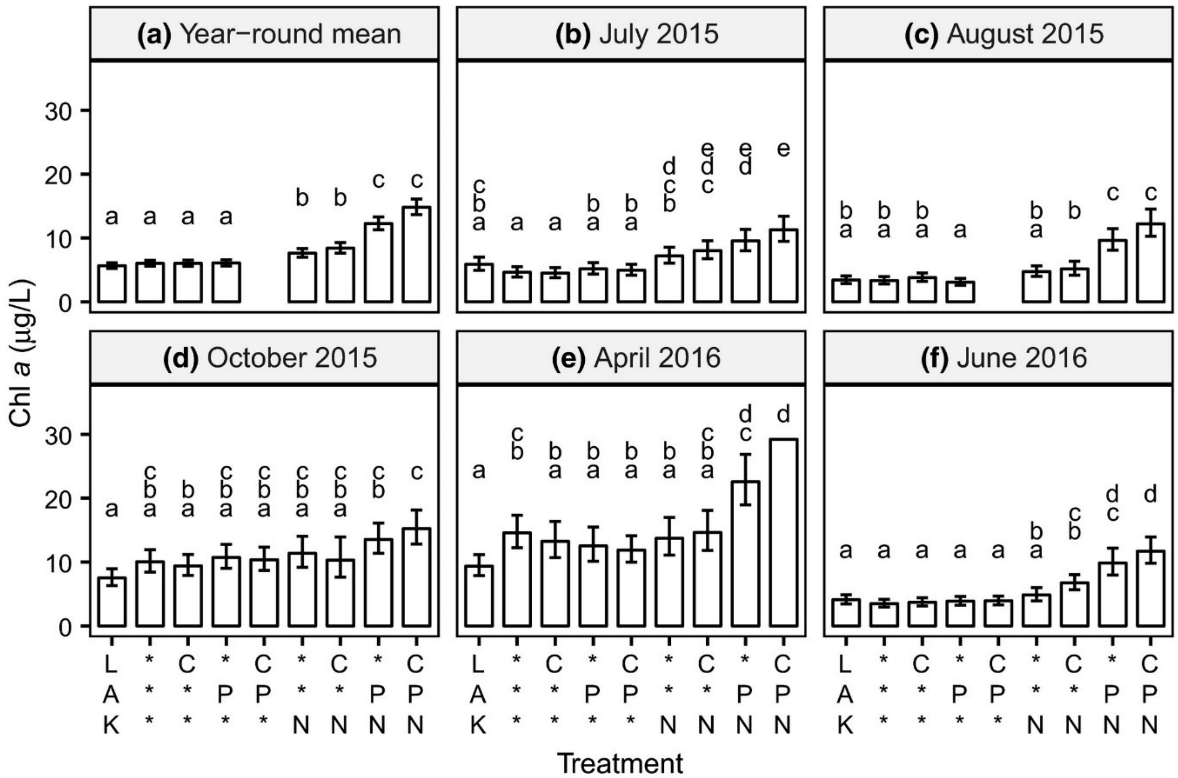

Figure 1.2: Model-estimated marginal means of the log total chlorophyll *a* (back-transformed to the response scale) in nitrogen (N), phosphorus (P) and CO_2 (C) treatments, controls (*) and in the Lake (LAK) on average (a) and per experiment (b-f). Error bars represent 95% confidence limits of the estimated marginal means. In each panel, letters represent groupings of treatments that were not significantly different from each other at the p<0.05 confidence level.

Second, we found an interaction between N and CO_2 (ANOVA: $F_{1,77}$=5.8, p=0.018). Across experiments, we found that CO_2 alone, or in combination with P, did not generate significant responses: -3% (95% CI: [-19%, 16%]) in both cases. However, it increased the effect of N addition from 23% (95% CI: [2%, 49%]) to 36% (95% CI: [12%, 66%]) in P-poor treatments (p=0.581) and from 81% (95% CI: [51%, 117%]) to 120% (95% CI: [80%, 160%]) in P-rich treatments (p=0.057). Across P treatments, the synergistic effect of CO_2 and N was 55% (95% CI: [6%, 128%]).

Table 1.1: N and P resource limitation across the five experiments. The effects of N, P, and N with P are percent increases in Chl *a* biomass relative to controls ("Incr."), with 95% confidence intervals ("CI") and p-values for their difference from zero ("p"). The synergistic effect is the percent difference between the effect of N with P and the sum of the effects of N and P separately. All the values are calculated in mesocosms at ambient CO_2 concentrations.

Experiment	Effect of N			Effect of P			Effect of N with P			Synergistic Effect			Limitation
	Incr.	CI	p	Incr.	CI	p	Incr.	CI	p	Incr.	CI	p	
June 2015	56	[010, 120]	0.008	12	[-021, 058]	0.823	106	[046, 192]	<0.001	58	[-025, 0230]	0.217	N-limitation
August 2015	43	[001, 102]	0.043	-07	[-034, 031]	0.938	189	[105, 309]	<0.001	435	[042, 1916]	0.015	Serial N, then P
October 2015	13	[-023, 067]	0.827	07	[-025, 051]	0.957	35	[-005, 091]	0.113	75	[-081, 1507]	0.612	No limitation
April 2016	-06	[-036, 039]	0.974	-14	[-042, 027]	0.717	55	[009, 119]	0.009				Simultaneous
June 2016	39	[-006, 104]	0.124	11	[-022, 057]	0.855	182	[092, 316]	<0.001	269	[029, 0958]	0.017	Simultaneous

We found that intra-annual variability in TN:TP ratios in control mesocosms could, in part, explain the intra-annual variability in the biomass responses to N and P additions. We found that three interactions were statistically significant: N, P and TN:TP ratios (ANOVA: $F_{1,71}$=10.8, p=0.002; Figure 1.3a); N, P and insolation (ANOVA: $F_{1,71}$=11.6, p=0.001; Figure 1.3b); N, P and water temperature (ANOVA: $F_{1,71}$=7.8, p=0.007; Figure 1.3c). We found that TN:TP ratios correlated positively with biomass in control mesocosms (p<0.001; Figure 1.3a), in mesocosms with N additions (p<0.001; Figure 1.3a), in mesocosms with P additions (p<0.001; Figure 1.3a), but not in mesocosms with combined N and P addition (p=0.893; Figure 1.3a). Instead, mesocosms with combined N and P addition appeared to be light limited, as their biomass correlated with insolation (p=0.076; Figure 1.3b). In contrast, the rest of the treatments had biomass values that correlated negatively with insolation (controls: p<0.001; N addition p=0.007; P addition p<0.001; Figure 1.3b).

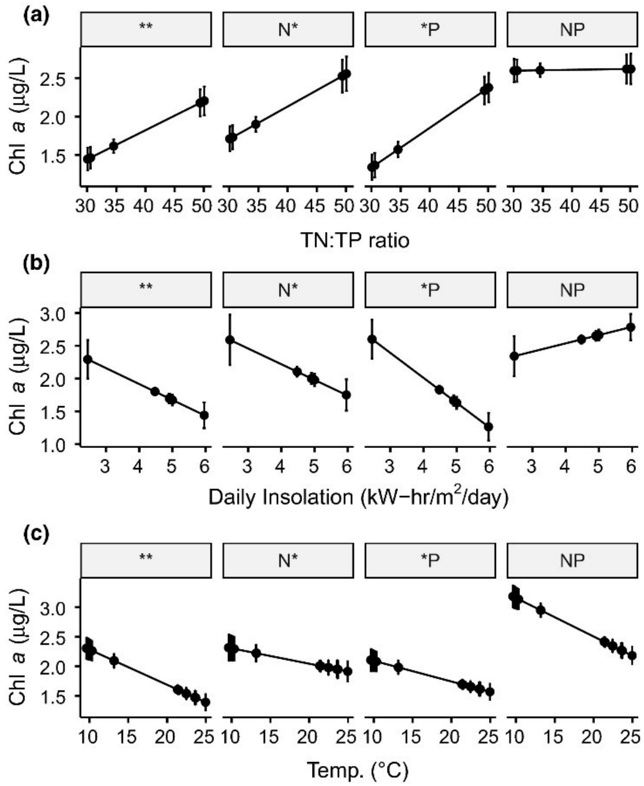

Figure 1.3: Model-estimated marginal means of different experimental treatments (Nitrogen, Phosphorus, and CO_2) as functions of (a) the mean TN:TP ratios in control mesocosms, (b) water temperature in each mesocosm and (c) average daily insolation across the duration of each experiment. For clarity, values are averaged over the two levels of the CO_2 treatment as its effects did not vary intra-annually (see text; Figure A1.2).

1.5.3 Community Composition Responses

Contrary to our hypothesis, we found that the effect of CO_2 on the chlorophyte community varied intra-annually and could depend on levels of P and N enrichment (ANOVA: $F_{4,70}$=1.4, p=0.253; Figure 1.4a). We found that in the October 2015 experiment, relative Chlorophyte density increased by 1.1% (95% CI: [-0.2%, 2.4%]) in response to CO_2 enrichment ANOVA: $F_{1,14}$=4.8, p=0.045). As hypothesized, this increase was accompanied by a decrease in cyanobacteria, although their relative density dropped by only 0.13% (95% CI: [-0.04%, 0.29%]; ANOVA: $F_{1,14}$=4.4, p=0.055). In the June 2015 experiment, we found that the treatments with added N, CO_2, but not P had 7.6% (95% CI: [0.4%, 14.7%]) more chlorophytes than the other treatments (ANOVA: $F_{1,16}=3$, p=0.101; Figure 1.4b). CO_2 did not affect chlorophyte relative abundance in any of the other experiments.

In the context of the community, we found that the interactive effects between N, P and CO_2 varied intra-annually (Roy's largest root=0.28, $F_{4,53}=3.7$, p=0.01). However, relative to natural succession, community composition was weakly affected by treatments (Figure 1.4; Mann-Whitney U test: p=0.0032). Whereas treatments generated a mean absolute effect size of 2.5 % (range: 0 to 14), changes between consecutive experiments resulted in a mean change of 14 % (range: 0 to 53).

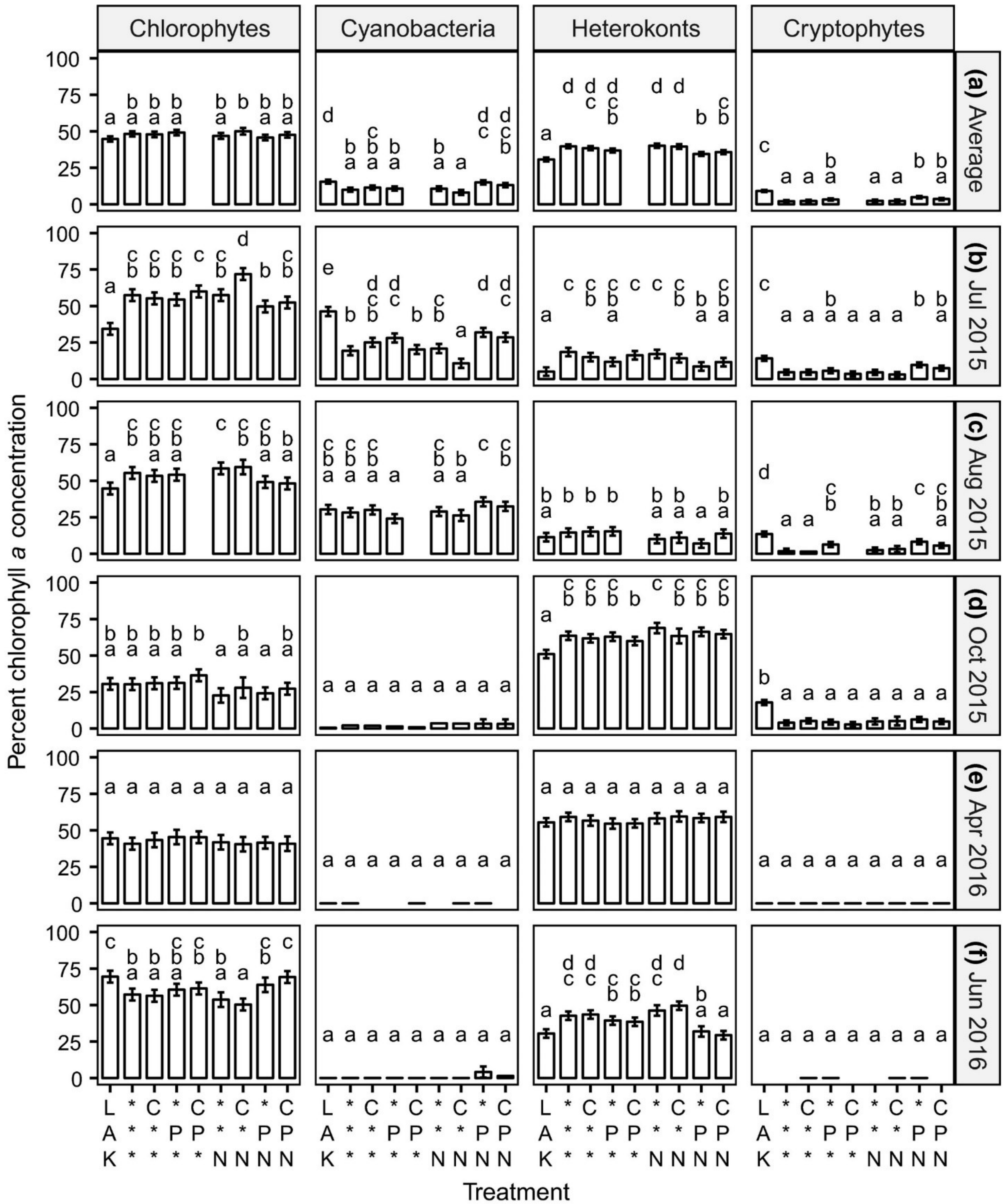

Figure 1.4: Model-estimated marginal means of relative densities of four taxonomic groups in treatments (N, P, C), controls (*) and the lake (LAK). See Figure 1.2 legend for details.

1.6 Discussion

The present study links to a large body of research that has used mesocosm and bioassay experiments to investigate (co-)limitation by nitrogen (N) and phosphorus (P) in temperate lakes (Harpole et al., 2011). Our study substantiates the discussion by adding a dimension of intra-annual variability, a third limiting resource (CO_2) and investigating the effects of resource addition on community composition. We found that: (1) the limiting, synergistic and community composition effects of N and P varied intra-annually; (2) the intra-annual variation of some effects of N and P addition on biomass could be predicted from TN:TP ratios, though solar irradiation and water temperature were also important factors; (3) although not limiting in and of itself, CO_2 had a synergistic effect with N addition that did not vary intra-annually; (4) the effect of CO_2 on community composition varied intra-annually and with N and P addition but was small when compared to the strong intra-annual patterns of phytoplankton community composition change. Below we discuss our main findings and evaluate the strength of inference derived from the series of mesocosm experiments.

1.6.1 Intra-annual variability of the effects of N and P

Although we found that TN:TP could not explain the response to either N or P additions, we did find that biomass responses were greater in response to combined N and P enrichment at low TN:TP ratios. This result suggests that overall, the lake is more strongly N-limited than P-limited, which is consistent with the measured biomass responses. However, this is not consistent with measurements in the central plains reservoirs of the USA which would suggest either co-limitation or P-limitation for the range of TN:TP ratios observed in Lac Hertel (Dzialowski et al., 2005). It is possible that measurements with higher concentrations of bioavailable resources, such as dissolved inorganic nitrogen and total dissolved phosphorus, may serve as better indicators of resource limitation (Maberly et al., 2002). Neither of these studies, however, report or explain the type of co-limitation (sensu Harpole et al., 2011). Furthermore, other factors such as temperature and light limitation were also found to affect biomass responses and should be considered.

We found that the strongest synergistic effect was in August, which is the time when resource limitation is expected to be most intense as streams run dry and the thermocline is fairly stable (Sommer et al., 1986). Three lacustrine studies, pulled from Elser (2007), that considered some form of intra-annual variability also found strongest synergistic effects in late summer (Bukaveckas & Crain, 2002; Maberly et al., 2002; Nydick et al., 2004). On the other hand, two other studies did not support this pattern, possibly due the indistinction between late summer and fall (Dzialowski et al., 2005), or due to oligotrophic conditions resulting in consistently strong resource limitation throughout the summer season (Nydick et al., 2003).

1.6.2 Multiple resource limitation – P and CO_2

We found several instances where N and P were simultaneous limiting, which according to most authors is evidence of co-limitation (e.g. Harpole et al., 2011). However, this result remains consistent with a single-resource limitation framework (sensu strictly essential resources (Sperfeld et al., 2016), as both resources could happen to be in equally low concentrations. In the August 2012 experiment, however, we found that although P was not limiting on its own, it had a positive synergistic effect with N. Similarly, CO_2 was not limiting but had a synergistic effect across experiments. Taken together, we find two independent synergistic effects of P and CO_2 with N. This suggests that under N-rich conditions, multiple resources are interactively essential, such that independent addition of either resource can result in increased phytoplankton biomass (sensu interactively essential resources (Sperfeld et al., 2016)). Whereas many studies have found that N and P are independently co-limiting (Harpole et al., 2011), this is the first time, to our knowledge, that CO_2 is categorized as such, suggesting that CO_2 can be one of the multiple limiting resources in freshwater ecosystems.

Few freshwater studies have looked at the effect of CO_2 on phytoplankton biomass (Hasler et al., 2016). Two previous mesocosm experiments in Lac Hertel have showed a synergistic effect of CO_2 with a large enrichment of commercial fertilizer containing N, P and other resources (Low-Décarie et al., 2015). Our study refines this result and demonstrates that it can be replicated even with moderate amounts of N enrichment. In another outdoor microcosm experiment with water taken from highly eutrophic Lake Taihu, CO_2 was found to increase biomass only in Spring, the only month when cyanobacteria were not dominating

(Shi et al., 2015). Cyanobacteria were not dominant in any of our experiments. However, certain cyanobacteria species have very efficient carbon uptake machinery (Tortell, 2000; Visser et al., 2016), so they may not have been limited even by the lowest CO_2 concentrations (270 ppm) to which they were exposed in the Shi et al. (2015) experiment. In line with our finding that CO_2 has no positive effect on biomass in nutrient-poor conditions, a study of 69 boreal, generally mesotrophic lakes (mean TN: 200±100 (±SD) µg/L, range: 100-600 µg/L) found no relationship between pCO_2 and Chl *a* in a multiple regression framework (Vogt et al., 2017). Jansson et al. (2012), on the other hand, found some strong effects on both primary production and biomass in response to reducing pCO_2 to ambient levels. However, they do not report the alkalinity of the lakes, which could be an important parameter in regulating the phytoplankton response via bicarbonate availability (Kragh & Sand-Jensen, 2018).

1.6.3 Community composition response to CO_2 enrichment

Based on previous predictions (Low-Décarie et al., 2014), competition assays (Low-Décarie et al., 2011) and mesocosm experiments in Lac Hertel (Low-Décarie et al., 2015), we expected that CO_2 should increase the frequency of chlorophytes relative to cyanobacteria in the phytoplankton community due to their generally weaker CO_2 uptake and binding efficiency (Tortell, 2000). In most experiments, we found that CO_2 had no effect on community composition, suggesting that coarse chemotaxonomic groups are unlikely to respond to CO_2 supersaturation. This is consistent with a survey of 69 boreal lakes which found no relationship between pCO_2 and community composition (Vogt et al., 2017). The efficiency of algal species and strains to fix carbon dioxide has been shown to be quite variable, even within the major groups (Low-Décarie et al., 2014; Maberly & Spence, 1983). Additionally, although bicarbonate use is usually less efficient than CO_2 (Hein, 1997; Moroney & Tolbert, 1985), certain species specialize in bicarbonate uptake and could be unaffected by changes in pCO_2 (Holland et al., 2012). Thus, intra-group variability seems to preclude generalized predictions based on major taxonomic groups.

On the other hand, our hypothesis was supported in two experiments: October 2015, with a ~2% increase in chlorophyte density, and June 2015, with a ~8% increase, though only in the N-rich, P-poor treatment. Previous experiments in Lac Hertel were also conducted in the autumn, consistent with the effect in October (Low-Décarie et al., 2015). Although the 2%

change in October was small, it might well represent a biologically meaningful result if one considers that acclimation to the altered conditions and biomass increase occurred over the relatively short experimental duration of 14 days. In June 2015, a complex interaction between resource concentrations shows that certain conditions, including high pCO_2, can lead to significant changes in community composition.

1.6.4 Limitation of the CO_2 treatment

Although the CO_2 press treatment provided a fair approximation of the current and predicted future atmospheric conditions (IPCC, 2013), it may have led to the underestimation of some of the effect sizes relative to the lake response. Essentially, the treatment did not account for seasonal pCO_2 fluctuations present in the lake (Figure 1.1). In the summer, for example, pCO_2 in the lake was near 50 ppm, whereas CO_2 controls were near 400 ppm. Thus, when added to the mesocosms, chlorophytes may have responded equally to both increases in pCO_2: from 50 ppm to 400 ppm in the controls and from 50 ppm to 1000 ppm in the treatments. The same could be said for Chl *a* in N-poor mesocosms. An alternative method would have been to periodically supplement treatment mesocosms with highly CO_2 supersaturated water and controls with untreated water (Paquette & Beisner, 2018). However, this method results in a series of pulses, contrary to what may be expected due to increasing atmospheric CO_2 and nutrient-rich treatments resulting in higher phytoplankton biomass would experience faster CO_2 drawdown than nutrient-poor treatments. Although this is an interesting interaction to study, the mesocosm design is likely to exacerbate CO_2 limitation given the wind-blocking effects of the mesocosm platform, likely leading to reduced gas exchange with the atmosphere.

1.6.5 Other Limitations

Our study has several other limitations. For example, our study does not distinguish between direct effects of nutrients on the phytoplankton community and indirect food web effects. Additionally, we cannot be certain that the responses observed in our mesocosm ecosystem are the same as those that would have transpired in the lake's natural pelagic ecosystem. Nevertheless, indirect food web effects are part of the lake's natural processes and by including these additional effects, we have a clearer picture of the net importance of our treatments on the phytoplankton community. Although mesocosms could affect observed responses, they provided us with the replication needed to run a factorial experiment while allowing for atmospheric gas exchange and longer duration compared to bottle experiments.

1.6.6 Conclusion

Our results reveal the intra-annual variability of limiting, synergistic and community composition effects of N and P. The intra-annual variability of biomass effects could be explained, in part, by TN:TP ratios, insolation, and water temperature. N alone or N with P were the more commonly limiting resources. Though CO_2 alone was not limiting, it had a synergistic effect with N across experiments. Furthermore, we found evidence of multiple resource limitation in N-rich treatments by CO_2 and P (Sperfeld et al., 2016). This is surprising given that at a pCO_2 of 400 ppm, one would not expect to see CO_2 limitation. We conclude that increased concentrations of CO_2 in eutrophic lakes could lead to further increases in biomass, at least in lakes of comparable alkalinity (soft water, bordering hardwater). Furthermore, our results suggest that pCO_2 can alter community composition at a coarse chemotaxonomic level in certain communities. We recommend that future research control for lower pCO_2 (e.g. 50 ppm) concentrations on phytoplankton communities to account for high CO_2 drawdown during periods of high phytoplankton biomass. Measuring species specific responses could also help us better understand community composition responses to changes in resource concentrations.

1.7 Acknowledgements

We thank the Natural Science and Engineering Research Council of Canada (NSERC), which funded both the Gault Mesocosm Facility and this work through grants to G.F.F. We thank Dr. Rene (Irene) Gregory-Eaves (McGill) and her laboratory, for feedback on the manuscript and for lending us a Fluoroprobe. Additional equipment was lent to us by the Gault Nature Reserve and the Centre de la Nature. We thank the summer interns (Marie-Claire Chiasson, Aurélie Hawes, Ashley Cameron, Andrea Cherry) and permanent staff (David Maneli, Charles Normandin, Sonya Tetrault, Christian Côté) of the Gault Nature Reserve, members of the McGill Outdoors Club mailing list, friends and family for help with sampling and the experimental set-up. We thank Katherine Velghe and Marilyne Robidoux (UQAM) for

nutrient sample processing. We thank Yves Prairie for sharing formulas for calculating pCO_2 and alkalinity.

1.8 Data Availability Statement

The data that support the findings of this study are openly available in Zenodo at http://doi.org/10.5281/zenodo.1318376, reference number 1318376.

1.9 Conflict of Interest Statement

The authors have no conflicts of interest to declare.

1.10 References

Allen, E. D., & Spence, D. H. N. (1981). The differential ability of aquatic plants to utilize the inorganic carbon supply in fresh waters. *New Phytologist, 87*(2), 269-283. doi:10.1111/j.1469-8137.1981.tb03198.x

de Baar, H. J. W. (1994). von Liebig's law of the minimum and plankton ecology (1899–1991). *Progress in Oceanography, 33*(4), 347-386. doi:10.1016/0079-6611(94)90022-1

Badger, M. R., Andrews, T. J., Whitney, S. M., Ludwig, M., Yellowlees, D. C., Leggat, W., & Price, G. D. (1998). The diversity and coevolution of Rubisco, plastids, pyrenoids, and chloroplast-based CO2-concentrating mechanisms in algae. *Canadian Journal of Botany, 76*(6), 1052-1071. doi:10.1139/b98-074

Badger, M. R., Kaplan, A., & Berry, J. A. (1980). Internal Inorganic Carbon Pool of *Chlamydomonas reinhardtii*: Evidence for a Carbon Dioxide-Concentrating Mechanism. *Plant Physiol, 66*(3), 407-413. doi:10.1104/pp.66.3.407

Bukaveckas, P. A., & Crain, A. S. (2002). Inter-annual, seasonal and spatial variability in nutrient limitation of phytoplankton production in a river impoundment. *Hydrobiologia, 481*(1), 19-31. doi:10.1023/A:1021388315552

Carpenter, S. R., Booth, E. G., & Kucharik, C. J. (2018). Extreme precipitation and phosphorus loads from two agricultural watersheds. *Limnology and Oceanography, 63*(3), 1221-1233. doi:10.1002/lno.10767

Catherine, A., Escoffier, N., Belhocine, A., Nasri, A. B., Hamlaoui, S., Yéprémian, C., . . . Troussellier, M. (2012). On the use of the FluoroProbe®, a phytoplankton quantification method based on fluorescence excitation spectra for large-scale surveys of lakes and reservoirs. *Water Research, 46*(6), 1771-1784. doi:10.1016/j.watres.2011.12.056

Chakraborty, P., Acharyya, T., Raghunadh Babu, P. V., & Bandyopadhyay, D. (2011). Impact of salinity and pH on phytoplankton communities in a tropical freshwater system: An investigation with pigment analysis by HPLC. *Journal of Environmental Monitoring*, 13(3), 614-620. doi:10.1039/C0EM00333F

Cole, J. J., & Prairie, Y. T. (2009). Dissolved CO2. In *G.E. Likens (ed.). Encyclopedia of Inland Waters*: Oxford: Elsevier.

Dzialowski, A. R., Wang, S.-H., Lim, N.-C., Spotts, W. W., & Huggins, D. G. (2005). Nutrient limitation of phytoplankton growth in central plains reservoirs, USA. *Journal of Plankton Research, 27*(6), 587-595. doi:10.1093/plankt/fbi034

Elser J.J., Bracken M.E.S., Cleland E.E., Gruner D.S., Harpole W.S., Hillebrand H., Ngai J.T., Seabloom E.W., Shurin J.B. & Smith J.E. (2007) Global analysis of nitrogen and phosphorus limitation of primary producers in freshwater, marine and terrestrial ecosystems. *Ecology Letters,* 10**,** 1135-1142.

ESRL, W. T. (2005). ESRL Global Monitoring Division-Global Greenhouse Gas Reference Network. Retrieved from https://www.esrl.noaa.gov/gmd/ccgg/trends/

Finlay, K., Vogt, R. J., Bogard, M. J., Wissel, B., Tutolo, B. M., Simpson, G. L., & Leavitt, P. R. (2015). Decrease in CO_2 efflux from northern hardwater lakes with increasing atmospheric warming. *Nature, 519*, 215. doi:10.1038/nature14172

Fox, J., & Weisberg, S. (2011). *An R companion to applied regression*: Sage Publications.

Gonçalves, A. M. M., Castro, B. B., Pardal, M. A., & Gonçalves, F. (2007). Salinity effects on survival and life history of two freshwater cladocerans (Daphnia magna and Daphnia longispina). *Annales de Limnologie - International Journal of Limnology., 43*(1), 13-20.

Goswami, S. R. (1971). Hydrologic Regime of Lake Hertel. *Journal (American Water Works Association), 63*(10), 671-675.

Hammer, K. J., Kragh, T., & Sand-Jensen, K. (2019). Inorganic carbon promotes photosynthesis, growth, and maximum biomass of phytoplankton in eutrophic water bodies. *Freshwater Biology, 64*(11), 1956-1970. doi:10.1111/fwb.13385

Harpole W.S., Ngai J.T., Cleland E.E., Seabloom E.W., Borer E.T., Bracken M.E.S., Elser J.J., Gruner D.S., Hillebrand H., Shurin J.B. & Smith J.E. (2011) Nutrient co-limitation of primary producer communities. *Ecology Letters,* 14**,** 852-862.

Hasler, C. T., Butman, D., Jeffrey, J. D., & Suski, C. D. (2016). Freshwater biota and rising pCO_2? *Ecology Letters, 19*(1), 98-108. doi:10.1111/ele.12549

Hein, M. (1997). Inorganic carbon limitation of photosynthesis in lake phytoplankton. *Freshwater Biology, 37*(3), 545-552. doi:10.1046/j.1365-2427.1997.00180.x

Hem, J. D. (1985). *Study and interpretation of the chemical characteristics of natural water* (U. G. Survey Ed. Third ed.).

Holland, D. P., Pantorno, A., Orr, P. T., Stojkovic, S., & Beardall, J. (2012). The impacts of a high CO2 environment on a bicarbonate user: The cyanobacterium *Cylindrospermopsis raciborskii*. *Water Research, 46*(5), 1430-1437. doi:10.1016/j.watres.2011.11.015

IPCC. (2013). Annex II: Climate System Scenario Tables. In: Working Group I Contribution to the IPCC Fifth Assessment Report (AR5), Climate Change 2013: The Physical Science Basis., 1395-1446.

Jansson, M., Karlsson, J., & Jonsson, A. (2012). Carbon dioxide supersaturation promotes primary production in lakes. *Ecology Letters, 15*(6), 527-532. doi:10.1111/j.1461-0248.2012.01762.x

Ji, X., Verspagen, J. M. H., Stomp, M., & Huisman, J. (2017). Competition between cyanobacteria and green algae at low versus elevated CO2: who will win, and why? *Journal of Experimental Botany, 68*(14), 3815-3828. doi:10.1093/jxb/erx027

Kalff, J. (1972). Net Plankton and Nanoplankton Production and Biomass in a Northern Temperate Zone Lake. *Limnology and Oceanography, 17*(5), 712-720. doi:10.4319/lo.1972.17.5.0712

Kaushal, S. S., Mayer, P. M., Vidon, P. G., Smith, R. M., Pennino, M. J., Newcomer, T. A., . . . Belt Kenneth, T. (2014). Land use and climate variability amplify carbon, nutrient, and contaminant pulses: A review with management implications. *Journal of the American Water Resources Association, 50*(3), 585-614. doi:10.1111/jawr.12204

Kragh, T., & Sand-Jensen, K. (2018). Carbon limitation of lake productivity. *Proceedings of the Royal Society B: Biological Sciences, 285*(1891), 20181415. doi:10.1098/rspb.2018.1415

Lenth, R. (2018). emmeans: Estimated Marginal Means, aka Least-Squares Means. Retrieved from https://CRAN.R-project.org/package=emmeans

Low-Décarie, E., Bell, G., & Fussmann, G. F. (2015). CO_2 alters community composition and response to nutrient enrichment of freshwater phytoplankton. *Oecologia, 177*(3), 875-883.

Low-Décarie, E., Fussmann, G. F., & Bell, G. (2011). The effect of elevated CO_2 on growth and competition in experimental phytoplankton communities. *Global Change Biology, 17*(8), 2525-2535. doi:10.1111/j.1365-2486.2011.02402.x

Low-Décarie, E., Fussmann, G. F., & Bell, G. (2014). Aquatic primary production in a high-CO_2 world. *Trends in ecology & evolution, 29*(4), 223-232.

Maberly, S. C., King, L., Dent, M. M., Jones, R. I., & Gibson, C. E. (2002). Nutrient limitation of phytoplankton and periphyton growth in upland lakes. *Freshwater Biology, 47*(11), 2136-2152. doi:10.1046/j.1365-2427.2002.00962.x

Maberly, S. C., & Spence, D. H. N. (1983). Photosynthetic inorganic carbon use by freshwater plants. *Journal of Ecology, 71*(3), 705-724. doi:10.2307/2259587

Martínez-Jerónimo, F., & Martínez-Jerónimo, L. (2007). Chronic effect of NaCl salinity on a freshwater strain of *Daphnia magna* Straus (Crustacea: Cladocera): A demographic study. *Ecotoxicology and Environmental Safety, 67*(3), 411-416. doi:10.1016/j.ecoenv.2006.08.009

Moroney, J. V., & Tolbert, N. E. (1985). Inorganic carbon uptake by *Chlamydomonas reinhardtii*. *Plant Physiol, 77*(2), 253-258. doi:10.1104/pp.77.2.253

Monod, J. (1950). Technique, theory and applications of continuous culture. *Ann. Inst. Pasteur, 79*(4), 390-410.

Nydick, K. R., Lafrancois, B. M., Baron, J. S., & Johnson, B. M. (2004). Nitrogen regulation of algal biomass, productivity, and composition in shallow mountain lakes, Snowy Range, Wyoming, USA. *Canadian Journal of Fisheries and Aquatic Sciences, 61*(7), 1256-1268. doi:10.1139/f04-085

Nydick, K. R., Moraska Lafrancois, B., Baron, J. S., & Johnson, B. M. (2003). Lake-specific responses to elevated atmospheric nitrogen deposition in the Colorado Rocky Mountains, U.S.A. *Hydrobiologia, 510*(1), 103-114. doi:10.1023/b:hydr.0000008636.13361.47

O'Neil, J. M., Davis, T. W., Burford, M. A., & Gobler, C. J. (2012). The rise of harmful cyanobacteria blooms: The potential roles of eutrophication and climate change. *Harmful Algae, 14*, 313-334. doi:10.1016/j.hal.2011.10.027

Pachauri, R. K., Allen, M. R., Barros, V. R., Broome, J., Cramer, W., Christ, R., . . . van Ypserle, J.-P. (2014). Climate Change 2014: Synthesis Report. Contribution of Working Groups I, II and III to the Fifth Assessment Report of the Intergovernmental Panel on Climate Change. Geneva, Switzerland: IPCC.

Paquette, C., & Beisner, B. E. (2018). Interaction effects of zooplankton and CO_2 on phytoplankton communities and the deep chlorophyll maximum. *Freshwater Biology, 63*(3), 278-292. doi:10.1111/fwb.13063

Patton, C. J., & Kryskalla, J. R. (2003). Methods of analysis by the U.S. Geological Survey National Water Quality Laboratory : evaluation of alkaline persulfate digestion as an alternative to Kjeldahl digestion for determination of total and dissolved nitrogen and phosphorus in water *Water-Resources Investigations Report*, 2003-4174. doi:10.3133/wri034174

Raven, J. A. & Johnston, A. M. (1991). Mechanisms of inorganic-carbon acquisition in marine phytoplankton and their implications for the use of other resources. *Limnology and Oceanography, 36*(8), 1701-1714. doi:10.4319/lo.1991.36.8.1701

Reynoso, G. T. & de Gamboa, B. A. (1982). Salt tolerance in the freshwater algae Chlamydomon as reinhardii: Effect of proline and taurine. *Comparative Biochemistry and Physiology Part A: Physiology, 73*(1), 95-99. doi:10.1016/0300-9629(82)90098-6

Rooney, N. & Kalff, J. (2003). Interactions among epilimnetic phosphorus, phytoplankton biomass and bacterioplankton metabolism in lakes of varying submerged macrophyte cover. *Hydrobiologia, 501*(1), 75-81. doi:10.1023/a:1026255302443

Schindler, D. W. (1977). Evolution of phosphorus limitation in lakes. *Science, 195*(4275), 260-262.

Schindler, D. W., Brunskill, G. J., Emerson, S., Broecker, W. S., & Peng, T.-H. (1972). Atmospheric carbon dioxide: Its role in maintaining phytoplankton standing crops. *Science, 177*(4055), 1192-1194. doi:10.1126/science.177.4055.1192

Schindler, D. W., Carpenter, S. R., Chapra, S. C., Hecky, R. E., & Orihel, D. M. (2016). Reducing phosphorus to curb lake eutrophication is a success. *Environmental Science & Technology, 50*(17), 8923-8929. doi:10.1021/acs.est.6b02204

Shi, X., Zhao, X., Zhang, M., Yang, Z., Xu, P., & Kong, F. (2015). The responses of phytoplankton communities to elevated CO_2 show seasonal variations in the highly eutrophic Lake Taihu. *Canadian Journal of Fisheries and Aquatic Sciences, 73*(5), 727-736. doi:10.1139/cjfas-2015-0151

Smith V.H. (1998) Cultural eutrophication of inland, estuarine, and coastal waters. In: *Successes, limitations, and frontiers in ecosystem science* pp. 7-49. Springer.

Sommer, U., Adrian, R., De Senerpont Domis, L., Elser, J. J., Gaedke, U., Ibelings, B., . . . Mooij, W. M. (2012). Beyond the Plankton Ecology Group (PEG) model: mechanisms driving plankton succession. *Annual Review of Ecology, Evolution, and Systematics, 43*, 429-448.

Sommer, U., Gliwicz, Z. M., Lampert, W., & Duncan, A. (1986). The PEG-model of seasonal succession of planktonic events in fresh waters. *Arch. Hydrobiol, 106*(4), 433-471.

Sperfeld, E., Martin-Creuzburg, D., & Wacker, A. (2012). Multiple resource limitation theory applied to herbivorous consumers: Liebig's minimum rule vs. interactive co-limitation. *Ecology Letters, 15*(2), 142-150. doi:10.1111/j.1461-0248.2011.01719.x

Sperfeld, E., Raubenheimer, D., & Wacker, A. (2016). Bridging factorial and gradient concepts of resource co-limitation: towards a general framework applied to consumers. *Ecology Letters, 19*(2), 201-215. doi:10.1111/ele.12554

Sterner, R. W., Elser, J. J., & Vitousek, P. (2002). *Ecological Stoichiometry: The Biology of Elements from Molecules to the Biosphere*. Princeton University Press.

Talling, J. F. (2010). Potassium — A non-limiting nutrient in fresh waters? *Freshwater Reviews, 3*(2), 97-104. doi:10.1608/FRJ-3.2.1

Thibodeau, G., Walsh, D. A., & Beisner, B. E. (2015). Rapid eco-evolutionary responses in perturbed phytoplankton communities. *Proceedings of the Royal Society B: Biological Sciences, 282*(1814). doi:10.1098/rspb.2015.1215

Tortell, P. D. (2000). Evolutionary and ecological perspectives on carbon acquisition in phytoplankton. *Limnology and Oceanography, 45*(3), 744-750. doi:10.4319/lo.2000.45.3.0744

Verschoor, A. M., Van Dijk, M. A., Huisman, J. E. F., & Van Donk, E. (2012). Elevated CO_2 concentrations affect the elemental stoichiometry and species composition of an experimental phytoplankton community. *Freshwater Biology, 58*(3), 597-611. doi:10.1111/j.1365-2427.2012.02833.x

Verspagen, J. M. H., Van de Waal, D. B., Finke, J. F., Visser, P. M., & Huisman, J. (2014a). Contrasting effects of rising CO2 on primary production and ecological stoichiometry at different nutrient levels. *Ecology Letters, 17*(8), 951-960. doi:10.1111/ele.12298

Verspagen, J. M. H., Van de Waal, D. B., Finke, J. F., Visser, P. M., Van Donk, E., & Huisman, J. (2014b). Rising CO_2 Levels Will Intensify Phytoplankton Blooms in Eutrophic and Hypertrophic Lakes. *PLOS ONE, 9*(8), e104325. doi:10.1371/journal.pone.0104325

Visser, P. M., Verspagen, J. M. H., Sandrini, G., Stal, L. J., Matthijs, H. C. P., Davis, T. W., . . . Huisman, J. (2016). How rising CO_2 and global warming may stimulate harmful cyanobacterial blooms. *Harmful Algae, 54*, 145-159. doi:10.1016/j.hal.2015.12.006

Vogt, R. J., St-Gelais, N. F., Bogard, M. J., Beisner, B. E., & del Giorgio, P. A. (2017). Surface water CO_2 concentration influences phytoplankton production but not community composition across boreal lakes. *Ecology Letters, 20*(11), 1395-1404. doi:10.1111/ele.12835

Wetzel, R., & Likens, G. (2000). Limnological Analyses. In: Springer, New York.

[dataset] Katkov, E. (2018). Dataset for Katkov et al. 2019: "Intra-annual variation in the response of phytoplankton to factorial manipulation of N, P and CO2 in a temperate mesotrophic lake". Zenodo. doi:10.5281/zenodo.1318376

2 Chapter 2: The Effect of Increasing Temperature and CO_2 on Experimental Pelagic Lake Communities

Egor Katkov[1], Gregor F. Fussmann[1]

[1] Department of Biology, McGill University, Montreal, Quebec, Canada H3A 1B1

2.1 Preamble

In Chapter 1, I found that, in a mesotrophic lake, increasing pCO_2 can affect (1) total phytoplankton biomass when other resources are added, namely nitrogen and phosphorus (2) phytoplankton community composition, albeit in different ways across the different intra-annual experiments. These findings indicate that anthropogenic changes, such as increased nutrient loading can cause CO_2 to become a co-limiting resource. Another important anthropogenic factor, caused by elevated atmospheric CO_2 itself, is increasing temperatures. However, no study, to our knowledge has considered the interactive effects of increasing temperatures and pCO_2 in phytoplankton assemblages in natural freshwater systems. In Chapter 2, I address this interaction to further understand the effects of increasing CO_2 on freshwater phytoplankton communities in the context of anthropogenic change. Although I find no evidence to support the existence of this interaction, both factors were found to have independent and even additive effects on biomass and community composition. Sampling efforts persisted twice per week over a period 41 day. As a result, the statistical models involve interaction between temperature increase, CO_2 enrichment, and the day since the start of experiment ("day," for short). When interpreting these models, it is important to focus on the highest-order interactions of statistical significance. When "day" was involved in such an interaction, this suggested that the effects of the other factor(s) involved in the interaction varied over the course of the experiment. An interaction involving both temperature and CO_2 would suggest that temperature modulates the effect of CO_2 on the response variable.

2.2 Abstract

As the global climate is changing, average water temperatures and the supply of CO_2 to water bodies are increasing. To determine how the effects of these changes on freshwater

communities will interact, we ran a month-long factorial mesocosm experiment, in which we manipulated water temperature and CO_2 concentrations. We found that while the phytoplankton community responded to the CO_2 and temperature treatments, no interactive effects were detected. Chlorophytes were strongly affected by temperature and CO_2, whereas heterokonts responded only to CO_2. At the end of the experiment, CO_2 had opposite effects on the two phytoplankton groups, resulting in no change in community biomass. CO_2 also affected seston C:N stoichiometry, though the experiment ended before we could observe any effects on the zooplankton community. However, we were able to detect a zooplankton community response to warming. We found that, in contrast to the effects of temperature, which can be explained based on temperature-dependent plankton growth curves, that responses of algal groups to pCO_2 were difficult to anticipate, despite the availability of system-specific priors. We conclude that species or strain-specific, or evolutionary responses may be important.

2.3 Introduction

Climate change is having major impacts on lake water temperatures around the world, but the ecological impacts of the many physical changes are not yet fully understood (Woolway *et al.*, 2020). Climate change is mainly caused by increasing levels of green house gasses in the atmosphere, primarily, CO_2, which cause increasing average global temperatures (IPCC, 2013). Many studies have investigated the effects of temperature and CO_2 on aquatic populations, communities and ecosystems, yet few have focused explicitly on the interaction of these two factors. The rise of the average temperatures of lakes worldwide is well documented (O'Reilly *et al.*, 2015), but less information is available on the long-term trends of partial pressure of carbon dioxide (pCO_2) in freshwaters. Because atmospheric CO_2 plays a role in controlling aquatic pCO_2 (Cole & Prairie, 2009) and other anthropogenic effects such as land use change can also cause aquatic pCO_2 to increase (Rebsdorf, Thyssen & Erlandsen, 1991; Gu, Xu & Li, 2022), it is reasonable to assume that temperature and pCO_2 simultaneously rise in many lakes.

Increasing temperatures are known to cause changes in phytoplankton and zooplankton community composition (Dupuis & Hann, 2009; Huisman *et al.*, 2018; da Silva, Torgan &

Schneck, 2019). In the most direct sense, maximum growth rates of populations are closely related to temperature for zooplankton (Gillooly, 2000) and phytoplankton (Paerl, Hall & Calandrino, 2011). Among the phytoplankton, cyanobacteria generally have the highest temperature for optimal growth, followed closely by chlorophytes, followed by dinoflagellates and finally diatoms (a class of heterokonts) (Paerl & Otten, 2013). Shifts in the phytoplankton community can also affect the zooplankton community; for example, increases in filamentous cyanobacteria can cause problems for the filtration apparatus of larger *Daphnia* species, whereas smaller species are less strongly affected (Gliwicz & Lampert, 1990; DeMott, Gulati & Van Donk, 2001; Huisman *et al.*, 2018).

Increasing atmospheric CO_2 can also result in increased growth rates, biomass and productivity of phytoplankton populations (Jansson, Karlsson & Jonsson, 2012; Low-Décarie, Bell & Fussmann, 2015; Shi *et al.*, 2015; Vogt *et al.*, 2017; Hamdan *et al.*, 2018; Katkov, Low-Décarie & Fussmann, 2020), though which specific groups benefit most strongly from this increase in CO_2 remains a topic for debate (Huisman *et al.*, 2018). Initial studies showed that cyanobacteria are generally able to take up CO_2 even when it is present at low concentrations (Shapiro, 1997). This led scientists to believe that green algae, or other eukaryotic phytoplankton species are better competitors at higher CO_2 concentrations (Shapiro, 1997; Low-Décarie, Fussmann & Bell, 2011; Low-Décarie *et al.*, 2015). Further studies found that increased CO_2 may have no effect at all on community composition (Vogt *et al.*, 2017), that there are seasonally varying effects on the competition between heterokonts and green algae (Katkov *et al.*, 2020) or alternatively, that cyanobacteria may, instead, benefit from increased CO_2 concentrations (Verspagen *et al.*, 2014; Ji *et al.*, 2020). Furthermore, increased CO_2 concentrations can cause phytoplankton to have higher proportions of carbon relative to nitrogen and phosphorus and have effects on algal fatty acid composition, which translates into reduced food quality for grazers (Urabe, Togari & Elser, 2003; Rossoll *et al.*, 2012; Schoo *et al.*, 2012; Meunier *et al.*, 2016). Finally, direct effects of CO_2 acidification can also slow growth rates of some zooplankton, though this effect is often weaker than indirect, food quality effects (Urabe *et al.*, 2003; Meunier *et al.*, 2016).

The interaction between temperature and CO_2, on the other hand, is much less studied. The best understood aspect of this interaction is the way in which temperature modulates the effects of differing food quality on zooplankton developmental rates. The three studies known to us found that temperature was an important modulator, but the specific relationship seemed to vary according to species (Persson *et al.*, 2010; Malzahn, Doerfler & Boersma, 2016; Garzke, Sommer & Ismar-Rebitz, 2020). Laboratory experiments with *Daphnia magna* found that decreasing food quality had a stronger impact on growth rates at higher temperatures (Persson *et al.*, 2010). In contrast, laboratory experiments with the calanoid copepod *Acartia tonsa* showed that decreasing food quality had stronger impacts at low temperatures (Malzahn *et al.*, 2016). A mesocosm experiment, also focused on *A. tonsa*, found that, in warm temperatures, increased pCO_2 promoted faster growth and developmental rates but greater mortality, while in colder temperatures, higher pCO_2 did not affect developmental rates but resulted in decreasing mortality rates (Garzke *et al.*, 2020).

To investigate the combined effects of increasing CO_2 and temperature on the phytoplankton and zooplankton communities, we conducted a mid-autumn mesocosm experiment in a mesotrophic lake. We chose the time of year because previous experiments performed at the same study site have shown significant effects of CO_2 on community composition at the same time of year (Low-Décarie *et al.*, 2015; Katkov *et al.*, 2020). We hypothesized that (1) chlorophyll a biomass (as a proxy for total phytoplankton biovolume) will increase as a result of both temperature and CO_2 increases, possibly in a synergistic manner; (2) independent of temperature, increasing pCO_2 will benefit chlorophytes, as in previous Fall experiments (Low-Décarie *et al.*, 2015; Katkov *et al.*, 2020); (3) independent of pCO_2, higher temperatures will benefit cyanobacteria and chlorophytes, possibly at the expense of heterokonts, as expected from the optimal temperature for maximal growth of each group (Paerl & Otten, 2013); (4) independent of temperature, food quality will decrease in response to increasing pCO_2 (measured as an increase in the seston carbon to nitrogen ratio) as expected from a number of laboratory experiments (Urabe *et al.*, 2003; Rossoll *et al.*, 2012; Schoo *et al.*, 2012; Meunier *et al.*, 2016); (5) the zooplankton community will be affected by temperature and CO_2 interactively, as a result of multiple drivers: direct species-specific effects of temperature on growth rates (Gliwicz & Lampert, 1990; DeMott *et al.*, 2001; Huisman *et al.*, 2018), indirect positive effects of temperature and CO_2 mediated by increased phytoplankton abundance, and indirect, and potentially interactive and species-specific negative effects caused by decreasing food quality (Persson *et al.*, 2010; Malzahn *et al.*, 2016; Garzke *et al.*, 2020).

2.4 Methods

2.4.1 Study Site

The study site was a floating platform located on Lac Hertel, Mont-Saint-Hilaire, Quebec, Canada. The platform was located 30 m offshore, near the deepest part of the lake. Lac Hertel is part of a UNESCO world heritage site, which compromises the Gault Nature Reserve, managed by McGill University; the watershed of the lake is primarily comprised of a hilly old-growth forest. The lake itself is dimictic, with a maximum depth of 8 m, a mean depth of 4.7 m and a surface area of 0.31 km^2 (Goswami, 1971; Rooney & Kalff, 2003). At the time of the experiment, we found that the average total phosphorus concentration near the surface of the lake was 24.9 μg L^{-1} and the total nitrogen concentration was 0.352 mg L^{-1}. Previous studies have qualified the lake as soft water, bordering on hard water, with summer alkalinity ranging from 0.48 to 0.66 meq/L (Kalff, 1972; Hem, 1985; Katkov *et al.*, 2020). Recently filled mesocosms were initially sampled on October 5th and 6th 2020 (days -2 and -1), the temperature treatment was first applied on October 7th 2020 (day 0) and the CO_2 treatments started on October 7th 2020 (day 1). The experiment ended on November 17th 2020 (day 41).

2.4.2 Mesocosms

The mesocosms were constructed from 165 gallon (246 L) vertical tanks (Norwesco Inc.) by sawing off the tops and adding 10 by 12 inch shelving brackets (Everbilt) to the tops of the tanks to prevent the mesocosms from escaping through the 1 m wide rings installed on the floating dock. The solid construction of the tanks (in lieu of polyethylene bags) was helpful to avoid the destruction of mesocosms by aquatic wildlife, to ensure a consistent water volume among tanks, and to reduce plastic pollution of the lake. The mesocosms were filled with unfiltered lake water from a depth of 1 m using a electric centrifugal pump.

2.4.3 Experimental design

The experiment consisted of 18 mesocosms, crossing two levels of temperature (ambient and heated) with three levels of CO_2 (low, medium and high), with three replicates. We aimed to generate a temperature difference of 2-3 °C, and pCO_2 levels of 250, 400 and 1000 ppm. Mesocosms assigned the heated level were heated using a 300 W aquarium heater (Eheim) and those assigned the ambient level were not. All mesocosms were bubbled with atmospheric air with altered levels of pCO_2 for 2 minutes per hour during the day, and for 2 minutes every two hours between 10 pm and 4 am. Bubbling was achieved by pumping air through weighted perforated placed inside each mesocosm and connected by weighted "Tornado" tubing (CanadianPond.ca; (Low-Décarie *et al.*, 2015)) to an air distribution network constructed with 1/2 inch polyethylene tubing inside the mesocosm platform. The low-CO_2 air was filtered through 2 L of soda lime (Fauna Marin Skim Breeze) to make it below ambient concentrations, medium-CO_2 air was untreated, and high-CO_2 air was enriched to 4500 ppm using pressurized CO_2.

2.4.4 Measurements

Twice per week, water temperature, pH, specific conductance and dissolved oxygen data were collected (in the mesocosms and in the lake close to the mesocosm platform) at a depth of 0.5 m using a YSI probe between 9 and 11 am. Simultaneously, samples for estimation of pCO_2 and phytoplankton communities were collected. Dissolved CO_2 was measured using the headspace method (Cole & Prairie, 2009). In summary, inside a sealed syringe, 30 mL of lake water were mixed with 30 mL of atmospheric air stripped of CO_2 with a soda lime column (Molecular Products). After equilibration, the air sample was injected into an infra-red gas analyser (IRGA, PP Systems). Dissolved CO_2 was then calculated from the pCO_2 of the air sample measured by the gas analyser. Water samples for phytoplankton analysis were collected in 30 mL polyethylene tubes covered in electric tape to avoid exposure to sunlight and kept in a cool environment. In the afternoon, they were analysed using a bench-top Fluoroprobe (bbe Moldaenke, GmbH) using default parameter settings to characterize the chlorophyll a biomass and the chemotaxonomic community composition (green algae, heterokonts and cyanobacteria) in a dark room.

Three times over the course of the experiment, zooplankton and nutrient samples were collected. We concentrated the zooplankton in ethanol by filtering 11 L of mesocosm water through a 30 μm mesh sieve. The filtered water was placed back into the mesocosm. All cladocerans and rotifers in 10% of each sample were identified and counted using a Nikon SMZ800 dissecting microscope, and a Nikon Eclipse TE2000-S inverted microscope (Thorp & Covich, 2001; Hudson & Lesko, 2003; Haney *et al.*, 2013) (species list: Suppl. Table A2.1). For each mesocosm, duplicate 40 mL samples were collected, in acid-washed glass tubes, for total and dissolved phosphorus and nitrogen. Total fractions did not require any filtration, while dissolved fractions were filtered through a GF/F filter using a manual syringe with a re-usable filter holder attachment. The filters were preserved for analysis of the particulate stoichiometry. Following digestion with potassium persulfate and the addition of an ammonium molybdate solution, total phosphorus concentrations were measured using colorimetric detection with a spectrophotometer at 890 nm (Wetzel & Likens, 2000). Total nitrogen concentrations were measured using a continuous flow analyser (ALPKEM Flow Solution IV, OI Analytical, College Station, Texas, USA) using an alkaline per-sulfate digestion method, coupled with a cadmium reactor (Patton & Kryskalla, 2003). Relative carbon and nitrogen concentrations of each GF/F filter were determined using a Carlo Erba 2500 elemental analyser.

2.4.5 Analysis

For measurements taken twice per week (temperature, pCO_2, chlorophyll a, phytoplankton community composition), a linear mixed model was fitted to simple and interactive effects of CO_2 treatment, temperature treatment and the day since the start of the experiment with each individual mesocosm as a random factor using the R package lme4 1.1.23 (Bates *et al.*, 2015). Note that we considered the day since the start of the experiment to be a factor, in order to capture responses that were non-linear with time. Using the fitted model, ANOVA statistics with p-values were calculated using the R package lmerTest 3.1.3 (Kuznetsova, Brockhoff & Christensen, 2017). For factors, or interactions between factors that were found to be significant ($p<0.05$), differences between the estimated marginal means of the model were used to determine which treatments were significantly different from each other ($p<0.05$) using the R package emmeans 1.6.0 (Lenth, 2021). If the interactions included the day since the start of the experiment, the comparisons were made separately for each day, and the days on which the effects were significant were reported.

For univariate measurements taken three times over the course of the experiment (e.g., seston stoichiometry), for each date, a linear model was fitted, with simple and interactive effects of temperature and CO_2 treatments as predictors. As for the mixed models, after calculating the ANOVA statistics for each model fit, significant factors ($p<0.05$) were analysed further by comparing estimated marginal means.

To detect shifts in the zooplankton community, we ran a redundancy analysis (RDA) on Hellinger-transformed community data with Temperature and CO_2 treatments as constraining variables for each of the three sampling dates using the R package vegan 2.5.7 (Oksanen *et al.*, 2020). For each RDA, we calculated an ANOVA table to determine which factors had a significant effect on the zooplankton community composition. All analyses were performed in R version 3.6.3 (2020-02-29).

2.5 Results

2.5.1 Treatment Effectiveness

Overall, we found that the CO_2 and temperature treatments were effective and near-independent of each other. On average, across all days, high-CO_2 treatments had, mean (±SEM) pCO_2 concentrations of 2038 ppm (±108), medium-CO_2 treatments had 677 ppm (±17) and the low-CO_2 treatments had 426 ppm (±12) (Figure 2.1a). The absolute CO_2 values attained in each treatment level were slightly higher than our target values but the differences among treatment levels were as expected and significant for nearly every sample date of the experiment. The temperature in unheated mesocosms was, on average, 9.2 °C (±0.3), while the temperature in heated mesocosms was 11.9 °C (±0.3) (Figure 2.1b). Over the course of the experiment, temperatures decreased, but remained significantly different between temperature treatments across nearly all days. Contrary to our expectations, pH was not affected by the CO_2 treatment (Suppl. Fig. A2.1). This could be attributed to low conductivity of the lake water (Suppl. Fig. A2.2h), which makes pH measurement less accurate (Busenberg & Plummer, 1987) but was not accounted for during sampling. Additionally, because CO_2 dissolves more effectively in cold water, pCO_2 concentrations were slightly higher in colder mesocosms, though this effect was significant at only one of ten sampling dates (Figure 2.1a). On day 15, the CO_2 treatments had a significant effect on temperature (Figure 2.1b), which can be explained by a single heater which became unplugged and caused average temperatures to drop in one of the the medium CO_2 mesocosms. The heater was immediately plugged back in, and the treatment was rapidly restored.

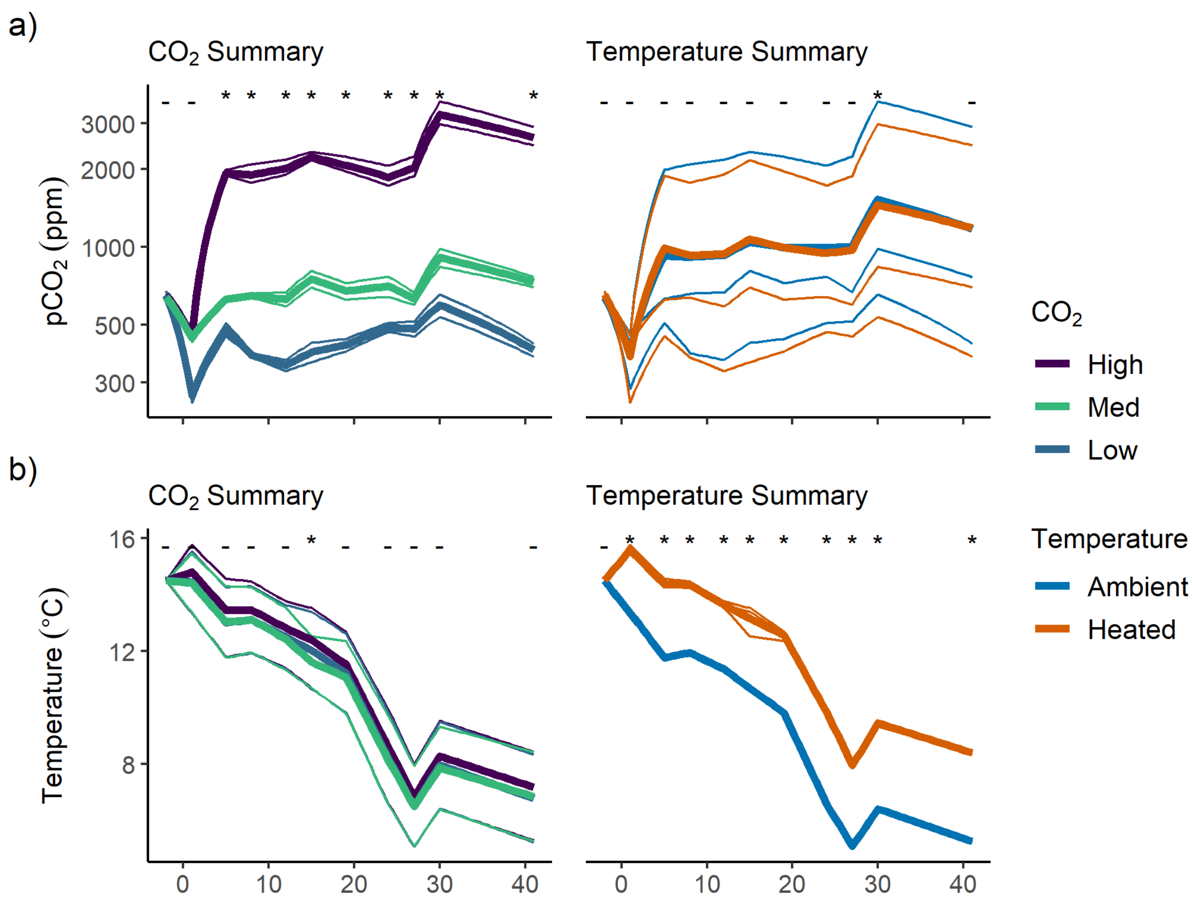

Figure 2.1: The effect of treatments on (a) pCO_2 and (b) temperature (y-axis) over time, expressed as the day since the start of the experiment (x-axis) in the mesocosms. In the "CO_2 Summary" panel, all lines are coloured by CO_2 treatment (see legend), thick lines represent averages of different CO_2 treatments regardless of temperature treatment, thin lines represent averages for each CO_2 and temperature combination, the "*" symbol represents days where at least one significant difference ($p=0.05$) between different CO_2 treatments were found (see text for details), and the "-" symbol represents days where no significant differences ($p>0.05$) between different CO_2 treatments were found. Note that no sampling events took place between days 31 and 41. The interpretation for the "Temperature Summary" panel is analogous to the "CO_2 Summary," but for temperature instead of CO_2 treatments. Overall, we find that both treatments had the desired effects. For a comparison with the lake, see Suppl. Fig. A2.2.

2.5.2 Phytoplankton community

We found that total chlorophyll a (measured as a proxy for phytoplankton biomass) was controlled by the independent effects of CO_2 and temperature, both of which varied by date (CO_2:Day ANOVA: $F_{20,107}=1.8$, $p<0.05$; Temperature:Day ANOVA: $F_{10,107}=4.5$, $p<0.001$; CO_2:Temperature:Day ANOVA: $F_{20,107}=0.7$, $p=0.86$; Figure 2.2a). We found a significant difference between low and high pCO_2 mesocosms on days 19, 24, and 27 of the experiment, whereas temperature caused chlorophyll a to significantly increase on days 24 and 30. See Tables A2.5.1.1 & A2.5.1.2 for contrasts.

The biomass of green algae was found to be affected by heating and, independently, CO_2 concentrations, though both effects varied according to the date (CO_2:Day ANOVA: $F_{20,107}=2.5$, $p<0.01$; Temperature:Day ANOVA: $F_{10,107}=11.2$, $p<0.001$; CO_2:Temperature:Day ANOVA: $F_{20,107}=0.7$, $p=0.8$; Figure 2.2b). On day 5, heating had a negative effect on green algal biomass, whereas on days 24, 27, 30, and 41, the effect was positive. The effect of CO_2 was more complex: on day 19, we found a significantly higher green algae biomass in high and medium CO_2 mesocosms, compared to low CO_2 mesocosms. On the other hand, on day 41, we found significantly lower green algae biomass in the high and medium pCO_2 mesocosms, compared to the low pCO_2 mesocosms. See Tables A2.5.2.1 & A2.5.2.2 for contrasts.

The biomass of heterokonts were found to be principally controlled by the CO_2 treatment, though the effect varied by day (CO_2:Day ANOVA: $F_{20,107}=3.1$, $p<0.001$; Temperature:Day ANOVA: $F_{10,107}=1.7$, $p=0.085$; CO_2:Temperature:Day ANOVA: $F_{20,107}=0.6$, $p=0.9$; Figure 2.2c). On days 19, 24, 27, 30, and 41, we found significantly higher biomass of heterokonts in the high versus the low pCO_2 mesocosms. See Tables A2.5.3.1 & A2.5.3.2 for contrasts.

Cyanobacteria, which comprised a much smaller proportion of the phytoplankton community by mid and late Fall, were also affected by temperature on certain days (CO_2:Day ANOVA: $F_{20,108}=0.3$, $p=1$; Temperature:Day ANOVA: $F_{10,108}=2.3$, $p<0.05$; CO_2:Temperature:Day ANOVA: $F_{20,108}=1.2$, $p=0.3$; Figure 2.2d). Cyanobacteria biomass was significantly higher in heated mesocosms on days 5 and 12. See Tables A2.5.4.1 & A2.5.4.2 for contrasts.

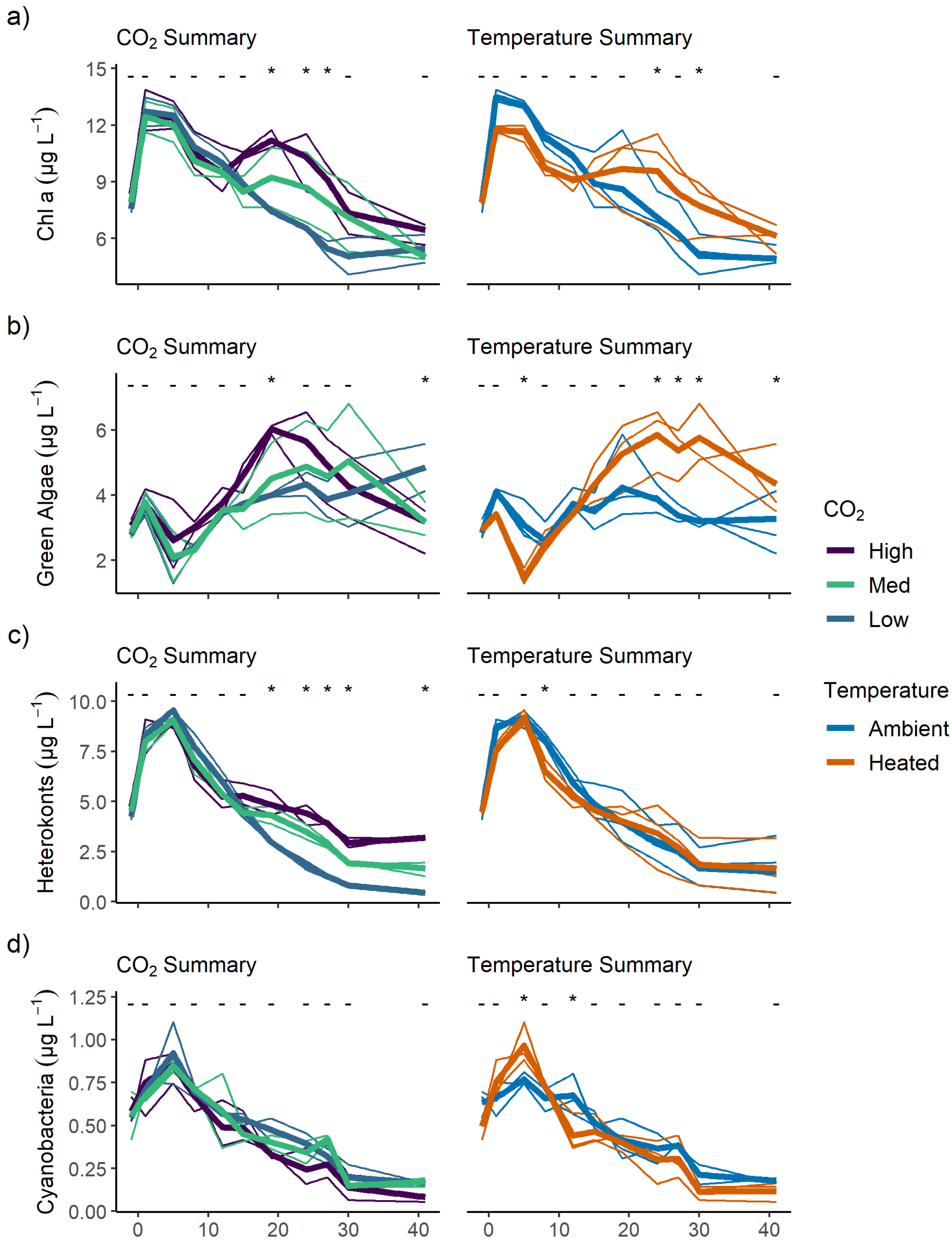
a)
b)
c)
d)
CO2 Summary
Temperature Summary
Chl a (μg L−1)
Green Algae (μg L−1)
Heterokonts (μg L−1)
Cyanobacteria (μg L−1)
CO2
High
Med
Low
Temperature
Ambient
Heated

Figure 2.2: Average (a) total chlorophyll a, and chlorophyll a contained in (b) green algae, (c) heterokonts, and (d) cyanobacteria as measured by the Floroprobe over the course of the experiment. For details about the meaning of the lines and symbols in each panel, see Figure 2.1 caption. For a comparison with the lake, see Suppl. Fig. A2.2. For a visualization of the treatment effects on relative densities of green algae, heterokonts, and cyanobacteria, see Suppl. Fig. A2.3.

2.5.3 Seston stoichiometry

We found some support for our hypothesis that the seston stoichiometry was affected by the CO_2 supply. Prior to the application of treatments, and mid-way through the experiment (day 19), the ratio of particulate C:N in mesocosms was not significantly affected by either treatment or their interaction. On the third (and last) sampling (day 31), on the other hand, we found that CO_2 had a significant effect on the seston C:N ratio (ANOVA: $F_{2,10}=17.6$, $p<0.001$), with a increase of 15 % in the high pCO_2 relative to low pCO_2 treatments ($p=0.0019$; Figure 2.3).

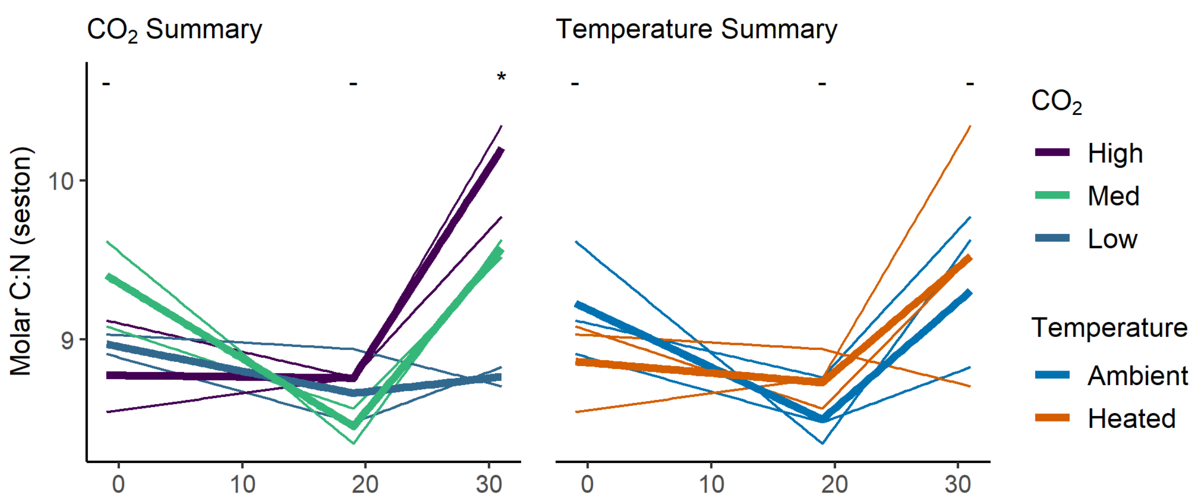

Figure 2.3: Molar C:N ratios of seston in the mesocosms (y-axis) over the course of the experiment (x-axis). For details about the meaning of the lines and symbols in each panel, see Figure 2.1 caption. For a comparison with the lake, see Suppl. Fig. A2.2.

2.5.4 Zooplankton community

Throughout the experiment, we found 13 distinct rotifer species, one of which was present in colonial and individual forms, 13 distinct crustacean species, copepodites, and nauplii, for a total of 29 taxa of zooplankton. Of these groups, only three rotifer species (*Keratella cochlearis*, *Polyarthra vulgaris* and *Ploesoma truncatum*), one cladoceran species (*Bosmina longirostris*), copepodites, and nauplii were present in all mesocosms on all three sampling dates. We found that temperature had a significant effect on the zooplankton community on the 15th day of the experiment ($p<0.05$), though this effect mostly dissipated by the next sampling date, on the 31st day of the experiment (Figure 2.4). *Bosmina longirostris* was positively associated with the heated temperature treatment, whereas *Polyarthra vulgaris* was associated with colder temperatures. None of the 27 other categories showed any statistically significant responses to the temperature treatment. Furthermore, CO_2 treatments had no statistically significant effects on the zooplankton community.

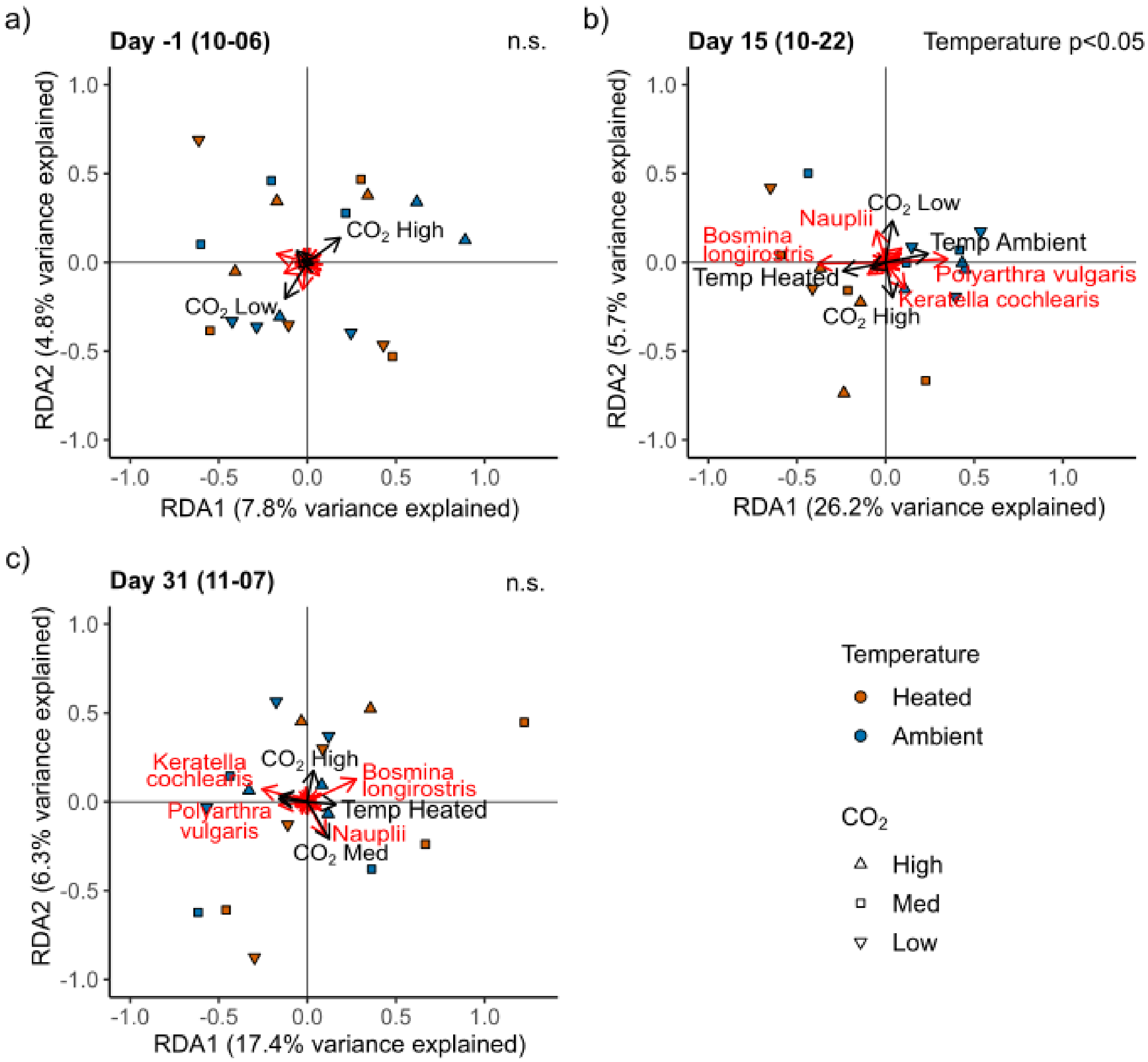

Figure 2.4: Redundancy analysis biplots for each of the dates when zooplankton were sampled (a-c). At the top right corner of each plot, we include statistically significant effects of experimental treatments on the community for that date (n.s. = no significant effects). Each point on the plot represents a mesocosm, where the color indicates the temperature and the shape the CO_2 treatment (see legend). The black text and arrows represent treatments and their associated scores, whereas red text and arrows represent categories of zooplankton and scores, respectivley.

2.6 Discussion

We found that CO_2 and temperature increases had independent effects on the phytoplankton community, though the effect was not consistent across all the days of the experiment. On days where CO_2 influenced community biomass, the effect was positive. This result is slightly surprising, because previous experiments in Lac Hertel concluded that increased nutrient addition was essential for CO_2 to have a positive effect on biomass (Low-Décarie *et al.*, 2015; Katkov *et al.*, 2020). It is possible that, because we used a model that allowed us to test the effect for each sampling date, we were able to detect transient effects that could have been missed in previous studies. Additionally, in contrast to Low-Décarie *et al.* (2015) and Katkov *et al.* (2020), this study featured a low pCO_2 treatment, intended to mimic pre-industrial levels of atmospheric pCO_2, which is involved in most of the significant CO_2 effects. Nevertheless, several studies have found that primary production and chlorophyll a biomass correlate with pCO_2 (Jansson *et al.*, 2012; Shi *et al.*, 2015; Vogt *et al.*, 2017; Hamdan *et al.*, 2018). The temperature effect, when present, also had a positive effect on community biomass as would be expected from the relationship between water temperatures and plankton population growth rates, which is positive unless temperatures become very high (Paerl *et al.*, 2011).

In our experiment, we did not observe synergistic interaction effects between the CO_2 and temperature treatments. The evidence from previous, marine studies is ambiguous. A microcosm study investigating a North Atlantic spring bloom community did find that, increased temperature and pCO_2 had a synergistic effect on chlorophyll *a* biomass (Feng *et al.*, 2009). However, a similar study found that pCO_2 and temperature had different effects at two different sites of the Bering Sea: a deep-water site and a one in the middle of a continental shelf (Hare *et al.*, 2007). A synergistic effect on chlorophyll *a* was observed at the offshore site, whereas, at the shelf site, increased temperature, pCO_2 and the combination of both all had comparable negative effects on chlorophyll *a* (Hare *et al.*, 2007). Adding to the puzzle is a third microcosm experiment in the South China Sea which showed that, although the chlorophyll *a* response to increased temperature was positive, this effect was countered by high pCO_2 conditions at both a near-shore and an off-shore site (Gao *et al.*, 2017). To our knowledge, no such studies were conducted in freshwater systems. But evidence from in marine systems suggests that the response of chlorophyll *a* to changing temperature and CO_2 appears to be highly system-specific, and likely depends on the community composition (Gao *et al.*, 2012). Additionally, we found that in one instance (sampling day 24), the positive effect of increasing CO_2 and temperature co-occurred on the same day, meaning that independent, additive effects should be considered.

In terms of phytoplankton community composition, we were surprised to find that increasing pCO_2 did not have a consistent positive effect on chlorophyte biomass as reported in previous experiments in Lac Hertel (Low-Décarie *et al.*, 2015; Katkov *et al.*, 2020). Only on two sampling days we observed a significant effect on chlorophytes, one with a positive, and another with a negative effect of pCO_2. Instead of chlorophytes, heterokonts benefited more strongly from increasing pCO_2 in the second half of the experiment (Figure 2.2b-d & Suppl. Fig. A2.3). This also contrasts with several marine studies which found shifts away from heterokonts in response to rising pCO_2 or acidification (Hare *et al.*, 2007; Petrou *et al.*, 2019). In our experiment, however, we did not find a significant impact of pCO_2 on pH (Suppl. Fig. A2.1), though small effects may have been missed because the readings were taken in cold, low salinity water. Regardless, some studies also found that communities can shift towards heterokonts in response to high pCO_2, or no shift at all (Kim *et al.*, 2006; Katkov *et al.*, 2020). Another study also reported that growth rates of different strains of the marine coccolithophore *Emiliania huxleyi* responded differently to changes in carbonate chemistry (Langer *et al.*, 2009). Thus, it seems likley that species- and strain-specific responses to changing pCO_2 (and concomitant acidification) might be responsible for the inconsistencies that we and others encountered when it comes to predicting community composition shifts among broader algal taxonomic groups.

In terms of temperature, we found that cyanobacteria, which represented a small fraction of the community, initially benefited from the warming treatment, though seasonally decreasing temperatures over the course of the experiment likely prevent their proliferation. This finding supports the idea that climate change is likely to prolong and exacerbate cyanobacterial blooms (Huisman *et al.*, 2018). Chlorophytes also benefited from increased temperature in the second half of the experiment. The initial heating, however, appeared to have a brief negative effect, possibly due to the shock caused by a rapid temperature change.

Overall, chlorophytes tend to have higher growth rates at warmer temperatures, which can explain this response (Paerl *et al.*, 2011). Heating, had no effect on heterokonts which, taken with the positive effects on chlorophytes and cyanobacteria, resulted in a net community biomass increase.

We found that C:N ratios of the seston increased in response to increasing pCO_2 concentrations. The effect only became apparent between days 15 and 31 of the experiment, which suggests a slow response in our *in-situ* experiment compared to incubation experiments that observed the same effect after five days or fewer (Burkhardt, Zondervan & Riebesell, 1999; Losh, Morel & Hopkinson, 2012). Population growth rates in our mesocosms might have been low due to resource limitation (the incubation experiments were supplemented with nutrients while our experiment was not), and this might have delayed the trickling down of carbon enrichment to seston stoichiometry. Alternatively, it is possible that nitrogen must become limiting before C:N ratio can increase (Healey & Hendzel, 1979; Guildford & Hecky, 2000; Stoyneva-Gärtner *et al.*, 2020). Regardless of the mechanism, the slow C:N response could explain why pCO_2 did not have a significant effect on the zooplankton community via food quality effects (Meunier *et al.*, 2016).

Indeed, the zooplankton community was only affected by temperature, not CO_2. Interestingly, temperature had an effect on day 15 after the start of the experiment, but this effect seemed to have mostly dissipated by day 31. While the cladoceran *Bosmina longirostris*, benefited from the heated treatment, the rotifer *Polyarthra vulgaris* had higher counts at ambient temperature. This finding is consistent with previous findings with regards to the effect of temperature on these two species. Though we are not aware of any studies focused specifically on the effects of temperature on *Bosmina longirostris*, another cladoceran, *Daphnia rosea* was found to have an optimal filtering rate at 20 °C (Burns & Rigler, 1967). In contrast, the growth rate of *Polyarthra vulgaris* appears to peak at lower temperatures, between 10 and 20 °C, and possibly as low as 5 °C (Buikema, Miller & Yongue, 1978).

In conclusion, we highlight that CO_2 can have opposing effects on different algal groups, resulting in changes in community composition but not community biomass. In contrast to temperature, CO_2 does not have a consistent effect on algal groups and we suggest that future research investigate species-specific responses. Although we did not find any evidence of interactive effects of temperature and CO_2, either for phytoplankton, or zooplankton, we found that additive effects are possible. Furthermore, we encourage further mesocosm studies to explore this interaction in different seasons, systems, and on longer time frames to have a better chance of capturing the indirect effects of phytoplankton biomass and food quality on higher trophic levels.

2.7 Acknowledgements

We thank Hilal Pilavci and Tina Le for their hard work and dedication to help develop and construct a mesocosm system that, we hope, will help future researchers keep plastic pollution out of Lac Hertel. We thank Hilal Pilavci, Julia Kossakowski, and Isabel Fernandez-McAuley for their invaluable help with the tedious work of preparing the nutrient and the concentrated zooplankton samples. We thank Michelle Gros for the challenging work of counting the zooplankton in each of our samples. We thank Étienne Low-Décarie for many helpful comments, suggestions, and discussions about this manuscript.

2.8 References

Bates D., Mächler M., Bolker B. & Walker S. (2015). Fitting Linear Mixed-Effects Models Using lme4. *Journal of Statistical Software* **67**. https://doi.org/10.18637/jss.v067.i01

Buikema A.L., Miller J.D. & Yongue W.H. (1978). Effects of algae and protozoans on the dynamics of *Polyarthra vulgaris*. *SIL Proceedings, 1922-2010* **20**, 2395–2399. https://doi.org/10.1080/03680770.1977.11896885

Burkhardt S., Zondervan I. & Riebesell U. (1999). Effect of CO_2 concentration on C:N:P ratio in marine phytoplankton: A species comparison. *Limnology and Oceanography* **44**, 683–690. https://doi.org/10.4319/lo.1999.44.3.0683

Burns C.W. & Rigler F.H. (1967). Comparison of Filtering Rates of *Daphnia Rosea* in Lake Water and in Suspensions of Yeast. *Limnology and Oceanography* **12**, 492–502. https://doi.org/10.4319/lo.1967.12.3.0492

Busenberg E. & Plummer L.N. (1987). *pH measurement of low-conductivity waters*. US Geological Survey.

Cole J.J. & Prairie Y.T. (2009). Dissolved CO_2. Oxford: Elsevier.

da Silva C.F.M., Torgan L.C. & Schneck F. (2019). Temperature and surface runoff affect the community of periphytic diatoms and have distinct effects on functional groups: evidence of a mesocosms experiment. *Hydrobiologia* **839**, 37–50. https://doi.org/10.1007/s10750-019-03992-6

DeMott W.R., Gulati R.D. & Van Donk E. (2001). Daphnia food limitation in three hypereutrophic Dutch lakes: Evidence for exclusion of large-bodied species by interfering filaments of cyanobacteria. *Limnology and Oceanography* **46**, 2054–2060. https://doi.org/10.4319/lo.2001.46.8.2054

Dupuis A.P. & Hann B.J. (2009). Warm spring and summer water temperatures in small eutrophic lakes of the Canadian prairies: potential implications for phytoplankton and zooplankton. *Journal of Plankton Research* **31**, 489–502. https://doi.org/10.1093/plankt/fbp001

Feng Y., Hare C., Leblanc K., Rose J., Zhang Y., DiTullio G., *et al.* (2009). Effects of increased pCO_2 and temperature on the North Atlantic spring bloom. I. The phytoplankton community and biogeochemical response. *Marine Ecology Progress Series* **388**, 13–25. https://doi.org/10.3354/meps08133

Gao G., Jin P., Liu N., Li F., Tong S., Hutchins D.A., *et al.* (2017). The acclimation process of phytoplankton biomass, carbon fixation and respiration to the combined effects of elevated temperature and pCO_2 in the northern South China Sea. *Marine Pollution Bulletin* **118**, 213–220. https://doi.org/10.1016/j.marpolbul.2017.02.063

Gao K., Xu J., Gao G., Li Y., Hutchins D.A., Huang B., *et al.* (2012). Rising CO_2 and increased light exposure synergistically reduce marine primary productivity. *Nature Climate Change* **2**, 519–523. https://doi.org/10.1038/nclimate1507

Garzke J., Sommer U. & Ismar-Rebitz S.M.H. (2020). Zooplankton growth and survival differentially respond to interactive warming and acidification effects. *Journal of Plankton Research* **42**, 189–202. https://doi.org/10.1093/plankt/fbaa005

Gillooly J.F. (2000). Effect of body size and temperature on generation time in zooplankton. *Journal of Plankton Research* **22**, 241–251. https://doi.org/10.1093/plankt/22.2.241

Gliwicz Z.M. & Lampert W. (1990). Food Thresholds in Daphnia Species in the Absence and Presence of Blue-Green Filaments. *Ecology* **71**, 691–702. https://doi.org/10.2307/1940323

Goswami S.R. (1971). Hydrologic regime of lake hertel. *Journal (American Water Works Association)* **63**, 671–675

Gu S., Xu Y.J. & Li S. (2022). Unravelling the spatiotemporal variation of pCO_2 in low order streams: Linkages to land use and stream order. *Science of The Total Environment* **820**, 153226. https://doi.org/10.1016/j.scitotenv.2022.153226

Guildford S.J. & Hecky R.E. (2000). Total nitrogen, total phosphorus, and nutrient limitation in lakes and oceans: Is there a common relationship? *Limnology and Oceanography* **45**, 1213–1223. https://doi.org/10.4319/lo.2000.45.6.1213

Hamdan M., Byström P., Hotchkiss E.R., Al-Haidarey M.J., Ask J. & Karlsson J. (2018). Carbon dioxide stimulates lake primary production. *Scientific Reports* **8**. https://doi.org/10.1038/s41598-018-29166-3

Haney J., Aliberti M., Allan E., Allard S., Bauer D., Beagen W., *et al.* (2013). An image-based key to the zooplankton of north america. *University of New Hampshire Center for Freshwater Biology*

Hare C., Leblanc K., DiTullio G., Kudela R., Zhang Y., Lee P., *et al.* (2007). Consequences of increased temperature and CO_2 for phytoplankton community structure in the Bering Sea. *Marine Ecology Progress Series* **352**, 9–16. https://doi.org/10.3354/meps07182

Healey F.P. & Hendzel L.L. (1979). Indicators of Phosphorus and Nitrogen Deficiency in Five Algae in Culture. *Journal of the Fisheries Research Board of Canada* **36**, 1364–1369. https://doi.org/10.1139/f79-195

Hem J.D. (1985). *Study and interpretation of the chemical characteristics of natural water*, Third.

Hudson P.L. & Lesko L.T. (2003). Free-living and parasitic copepods of the laurentian great lakes: Keys and details on individual species. *US Geological Survey, Great Lakes Science Center, Ann Arbor, Michigan.*

Huisman J., Codd G.A., Paerl H.W., Ibelings B.W., Verspagen J.M.H. & Visser P.M. (2018). Cyanobacterial blooms. *Nature Reviews Microbiology* **16**, 471–483. https://doi.org/10.1038/s41579-018-0040-1

IPCC (2013). Summary for policymakers. (Eds T.F. Stocker, D. Qin, G.-K. Plattner, M. Tignor, S.K. Allen, J. Boschung, et al.), p. 130. Cambridge University Press, Cambridge, United Kingdom; New York, NY, USA.

Jansson M., Karlsson J. & Jonsson A. (2012). Carbon dioxide supersaturation promotes primary production in lakes. *Ecology Letters* **15**, 527–532. https://doi.org/10.1111/j.1461-0248.2012.01762.x

Ji X., Verspagen J.M.H., Van de Waal D.B., Rost B. & Huisman J. (2020). Phenotypic plasticity of carbon fixation stimulates cyanobacterial blooms at elevated CO_2. *Science Advances* **6**, eaax2926. https://doi.org/10.1126/sciadv.aax2926

Kalff J. (1972). Net plankton and nanoplankton production and biomass in a northern temperate zone lake. *Limnology and Oceanography* **17**, 712–720. https://doi.org/10.4319/lo.1972.17.5.0712

Katkov E., Low-Décarie É. & Fussmann G.F. (2020). Intra-annual variation of phytoplankton community responses to factorial N, P, and CO_2 enrichment in a temperate mesotrophic lake. *Freshwater Biology* **65**, 960–970. https://doi.org/https://doi.org/10.1111/fwb.13482

Kim J.-M., Lee K., Shin K., Kang J.-H., Lee H.-W., Kim M., *et al.* (2006). The effect of seawater CO_2 concentration on growth of a natural phytoplankton assemblage in a controlled mesocosm experiment. *Limnology and Oceanography* **51**, 1629–1636. https://doi.org/10.4319/lo.2006.51.4.1629

Kuznetsova A., Brockhoff P.B. & Christensen R.H.B. (2017). lmerTest Package: Tests in Linear Mixed Effects Models. *Journal of Statistical Software* **82**. https://doi.org/10.18637/jss.v082.i13

Langer G., Nehrke G., Probert I., Ly J. & Ziveri P. (2009). Strain-specific responses of *Emiliania huxleyi* to changing seawater carbonate chemistry. *Biogeosciences* **6**, 2637–2646. https://doi.org/10.5194/bg-6-2637-2009

Lenth R.V. (2021). *Emmeans: Estimated marginal means, aka least-squares means*.

Losh J., Morel F. & Hopkinson B. (2012). Modest increase in the C:N ratio of N-limited phytoplankton in the California Current in response to high CO_2. *Marine Ecology Progress Series* **468**, 31–42. https://doi.org/10.3354/meps09981

Low-Décarie E., Bell G. & Fussmann G.F. (2015). CO_2 alters community composition and response to nutrient enrichment of freshwater phytoplankton. *Oecologia* **177**, 875–883

Low-Décarie E., Fussmann G.F. & Bell G. (2011). The effect of elevated CO_2 on growth and competition in experimental phytoplankton communities. *Global Change Biology* **17**, 2525–2535. https://doi.org/10.1111/j.1365-2486.2011.02402.x

Malzahn A.M., Doerfler D. & Boersma M. (2016). Junk food gets healthier when it's warm. *Limnology and Oceanography* **61**, 1677–1685. https://doi.org/10.1002/lno.10330

Meunier C.L., Algueró-Muñiz M., Horn H.G., Lange J.A.F. & Boersma M. (2016). Direct and indirect effects of near-future pCO_2 levels on zooplankton dynamics. *Marine and Freshwater Research* **68**, 373–380. https://doi.org/10.1071/MF15296

O'Reilly C.M., Sharma S., Gray D.K., Hampton S.E., Read J.S., Rowley R.J., *et al.* (2015). Rapid and highly variable warming of lake surface waters around the globe. *Geophysical Research Letters* **42**. https://doi.org/10.1002/2015gl066235

Oksanen J., Blanchet F.G., Friendly M., Kindt R., Legendre P., McGlinn D., *et al.* (2020). *Vegan: Community ecology package*.

Paerl H.W., Hall N.S. & Calandrino E.S. (2011). Controlling harmful cyanobacterial blooms in a world experiencing anthropogenic and climatic-induced change. *Science of The Total Environment* **409**, 1739–1745. https://doi.org/10.1016/j.scitotenv.2011.02.001

Paerl H.W. & Otten T.G. (2013). Harmful Cyanobacterial Blooms: Causes, Consequences, and Controls. *Microbial Ecology* **65**, 995–1010. https://doi.org/10.1007/s00248-012-0159-y

Patton C.J. & Kryskalla J.R. (2003). *Methods of analysis by the u.s. Geological survey national water quality laboratory : Evaluation of alkaline persulfate digestion as an alternative to kjeldahl digestion for determination of total and dissolved nitrogen and phosphorus in water*.

Persson J., Wojewodzic M.W., Hessen D.O. & Andersen T. (2010). Increased risk of phosphorus limitation at higher temperatures for Daphnia magna. *Oecologia* **165**, 123–129. https://doi.org/10.1007/s00442-010-1756-4

Petrou K., Baker K.G., Nielsen D.A., Hancock A.M., Schulz K.G. & Davidson A.T. (2019). Acidification diminishes diatom silica production in the Southern Ocean. *Nature Climate Change* **9**, 781–786. https://doi.org/10.1038/s41558-019-0557-y

Rebsdorf A., Thyssen N. & Erlandsen M. (1991). Regional and temporal variation in pH, alkalinity and carbon dioxide in Danish streams, related to soil type and land use. *Freshwater Biology* **25**, 419–435. https://doi.org/10.1111/j.1365-2427.1991.tb01386.x

Rooney N. & Kalff J. (2003). Interactions among epilimnetic phosphorus, phytoplankton biomass and bacterioplankton metabolism in lakes of varying submerged macrophyte cover. *Hydrobiologia* **501**, 75–81. https://doi.org/10.1023/a:1026255302443

Rossoll D., Bermúdez R., Hauss H., Schulz K.G., Riebesell U., Sommer U., *et al.* (2012). Ocean Acidification-Induced Food Quality Deterioration Constrains Trophic Transfer. *PLoS ONE* **7**, e34737. https://doi.org/10.1371/journal.pone.0034737

Schoo K.L., Malzahn A.M., Krause E. & Boersma M. (2012). Increased carbon dioxide availability alters phytoplankton stoichiometry and affects carbon cycling and growth of a marine planktonic herbivore. *Marine Biology* **160**, 2145–2155. https://doi.org/10.1007/s00227-012-2121-4

Shapiro J. (1997). The role of carbon dioxide in the initiation and maintenance of blue-green dominance in lakes. *Freshwater Biology* **37**, 307–323. https://doi.org/10.1046/j.1365-2427.1997.00164.x

Shi X., Zhao X., Zhang M., Yang Z., Xu P. & Kong F. (2015). The responses of phytoplankton communities to elevated CO_2 show seasonal variations in the highly eutrophic lake taihu. *Canadian Journal of Fisheries and Aquatic Sciences* **73**, 727–736. https://doi.org/10.1139/cjfas-2015-0151

Stoyneva-Gärtner M.P., Morana C., Borges A.V., Okello W., Bouillon S., Deirmendjian L., *et al.* (2020). Diversity and ecology of phytoplankton in Lake Edward (East Africa): Present status and long-term changes. *Journal of Great Lakes Research* **46**, 741–751. https://doi.org/10.1016/j.jglr.2020.01.003

Thorp J.H. & Covich A.P. (2001). *Ecology and classification of north american freshwater invertebrates*. Elsevier.

Urabe J., Togari J. & Elser J.J. (2003). Stoichiometric impacts of increased carbon dioxide on a planktonic herbivore. *Global Change Biology* **9**, 818–825. https://doi.org/10.1046/j.1365-2486.2003.00634.x

Verspagen J.M.H., Van de Waal D.B., Finke J.F., Visser P.M., Van Donk E. & Huisman J. (2014). Rising CO_2 levels will intensify phytoplankton blooms in eutrophic and hypertrophic lakes. *PLOS ONE* **9**, e104325. https://doi.org/10.1371/journal.pone.0104325

Vogt R.J., St-Gelais N.F., Bogard M.J., Beisner B.E. & del Giorgio P.A. (2017). Surface water CO_2 concentration influences phytoplankton production but not community composition across boreal lakes. *Ecology Letters* **20**, 1395–1404. https://doi.org/10.1111/ele.12835

Wetzel R.G. & Likens G.E. (2000). *Limnological analyses*. Springer New York.

Woolway R.I., Kraemer B.M., Lenters J.D., Merchant C.J., O'Reilly C.M. & Sharma S. (2020). Global lake responses to climate change. *Nature Reviews Earth & Environment* **1**, 388–403. https://doi.org/10.1038/s43017-020-0067-5

3 Chapter 3: Predicting Long-Term Evolutionary Responses of Phytoplankton to Rising CO_2 Concentrations

Egor Katkov[1], Gregor Fussmann[1], Jef Huisman[2], Jolanda M.H. Verspagen[2]

[1] Department of Biology, McGill University, Montreal, Canada.

[2] Department of Freshwater and Marine Ecology, Institute for Biodiversity and Ecosystem Dynamics, University of Amsterdam, Amsterdam, The Netherlands.

3.1 Preamble

In Chapters 1 and 2, I focused on the ecological effects of increasing pCO_2 on semi-natural phytoplankton communities. However, ecological changes are often associated with evolution and changing fitness landscapes. In Chapter 3, I address how evolution can alter the effects of increasing atmospheric CO_2 on phytoplankton populations and communities using modelling and computer simulations. I find that evolution can change how competition might play out when populations are competing for dissolved inorganic carbon. Model simulations that allow phytoplankton populations to evolve also predicted slightly higher phytoplankton biomass than simulations that only incorporate ecological mechanisms.

3.2 Abstract

One of the most pressing scientific questions is to what extent species can adapt to global change, yet theoretical work in this research domain remains limited. Here, we investigate evolutionary adaptation of phytoplankton to rising CO_2. Phytoplankton can assimilate both CO_2 and bicarbonate (HCO_3^-) into their biomass but display considerable intra- and interspecific variation in their carbon uptake kinetics. These kinetics can evolve to maximize fitness by a trade-off between the ability to take up more inorganic carbon at high concentration and the ability to efficiently assimilate inorganic carbon at low concentration. We consider two species: a CO_2 specialist that only uses CO_2, and a generalist that uses both CO_2 and HCO_3^-. We show that evolutionary adaptation alters the carbon uptake kinetics of both species and can change the outcome of competition between the CO_2 specialist and the generalist. We found that evolution favoured the generalist in environments with high HCO_3^- concentrations. Simulations across a range of atmospheric CO_2 concentrations predicted that

evolution was effective at increasing phytoplankton biomass in response to increasing atmospheric CO_2, especially in those cases where potential benefits from evolutionary adaptation of the carbon uptake kinetics were high, e.g., for generalist species in low alkaline waters with low HCO_3^- concentrations.

3.3 Introduction

Species across the tree of life are confronted with resource limitation, leading to competition between species requiring the same essential resources (Hutchinson, 1961; Tilman, 1977, 1982; Chesson, 2000). Consequently, resource competition is likely an important evolutionary driver for organisms, though conclusive evidence remains limited (Dykhuizen, 1990; Grant, 1999; Adamec, 2010; Simmons & Altwegg, 2010). Evolutionary experiments with microbes demonstrate that evolution in response to resource limitation is possible (Gresham *et al.*, 2008; Tamminen *et al.*, 2018) and has the potential to alter the outcome of competition (Bernhardt *et al.*, 2020). Here we develop and analyze an eco-evolutionary mathematical model of phytoplankton species that compete for dissolved inorganic carbon (DIC) in water. The competitive scenario is complex because DIC exists as a dynamical equilibrium between three dissolved carbon compounds: CO_2, HCO_3^- and CO_3^{2-} (Cole & Prairie, 2009). CO_2 and HCO_3^- can be used as inorganic carbon resources by phytoplankton, though uptake efficiencies vary by species, carbon compound, and through time (Ji *et al.*, 2020).

Although, on geological time scales, the carbon uptake machinery of phytoplankton has evolved (Giordano, Beardall & Raven, 2005), whether evolution is helping phytoplankton to adapt to our rapidly changing world is still a subject of scientific inquiry (Dlugokencky & Tans, 2021). A series of laboratory experiments determined that increasing CO_2 concentrations did not result in any specific adaptations that increase fitness in a range of freshwater phytoplankton species and strains (Collins & Bell, 2004, 2005; Low-Décarie *et al.*, 2013). More recent experiments, on the other hand, showed that increasing pCO_2 can result in evolutionary changes in several marine and freshwater phytoplankton species (Lohbeck *et al.*, 2013; Schaum & Collins, 2014; Scheinin *et al.*, 2015; Lindberg & Collins, 2020). Whereas these experiments focused on adaptive evolutionary responses within a single lineage or species, there is also evidence for CO_2-driven natural selection among genotypes with different carbon-concentrating mechanisms of the freshwater cyanobacterium *Microcystis* in both laboratory and field populations (Sandrini *et al.*, 2016). Sandrini *et al.* (2016) found that in a eutrophic lake, low CO_2 conditions benefited strains of *Microcystis* spp. that had both a high-affinity low-flux and a low-affinity high-flux gene for HCO_3^- uptake, whereas at high CO_2, the genotype with only the low-affinity high-flux gene became dominant. Though more research is needed, these studies demonstrate that changing CO_2 concentrations can drive adaptation and selection of different carbon uptake kinetics.

Few other studies, however, have considered the role of HCO_3^- as an alternative carbon source that can affect evolutionary outcomes. Compared to CO_2, HCO_3^- is typically more costly for the organism to take up because it requires additional cellular machinery to be converted to CO_2 prior to being used for photosynthesis (Price *et al.*, 2007; Sandrini *et al.*, 2013; Verspagen *et al.*, 2014). Nevertheless, HCO_3^- is the dominant form of inorganic carbon in aquatic systems with pH values between ~6 and ~10 whereas CO_2 is dominant at pH below ~6 (Maberly & Gontero, 2017). In aquatic plants the importance of HCO_3^- use is reflected in their distribution across the landscape, which shows a correlation between species' abilities to use HCO_3^- and the actual HCO_3^- concentration (Titus & Pagano, 2017; Iversen *et al.*, 2019).

Classical resource competition states that the resource (R) that is present in the lowest concentration relative to demand becomes limiting for growth (Tilman, 1977). A single population growing in isolation will lower the resource concentration until its net growth rate reaches zero and the system reaches a dynamic equilibrium. The resource concentration at which this equilibrium is reached is denoted R^*. In a competitive scenario, with several populations limited by a single resource, the population with the lowest R^* will inevitably outcompete all other populations. As more resources are included, more species can co-exist, if they are limited by different resources. When incorporating evolution into such models, it is important to consider any potential trade-offs that might constrain evolutionary change. Some studies find proof for a trade-off between the uptake rates of different resources (Spijkerman, de Castro & Gaedke, 2011), while other studies find no evidence for a trade-off (Bernhardt *et al.*, 2020).

To investigate the effects that evolutionary responses to changing carbon availability might have on uptake kinetics of phytoplankton and how that might affect the outcomes of competition, we developed and analyzed a mathematical model featuring two phytoplankton populations with different carbon uptake strategies that are competing for two complementary carbon resources: CO_2 and HCO_3^-. We hypothesized that (1) in the single species case, evolution should work to optimize the growth of the population and enable it to draw down the resource concentrations to lower levels (i.e., to a lower R^*) than without evolution such that an evolving strain can out-compete the non-evolving strain of the same species; (2) similarly, in the multi-species case, evolution can change the outcome of competition in a context where a species' R^* evolves to be lower than that of the competitors, (3) at equilibrium, evolving populations, compared to non-evolving ones, should benefit more strongly, in terms of biomass, from increasing atmospheric CO_2 because the uptake parameters can be fine-tuned to the changing resource availabilities.

3.4 Methods

3.4.1 Model

Our model is built upon the model from Ji *et al.* (2020) without phenotypic plasticity. In summary, the model considers n phytoplankton species and two carbon resources: $\mathrm{CO_2}$ and $\mathrm{HCO_3^-}$. The change in population size, which we measure in units of biovolume, of species i (X_i) is primarily controlled by the sum of the rates of uptake of carbon resource j ($v_{i,j}$) relative to the cellular demand for carbon ($Q_{C,i}$) of this species. Additionally, the species-specific mortality rate (m_i) decreases the population size (Eqn. 3.1). For simplicity, we assume that population growth does not affect the alkalinity (see (Ji *et al.*, 2020)), nor do we consider any other factors that may play a role in the real world. However, we do assume a fixed effect of light limitation (see Supplemental Text A3.1).

$$\frac{dX_i}{dt} = \left(\frac{v_{i,\mathrm{CO_2}} + v_{i,\mathrm{HCO_3^-}}}{Q_{C,i}} - m_i\right) X_i \qquad i = 1, \ldots, n \tag{3.1}$$

Following the classic Michaelis-Menten uptake kinetics, the uptake rate for carbon resource j ($v_{i,j}$) is determined by the resource concentration (R_j), the maximum uptake rate of a resource ($V_{\max,i,j}$) and the species-specific affinity ($A_{i,j}$; Eqn. 3.2). Mathematically, affinity is defined as the maximum uptake rate of a resource ($V_{\max,i,j}$) divided by the half-saturation constant ($k_{i,j}$).

$$v_{i,j} = \frac{V_{\max,i,j} R_j}{\left(V_{\max,i,j}/A_{i,j}\right) + R_j} \tag{3.2}$$

Two carbon resources are considered in this model: CO_2 and HCO_3^-. Along with carbonate (CO_3^{2-}), which is not bioavailable, CO_2 and HCO_3^- form the carbonate system. All three components of the carbonate system are in a dynamic equilibrium, which is re-calculated at every time-step of each simulation. This equilibrium is controlled by the partial pressure of atmospheric CO_2, the concentration of dissolved inorganic carbon ([DIC], i.e., the sum of dissolved CO_2, HCO_3^- and CO_3^{2-}), pH, temperature, and salinity (Verspagen *et al.*, 2014). In our model, the DIC concentration is a variable that changes due to CO_2 exchange with the atmosphere and uptake of CO_2 and HCO_3^-- by the phytoplankton species:

$$\frac{d[\mathrm{DIC}]}{dt} = \frac{g}{z_m}\left([\mathrm{CO_2}]^{\mathrm{atm}} - [\mathrm{CO_2}]\right) - \sum_{i=1}^{n}\left(v_{i,\mathrm{CO_2}} + v_{i,\mathrm{HCO_3^-}}\right) X_i \tag{3.3}$$

where g is the gas transfer velocity (piston velocity) across the air-water interface, z_m is the depth of the water body, $[\mathrm{CO_2}]^{\mathrm{atm}}$ is the atmospheric CO_2 concentration and $[\mathrm{CO_2}]$ is the dissolved CO_2 concentration. Note that we here assume that g has a fixed value that ignores chemical enhancement (see (Ji *et al.*, 2020)).

3.4.1.1 Evolution

To introduce evolution into the model, we allow the affinity parameter to evolve through time since resource affinity is considered one of the main factors governing a population's competitive ability (Aksnes & Egge, 1991). First, to prevent run-away evolution, we introduce constraints (Fussmann & Gonzalez, 2013). We assume that there is a trade-off between the affinity and the maximum uptake rate for each carbon resource. That is, an increase in affinity is assumed to lead to a decrease in the maximum uptake rate (Figure 3.1). We use a simple power function, with an exponent ($p_{i,j}$) and a constant ($c_{i,j}$), which determine the shape and intensity of the trade-off:

$$V_{\max,i,j}^{-1} = c_{i,j} \cdot A_{i,j}^{p_{i,j}} \qquad \text{where } c_{i,j} > 0; p_{i,j} > 0 \tag{3.3}$$

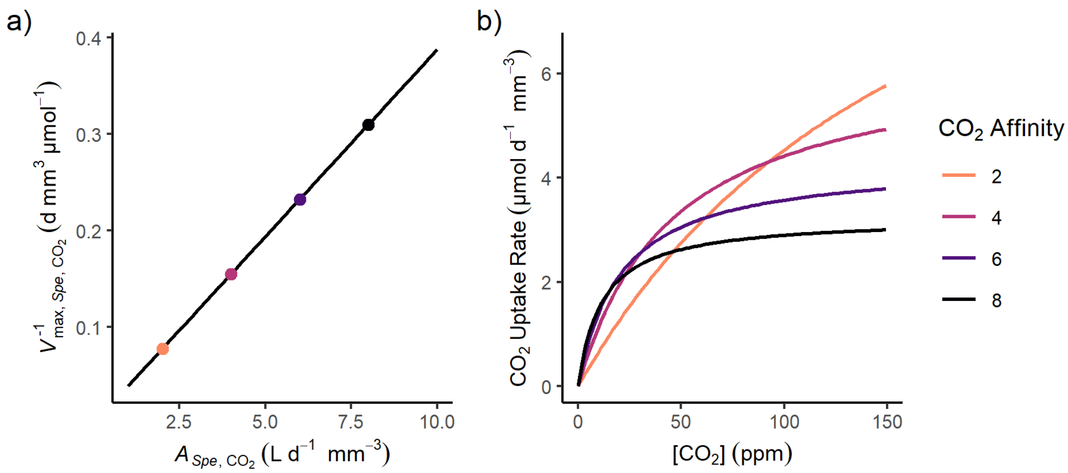

Figure 3.1: (a) The trade-off between the maximum uptake rate ($V^{-1}_{\max,Spe,CO_2}$; x-axis) and affinity (A_{Spe,CO_2}; y-axis) for CO_2, for a specialist phytoplankton species. Specific affinities are highlighted with coloured points (see colour legend in b). (b) CO_2 uptake rates (y-axis) across a range of CO_2 concentrations (x-axis) for each of the affinity values highlighted in (a) (colour legend). Note that a high affinity is advantageous when resource concentrations are low and vice-versa. The equation is parameterised for the CO_2 uptake of a CO_2 specialist species (Table A3.2.2), though the same principle applies to other species and resources (e.g., Figure A3.1.1). In this case, $p_{Spe,CO_2} = 1$ and $c_{Spe,CO_2} = 3.87 \cdot 10^4$ d^2 mm^6 L^{-1} mol^{-1}.

Assuming that affinity is a quantitative trait, we then allow $A_{i,j}$ (and hence also $V_{\max,i,j}$) to evolve through time based on the fitness landscape, following the method of Lande (1976). This method assumes that selection occurs on existing variation in the population and increases the specific growth rate (fitness) of the population. Mathematically, the operation involves taking the derivative of the specific growth rate $(1/X_i)(dX_i/dt)$ with respect to affinity $A_{i,j}$. Inherent to the model, a higher growth rate means a faster rate of resource uptake, which also means a lower R^*. Here, we assume that evolution of the CO_2 uptake kinetics does not affect the HCO_3^- uptake kinetics.

$$\frac{dA_{i,j}}{dt} = \varepsilon_{i,j} \frac{\partial(d\ln X_i/dt)}{\partial A_{i,j}} \tag{3.4}$$

where $\varepsilon_{i,j}$ is the rate of evolutionary change, and for notational convenience we have written the specific growth rate as $d\ln X_i/dt$.

3.4.2 Mathematical Simulations

We explored the parameter space of the model by running many simulations with various rates of evolutionary change (ε), shapes of evolutionary trade-offs (p) and resource concentrations. To present the results in a compact manner, we selected values of ε for which evolutionary endpoints were reached within a timeframe of 300 days from realistic initial concentrations (Table A3.2.2). Although rapid rates of evolution can be seen as unrealistic, most of our analyses are focused on the equilibrium conditions, which do not depend on the evolutionary rates. Additionally, selection on standing variation can happen quickly in rapidly proliferating organisms like phytoplankton (Padfield *et al.*, 2016; Bach *et al.*, 2018). We set the trade-off variable $p_{i,j} = 1$ for all species and resources for all the simulations presented here, though we explore the effect of different values in the supplemental materials (Figure A3.1.2).

We first analytically explored the effect that different affinities might have on species' R^* values. Next, we chose a fixed $[\mathrm{CO_2}]^{\mathrm{atm}}$ and $[\mathrm{HCO_3^-}]_{\mathrm{in}}$ which allowed us to highlight the role of evolution in a competitive context (Table A3.2.1). Next, to explore the role of changing $[\mathrm{CO_2}]^{\mathrm{atm}}$ and $[\mathrm{HCO_3^-}]_{\mathrm{in}}$ on individual species' biovolumes and CO_2 and HCO_3^- affinities, we ran hundreds of simulations until equilibrium was reached to get a sense of the equilibrium conditions across CO_2 supply rates ranging from 250 to 10,000 ppm, capturing pre-industrial atmospheric CO_2, future atmospheric CO_2 and highly supersaturated lakes (Cole *et al.*, 1994) and for three initial HCO_3^- concentrations (Table A3.2.1).

Note that although most computations for CO_2 are made in units of mol L^{-1}, to allow most readers a better grasp on the values, we report them in ppm assuming a temperature of 24 °C and total pressure of 1 atm. For reference, a pCO_2 of 400 ppm corresponds to a dissolved CO_2 concentration of 14 µmol L^{-1} (Table A3.2.1).

3.5 Results

3.5.1 Analytical Results

3.5.1.1 Resource equilibria (R^*)

It is possible to calculate a range of possible equilibrium resource concentrations (R^*) for CO_2 ($[\mathrm{CO_2}]_i^*$) and HCO_3^- ($[\mathrm{HCO_3^-}]_i^*$) by assuming that dX/dt and $d[\mathrm{DIC}]/dt$ are equal to zero and substituting Eqn. 3.1 into Eqn. 3.3:

$$\begin{aligned} [\mathrm{CO_2}]_i^* &= \frac{V_{\max,i,\mathrm{CO_2}}\left(m_i\ Q_{C,i} - v_{i,\mathrm{HCO_3^-}}\right)}{A_{i,\mathrm{CO_2}}\left(V_{\max,i,\mathrm{CO_2}} - m_i\ Q_{C,i} + v_{i,\mathrm{HCO_3^-}}\right)} \\ [\mathrm{HCO_3^-}]_i^* &= \frac{V_{\max,i,\mathrm{HCO_3^-}}\left(m_i\ Q_{C,i} - v_{i,\mathrm{CO_2}}\right)}{A_{i,\mathrm{HCO_3^-}}\left(V_{\max,i,\mathrm{HCO_3^-}} - m_i\ Q_{C,i} + v_{i,\mathrm{CO_2}}\right)} \end{aligned} \tag{3.5}$$

A species' R^* corresponds to the resource concentration at which a population of that species can maintain its population size. Thus, the species with the lowest R^* can outcompete its competitor (Tilman, 1980). We first consider a CO_2 specialist, which can only take up CO_2. The CO_2 specialist has a $[\mathrm{CO_2}]^*$, which does not change regardless of the HCO_3^- concentration in the medium (vertical green line in Figure 3.2). Next, we consider a generalist, which can take up both CO_2 and HCO_3^-. In this case, the $[\mathrm{CO_2}]^*$ and $[\mathrm{HCO_3^-}]^*$ are inter-dependent (Eqn. 3.5) and together, produce a curve, called the zero net-growth isocline (ZNGI; red line in Figure 3.2). The intersection of the ZNGIs of two competing species indicates the existence of a coexistence equilibrium, at the resource concentrations defined by the coexistence point (Figure 3.2).

In the classical graphical approach to competition for two limiting resources, the stability of the coexistence equilibrium depends on the configuration of the consumption vectors of the two species (Tilman, 1982). Here, our model deviates from the classical resource competition models. In the classical models, each species has its own consumption vector, defined by the ratio at which the two resources are consumed by this species. Hence, with two species, there are two consumption vectors and the area delineated by the two consumption vectors allows for either stable species coexistence or alternative stable states. In our model, the two species also differ in the ratios at which they consume the two resources, but the chemical equilibrium reactions of the carbonate system rapidly redistribute the concentrations of dissolved CO_2, HCO_3^- and CO_3^{2-}. Consequently, instead of two species-specific consumption vectors, both species follow the same carbon depletion trajectory dictated by the chemical equilibration of the carbonate system. This carbon depletion trajectory can be plotted as a trajectory in the plane of $[CO_2]$ and $[HCO_3^-]$, that starts at a supply point $([CO_2]^{atm}, [HCO_3^-]_{in})$ given by the dissolved CO_2 and HCO_3^- concentrations in the absence of phytoplankton and tracks the changes of $[CO_2]$ and $[HCO_3^-]$ due to inorganic carbon uptake by the phytoplankton populations. Hence, each supply point in the plane of $[CO_2]$ and $[HCO_3^-]$ has its own unique carbon depletion trajectory.

An important implication is that contrary to the classical resource competition models, our model does not predict a region of stable species coexistence or alternative stable states. Instead, there is a single boundary line separating the supply points where the CO_2 specialist wins from the supply points where the generalist wins (black line in Figure 3.2; Supplemental Text A3.2). This boundary line is given by the carbon depletion trajectory that leads to the coexistence point. For all supply points that fall in the green area below the boundary line, the CO_2 specialist wins. Conversely, for all supply points that fall in the red area above the boundary line, the generalist wins (Figure 3.2).

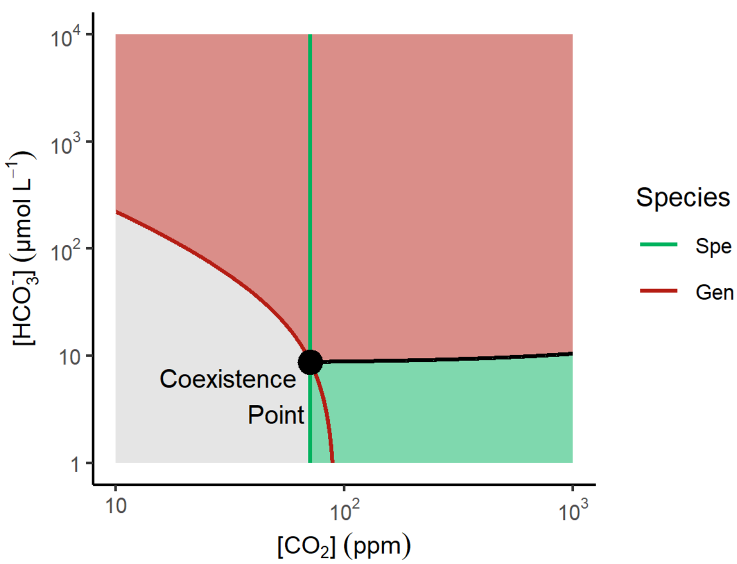

Figure 3.2: Graphical analysis of competition between two species: a CO_2 specialist (green), which relies solely on CO_2, and a generalist (red), which can take up CO_2 and HCO_3^-. The resource space spans a range of CO_2 (x-axis) and HCO_3^- concentrations (y-axis). The green and red lines denote the ZNGIs of the CO_2 specialist and the generalist, respectively. The black line is the boundary line between the supply points for which the CO_2 specialist wins and the supply points for which the generalist wins. If the supply point ($[\mathbf{CO_2}]^{\mathbf{atm}}$, $[\mathbf{HCO_3^-}]_{\mathbf{in}}$) is positioned along this boundary line, the resource concentrations will reach the coexistence point (black), with both species coexisting. If the supply point is positioned in the green area, the CO_2 specialist is the winner of the competition. If the supply point is in the red area, the generalist is the winner. In the grey area, the resource concentrations are insufficient to sustain the growth of either species. The parameter values for both species can be found in Table A3.2.2.

3.5.1.2 Eco-evolutionary dynamics of a CO_2 specialist

To study the eco-evolutionary dynamics, we first focus on CO_2 uptake by a single species only and assume that HCO_3^- uptake is negligible. Furthermore, we assume that chemical processes of the carbonate system occur at a much faster rate than the population dynamics and evolutionary dynamics of this species. Hence, the carbonate system rapidly approaches a quasi-equilibrium ($d[\mathrm{DIC}]/dt \approx 0$) with the extant population density and evolutionary status. In this case, eco-evolutionary adaptation of the CO_2 uptake kinetics of a species can be analyzed as a two-dimensional problem governed by its ecological dynamics (dX/dt) and evolutionary dynamics (dA/dt). Figure 3.3a plots ZNGI's of the ecological and evolutionary dynamics in the plane of $[CO_2]$ and the evolving trait (CO_2 affinity).

Ecological dynamics: Inserting the trade-off between CO_2 affinity and maximum uptake rate of CO_2 (Eqn. 3.3) into Eqn. 3.1 , 3.2, the population dynamics of a species can be written as:

$$\frac{dX_i}{dt} = \left(\frac{1}{Q_{C,i}}\left(\frac{A_i[\mathrm{CO_2}]}{1 + c_i(A_i)^{1+p_i}[\mathrm{CO_2}]}\right) - m_i\right)X_i \tag{3.6}$$

where we have simplified the notation by dropping the subject j. The ecological zero isocline is obtained by solving the population dynamics for equilibrium, i.e., $dXi/dt = 0$. This gives:

$$[\mathrm{CO_2}]_{\mathrm{eco}} = \frac{m_i Q_{C,i}}{A_i \left(1 - m_i Q_{C,i} c_i (A_i)^{p_i}\right)} \tag{3.7}$$

According to this equation, the ecological zero isocline is a U-shaped function of the CO_2 affinity, bounded between two vertical asymptotes, at A_i equals 0 and A_i equals the pith-root of $1/\left(m_i Q_{C,i} c_i\right)$. An example of this U-shaped function is plotted in Figure 3.3a. The minimum value of this U-shaped function is located at:

$$A_i = \frac{1}{\sqrt[p_i]{(p_i + 1)\, m_i\, Q_{C,i}\, c_i}} \tag{3.8}$$

Evolutionary dynamics: Evolutionary adaptation of the CO_2 affinity is assumed to be proportional to the fitness gradient. According to Eq.7, after incorporation of the trade-off between CO_2 affinity and maximum CO_2 uptake rate, the fitness gradient with respect to CO_2 affinity equals:

$$\frac{\partial(d\ln X_i/dt)}{\partial A_i} = \frac{[\mathrm{CO_2}]}{Q_{C,i}} \left(\frac{1 + c_i\, A_i^{1+p_i}\, [\mathrm{CO_2}] - (1 + p_i)\, c_i\, A_i^{1+p_i} [\mathrm{CO_2}]}{\left(1 + c_i\, A_i^{1+p_i}\, [\mathrm{CO_2}]\right)^2} \right) \tag{3.9}$$

Some terms in this equation cancel out. Hence, the evolutionary dynamics can be written as

$$\frac{dA_i}{dt} = \varepsilon_i \frac{[\mathrm{CO_2}]}{Q_{C,i}} \left(\frac{1 - p_i\, c_i\, A_i^{1+p_i} [\mathrm{CO_2}]}{\left(1 + c_i\, A_i^{1+p_i}\, [\mathrm{CO_2}]\right)^2} \right) \tag{3.10}$$

The evolutionary zero isocline is obtained by solving the evolutionary dynamics for equilibrium (i.e., $dA_i/dt = 0$). This gives:

$$[\mathrm{CO_2}]_{\mathrm{evo}} = \frac{1}{p_i\, c_i\, (A_i)^{1+p_i}} \tag{3.11}$$

Accordingly, the evolutionary zero isocline is a decreasing convex function of the CO_2 affinity. We explore the non-equilibrium dynamics in the supplemental materials (Supplemental Text A3.3).

Eco-evolutionary equilibrium: The ecological and evolutionary dynamics are both at equilibrium at the intersection of the two zero isoclines. According to Eqn. 3.7 , 3.11, this intersection point is given by

$$\frac{1}{p_i\ c_i\ (A_i)^{1+p_i}} = \frac{m_i Q_{C,i}}{A_i\ \left(1 - m_i Q_{C,i} c_i (A_i)^{p_i}\right)} \tag{3.12}$$

Solving this equality for A_i gives Eqn. 3.8. That is, the two zero isoclines intersect at the minimum of the U-shaped ecological isocline. This is a very important result. It shows that the CO_2 uptake kinetics of a species will evolve towards an eco-evolutionary equilibrium at which this species can deplete the dissolved CO_2 concentration to the lowest possible level.

3.5.1.3 Eco-evolutionary dynamics of a generalist

Many phytoplankton species can use both CO_2 and HCO_3^- as inorganic carbon sources, and hence are generalists. Therefore, as a next step, we now consider the eco-evolutionary dynamics of a generalist species by incorporating HCO_3^- uptake in the model. For simplicity, we first assume that the HCO_3^- concentration is at a fixed value (which may serve as a valid first approximation for the oceans, where the HCO_3^- concentration is ∼2 mmol L^{-1}) and ignore evolution of the HCO_3^- uptake kinetics. In this case, the population dynamics of a species can be written as:

$$\frac{dX_i}{dt} = \left(\frac{1}{Q_{C,i}}\left(\frac{A_i[\mathrm{CO_2}]}{1 + c_i (A_i)^{1+p_i}[\mathrm{CO_2}]} + v_{i,\mathrm{HCO_3^-}}\right) - m_i\right) X_i \tag{3.13}$$

The ecological zero isocline for CO_2 is now given by:

$$[\mathrm{CO_2}]_{\mathrm{eco}} = \frac{m_i Q_{C,i} - v_{i,\mathrm{HCO_3^-}}}{A_i\ \left(1 - \left(m_i Q_{C,i} - v_{i,\mathrm{HCO_3^-}}\right) c_i (A_i)^{p_i}\right)} \tag{3.14}$$

Its minimum value is now given by:

$$A_i = \frac{1}{\sqrt[p_i]{(p_i + 1)\ \left(m_i\ Q_{C,i} - v_{i,\mathrm{HCO_3^-}}\right)\ c_i}} \tag{3.15}$$

According to this equation, the ecological zero isocline is again a U-shaped function of the CO_2 affinity, bounded between two vertical asymptotes. All else being equal, the U-shaped zero isocline of a generalist species will be both wider and deeper than the zero isocline of the CO_2 specialist (Figure 3.3b). Moreover, when its HCO_3^- uptake rate increases, the U-shape zero isocline of the generalist will widen and deepen further.

In our model, the CO_2 uptake kinetics are not affected by HCO_3^- uptake. Consequently, the fitness gradient with respect to CO_2 affinity and hence the evolutionary dynamics remain the same as in Eqn. 3.9 , 3.10. Hence, the evolutionary zero isocline is still the same convex decreasing function of CO_2 affinity described by Eqn. 3.11.

Analogous to our previous derivations for the CO_2 specialist, it can be shown that the ecological and evolutionary zero isocline of the generalist species again intersect at the minimum of the U-shaped ecological isocline. This implies that the CO_2 uptake kinetics of a generalist species will again evolve towards an eco-evolutionary equilibrium (EEE) at which this species can deplete the dissolved CO_2 concentration to the lowest possible level. However, the U-shaped zero isocline of the generalist species extends deeper than that of the CO_2 specialist, and hence at this EEE, the generalist species will deplete the dissolved CO_2 concentration to a lower level than the CO_2 specialist. Thus, because the generalist species has access to HCO_3^- as an additional carbon source, it becomes a stronger competitor for CO_2 than the specialist species.

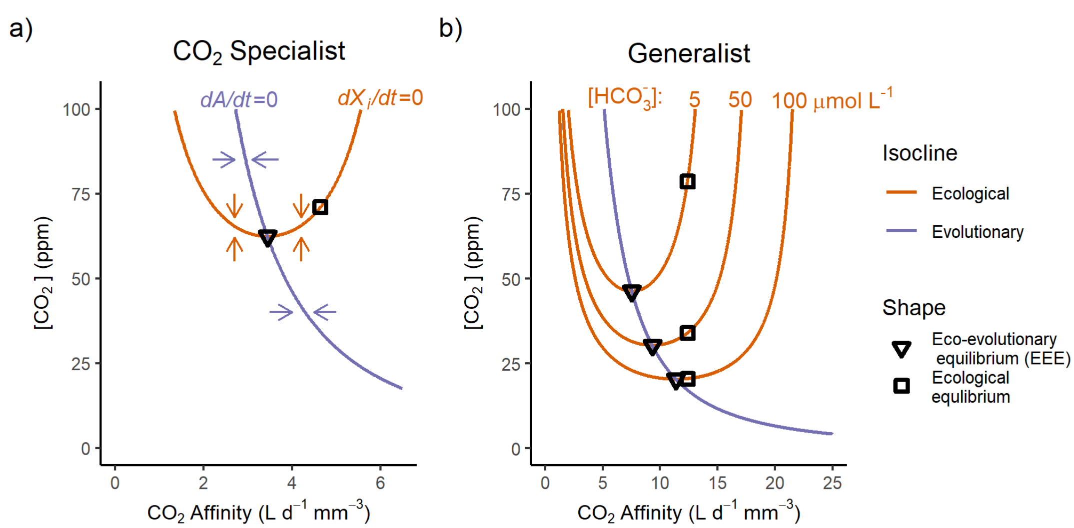

Figure 3.3: In resource ($[CO_2]$; y-axis) and CO_2 affinity (A_i; x-axis) space, the orange line represents the ecological (zero-growth) isocline (i.e., $dX_i/dt = 0$) whereas purple line represents the evolutionary isocline (i.e., $dA_i/dt = 0$). The square represents the ecological equilibrium, based on the species' initial affinity, whereas the triangle represents the eco-evolutionary equilibrium (i.e., $dX_i/dt = dA_i/dt = 0$). In (a), parameter values for the CO_2 specialist are used; orange arrows represent the direction of change of $[CO_2]$ and purple arrows the directon of change of A_i. In (b), parameter values for the generalist are used and three different fixed bicarbonate concentrations are exemplified. For parameter values, see Table A3.2.2.

3.5.1.4 Competition Between a CO_2 Specialist and a Generalist Species

As discussed, the population that has the lowest R^* is the best competitor. By comparing the R^*s of evolving and non-evolving strains of different species, we can predict the outcome of competition. Here, we make the simplifying assumption that HCO_3^- concentrations and HCO_3^- affinity are fixed, which reduces the dimensionality of the problem from 4 to 2. In the simplest case, neither species can evolve, meaning that the affinity is fixed at the starting value for each species (squares in Figure 3.3). When HCO_3^- concentrations are minimal, the CO_2 specialist has a lower $[CO_2]^*$ than the generalist, and is expected to win the competition (compare the square in Figure 3.3a with the square on the 5 μmol L^{-1} line in Figure 3.3b). As the HCO_3^- concentration increases, however, the $[CO_2]^*$ becomes lower for the generalist (compare the squares along different lines in Figure 3.3b), but does not change for the CO_2 specialist since it is unable to take up HCO_3^-. With a sufficiently high $[HCO_3^-]^*$ (>10 μmol L^{-1}), the generalist is guaranteed to win the competition (Figure 3.2 & 3.3). With evolution, the affinity is expected to change in a way that minimizes the $[CO_2]^*$ and reach the EEE (triangles in Figure 3.3). In this case, the generalist is able to out-compete the CO_2 specialist as it has the potential to evolve to a lower $[CO_2]^*$, irrespective of the HCO_3^- supply concentration (compare the triangles in Figure 3.3a,b). Note that it is possible to envision a scenario where a different evolving CO_2 specialist species could out-compete the evolving generalist for some range of HCO_3^- concentrations by adjusting p, c, or Q_C parameters (Figure A3.1.2).

3.5.2 Simulation Results

3.5.2.1 Single Species

Here, we illustrate the model described above for a single species, using the CO_2 specialist as an example, growing without competition, at $[CO_2]^{atm}$=400 ppm, and a very low starting HCO_3^- concentration of 5.0 μmol L^{-1}. The results are similar for the generalist species (Supplemental Text A3.4). Evolution had a positive effect on the biovolume of the CO_2 specialist, increasing it to 1.35 mm^3 L^{-1} from 1.28 mm^3 L^{-1} (Figure 3.4a,d), and on the maximum observed growth rate, increasing it to 0.41 d^{-1}, compared to 0.317 d^{-1}. Note that the effect of evolution on equilibrium biomass was quite subtle because the starting affinity of the population was relatively close to the EEE (Figure 3.3a). With evolution, the CO_2 concentration at equilibrium ($[CO_2]^*$) was drawn down to 72.8 ppm, compared to 91.9 ppm, without evolution. Due to the chemical equilibrium between CO_2 and HCO_3^-, the HCO_3^- concentrations also decreased from 3.92 μmol L^{-1} without evolution to 3.83 μmol L^{-1} with evolution (Figure 3.4b,e). With evolution, the CO_2 affinity decreased to a new EEE, 3.19 L d^{-1} mm^{-3}, compared to 4.64 L d^{-1} mm^{-3} without evolution. (Figure 3.4c,f).

In a competitive scenario with both the non-evolving and the evolving strain, the evolving strain could outcompete the non-evolving strain (Figure 3.4g,h,i). The final resource concentration was determined by the evolving strain (Figure 3.4g) and the affinities behaved in essentially the same way as when the evolving strain was growing alone (Figure 3.4i). This finding confirms our first hypothesis that evolution should work to optimize the growth of the population and enable it to draw down the resource concentrations to lower levels than without evolution such that a strain of the same species that can evolve can out-compete the non-evolving strain. The same principles apply to the generalist strains (Supplemental Text A3.4).

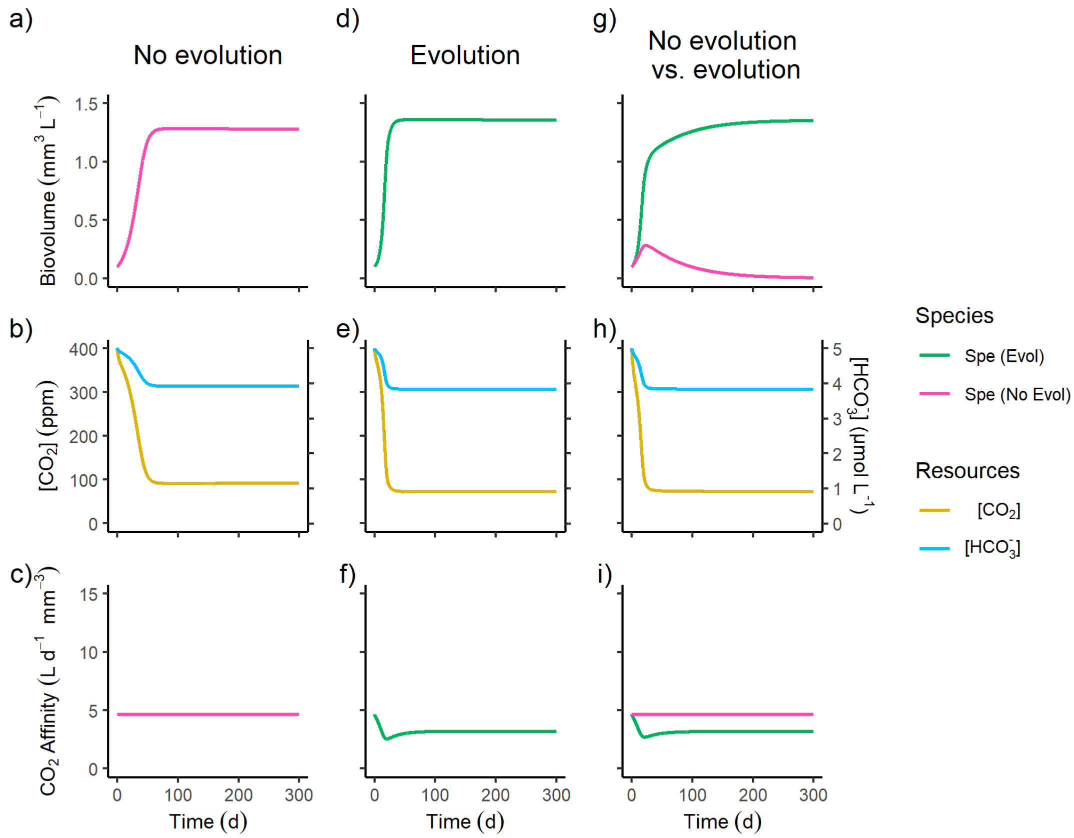

Figure 3.4: Simulations featuring a single non-evolving strain of the CO_2 specialist (a-c), a single evolving strain of the same species (d-f), and a competitive scenario between both strains (g-i). We compare the biovolume concentration (a, d, g), the resource concentrations CO_2 and HCO_3^- (b, e, h) and each population's CO_2 affinity (c, f, i).

3.5.2.2 Interspecific Competition

As predicted from the eco-evolutionary dynamics in Figure 3.3, when competing without evolution, the CO_2 specialist could outcompete the generalist at $[CO_2]^{atm}$=400 ppm and a very low starting HCO_3^- concentration of 5.0 µmol L^{-1} (Figure 3.5a). With evolution, on the other hand, the generalist outcompetes the specialist (Figure 3.5d). In both cases, the winning species determined the equilibrium biovolume and resource concentrations, which were essentially the same as when the winning species was growing alone (compare Figure 3.5 with Figure 3.4 & A3.4.1). The CO_2 and HCO_3^- affinities of the evolving generalist also reached the same EEE as in isolation (Figure 3.5f & A3.4.1f). The CO_2 affinity of the evolving

CO_2 specialist, however, increased above its single-species EEE of 3.19 L d^{-1} mm^{-3}, up to 3.86 L d^{-1} mm^{-3} (Figure 3.4f & 3.5g).

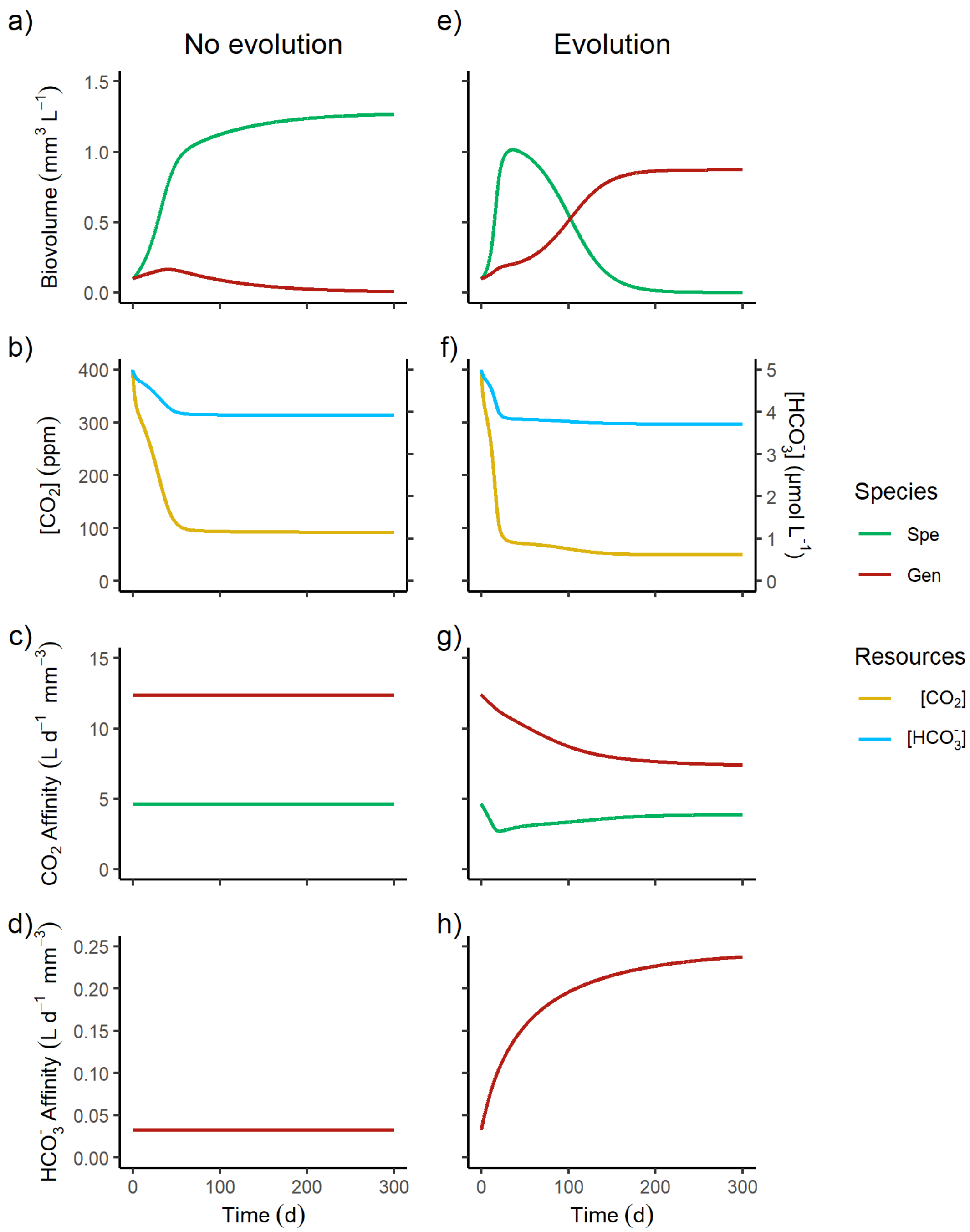

Figure 3.5: Simulations featuring two non-evolving strains of the generalist and the CO_2 specialist (a-d) and two evolving strains of the same species (e-h). We compare the biovolume concentration (a, e), the resource concentrations (b, f) and each population's CO_2 affinity (c, g) and HCO_3^- (d,h).

3.5.2.3 The Effect of Rising Atmospheric CO_2

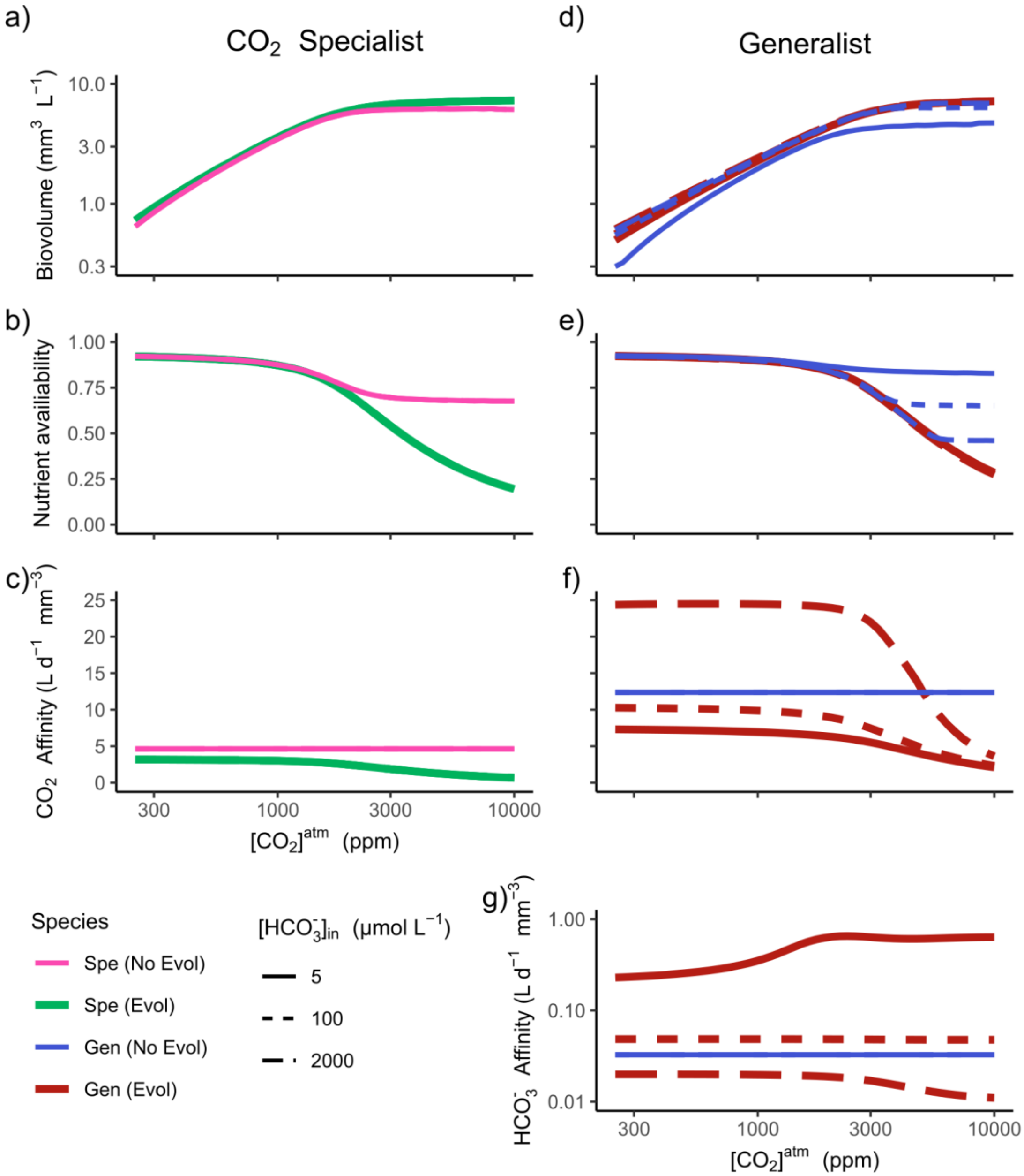

Figure 3.6: Effects of resource supply on the CO_2 specialist (left column) and the generalist (right column) in non-evolutionary and evolutionary scenarios (equilibrium values are plotted). Specifically, the effect of varying atmospheric CO_2 concentrations (x-axis) on biovolume (a,d), nutrient availability relative to species' demand, where 1 means no nutrient limitation and 0 means extreme nutrient limitation (b,e; see Supplemental Text A3.5 for details about $f_{i,\mathrm{P}}$), CO_2 affinity (c,f), HCO_2 affinity (g). Three different starting HCO_3^- concentrations were considered: very low (5 µmol L^{-1}), low (100 µmol L^{-1}) and an average marine and freshwater HCO_3^- (2000 µmol L^{-1}; line type) (USEPA (US Environmental Protection Agency), 2009).

We explored the effects of increasing atmospheric CO_2 at different starting HCO_3^- concentrations ($[\mathrm{HCO_3^-}]_{\mathrm{in}}$) and the evolution of species in monoculture. We did not focus on competition because without evolution, the outcome of competition can be determined by calculating each population's ZNGI (Figure 3.2), whereas with evolution, the generalist always outcompetes the CO_2 specialist (Figure 3.3, 3.5). Additionally, to make the model more realistic, we incorporated independent nutrient co-limitation to prevent unlimited growth (Sperfeld, Raubenheimer & Wacker, 2016). Note that the generalist and the specialist both have the same nutrient uptake kinetics (Table A3.2.2).

We found that the equilibrium biovolume of the evolving CO_2 specialist was consistently higher than that of the non-evolving strain, though the percent increase varied with $[\mathrm{CO_2}]^{\mathrm{atm}}$ whereas the effects of $[\mathrm{HCO_3^-}]_{\mathrm{in}}$ were negligible (Figure 3.6b). At $[\mathrm{CO_2}]^{\mathrm{atm}}$=250 ppm, evolution generated a 12.4 % increase. The effect reached a minimum of 3.26 % at $[\mathrm{CO_2}]^{\mathrm{atm}}$=1,100 ppm, and a maximum of 18.8 % at $[\mathrm{CO_2}]^{\mathrm{atm}}$=10,000 ppm (Figure 3.6a). As $[\mathrm{CO_2}]^{\mathrm{atm}}$ increased, nutrient availability decreased (Figure 3.6b), which correlated with a decline in the CO_2 affinity of the evolving strain (Figure 3.6c). Because a decreased affinity trades off to a higher maximum uptake rate (Figure 3.1), this strategy allowed the evolving strain to benefit more strongly from the independent co-limitation of carbon and nutrient than the non-evolving strain. As a result, the greatest effect of evolution on biovolume occurs at extreme values of $[\mathrm{CO_2}]^{\mathrm{atm}}$ (Figure 3.6a).

For the generalist, the results are similar, but we found that $[\mathrm{HCO_3^-}]_{\mathrm{in}}$ can also play an important role in controlling biomass, nutrient availability, CO_2 affinity and HCO_3^- affinities

(Figure 3.6d,e,f,g). Interestingly, at $[HCO_3^-]_{in}$=5 µmol L^{-1}, evolution resulted in biomass increases of 79.3% and 51.9% at $[CO_2]^{atm}$=250 and 10,000 ppm, respectively (Figure 3.6d). In contrast, these values were 1.58% and 13.7% at $[HCO_3^-]_{in}$=100 µmol L^{-1} and 0.914% and 3.9% at $[HCO_3^-]_{in}$=2,000 µmol L^{-1}. We found that at low $[CO_2]^{atm}$ and at $[HCO_3^-]_{in}$=5 and 100 µmol L^{-1}, CO_2 affinity tends to decrease and HCO_3^- affinity increases relative to the non-evolving strain, while at $[HCO_3^-]_{in}$=2,000 µmol L^{-1}, CO_2 affinity increases and HCO_3^- affinity decreases (Figure 3.6f,g). Because $[HCO_3^-]_{in}$ affects the alkalinity of the system, which controls the CO_2:HCO_3^- ratio, the CO_2 and HCO_3^- affinity responses are opposed at low $[CO_2]^{atm}$. At high $[CO_2]^{atm}$ values, however, nutrient availability decreases, causing excess CO_2 to build up which and the CO_2 affinities to converge to the same value regardless of $[HCO_3^-]_{in}$ (Figure 3.6e,f). Notably, we found that at $[HCO_3^-]_{in}$=5 µmol L^{-1}, the HCO_3^- affinity increases by an order of magnitude, relative to the non-evolving strain, across the range of $[CO_2]^{atm}$ (Figure 3.6e,g). By running additional simulations and allowing either CO_2 or HCO_3^- affinities to evolve, we found that despite this dramatic increase, it is the decrease in CO_2 affinity which was instrumental in the evolutionary-driven biomass increase (Figure A3.1.3).

In summary, we find that, given our assumptions, increasing $[CO_2]^{atm}$, evolution, and different $[HCO_3^-]_{in}$ can interact to affect a population's equilibrium biomass and carbon uptake to different degrees. Evolutionary-induced biomass increases are most prominent when the population is far from the EEE in a given resource space, such as the generalist growing under very low $[HCO_3^-]_{in}$ or when evolution allows the population to benefit from independent co-limitation of carbon and a nutrient. Additionally, we found that repeating the experiment with a number of species with different carbon uptake kinetics supports our conclusion that increasing $[CO_2]^{atm}$, evolution, and different $[HCO_3^-]_{in}$ can interact to affect equilibrium biomass and carbon uptake (Figure A3.1.4). Interestingly, we found that in the cases of *Microcystsis aerguinosa* and *Chlamydomonas reinhardtii*, evolution allowed populations that were unable to survive in conditions with very low $[HCO_3^-]_{in}$ to adapt (Figure A3.1.4).

3.6 Discussion

Our modelling study is based on the principles of classic, dynamic resource competition theory (Tilman, 1977; Chesson, 2000) and aimed to merge this approach with trait-based evolutionary adaptation that follows a fitness-increasing trajectory (Lande, 1976). While our more basic results confirm our expectations, we were able to provide new insights that arise from the interaction of resource competition and evolutionary dynamics predicted by our model. Our study also contributes to an improved understanding of the dynamic competition for substitutable resources; more concretely, for CO_2 and HCO_3^-, which, in water, are linked by a dynamical chemical equilibrium.

First, we found that the model functions in a way consistent with our understanding of evolution. Populations that can adapt to the carbon-limited environment became better competitors compared to the ancestral populations. Mathematically, we showed that CO_2 uptake kinetics of a species evolve towards an EEE at which this species can deplete the dissolved CO_2 concentration to the lowest possible level (Eqn. 3.8 , 3.15). This finding is consistent with the literature on local adaptation, which shows that populations adapted to local conditions frequently have higher levels of fitness than immigrant populations of the same species (Leimu & Fischer, 2008; Hereford, 2009). This finding confirms Hypothesis 1 and is fairly intuitive as natural selection acts by selecting for better adapted individuals.

Second, we found that evolution can change the outcome of competition (consistent with Hypothesis 2). Although not surprising *per se*, it is noteworthy that we observed this result using a modelling approach that implements evolutionary dynamics at the time scale of the ecological dynamics, based on the competing organisms' generation times. Thus, our finding supports what we know to be true on long timescales to be possible on shorter ones. This finding is consistent with another study, where the incorporation of contemporary evolutionary dynamics with population models was shown to explain otherwise anomalous experimental results (Rael, Vincent & Cushing, 2011).

Hendry (2016), in his book on eco-evolutionary dynamics, suggests that evolution generally promotes coexistence. Indeed, a theoretical study using a similar approach to ours, based on R* theory, was able to show that evolution has a stabilizing effect in the case of two consumers competing for two resources, with each resource containing a fixed proportion of two possible essential nutrients (Vasseur & Fox, 2011). In our model, on the other hand, we investigated competition for two substitutable resources, which are further linked via chemical equilibrium. In this case, however, we find that evolution does not promote coexistence between the resource specialist and generalist populations.

In the context of the specialist vs. generalist concept we also observed that it mattered to differentiate the degrees to which different species can evolve. We found that, while the CO_2 specialist evolved to the same EEE, regardless of the initial HCO_3^- concentration, the generalist could reach many different EEE's depending on the initial HCO_3^- concentration. In our example parametrization, the evolving generalist was always able to deplete CO_2 concentrations below the R^* of the CO_2 specialist. Granted, different parametrizations could result in a more efficient CO_2 specialist or less efficient generalist for some range of HCO_3^- values. For example, a CO_2 specialist with a lower carbon content (Q_{C}) could outcompete a specialist across a much wider range of initial HCO_3^-- concentrations (Figure A3.1.2). Furthermore, a trade-off between HCO_3^- and CO_2 could also limit the evolutionary potential of the generalist (discussed below). Nevertheless, by providing an evolutionary mechanism, this finding goes beyond other studies which reported that generalist plant species were often better competitors (Denelle *et al.*, 2020). Indeed, most phytoplankton species are generalist species that can take up both CO_2 and HCO_3^- (Giordano *et al.*, 2005) that occupy a wide variety of niches, whereas CO_2 specialists are often restricted to oligotrophic lakes with relatively high CO_2 concentrations (Raven *et al.*, 2005; Maberly *et al.*, 2009). Furthermore, our results indicate that the benefits of a generalist strategy go beyond the immediate effects of greater resource availability by increasing the evolutionary potential of the population. This result also aligns with a meta-analysis of microbial genomes suggesting that generalist species are the drivers of speciation, whereas specialists are often evolutionary dead-ends (Sriswasdi, Yang & Iwasaki, 2017).

Third, consistent with Hypothesis 3, we found that evolving populations were able to reach higher equilibrium biomass than their non-evolving counterparts, however, differences in biovolume varied widely across different species, atmospheric CO_2 concentrations, and, for the generalist, starting HCO_3^- concentrations. Specifically, extreme resource concentrations maximized the potential for evolution to drive biomass increases because populations were far from their EEE. Several studies focusing on the adaptation of phytoplankton to $[CO_2]^{atm}$=1000 ppm failed to detect adaptive responses, which corresponds to the $[CO_2]^{atm}$ where we find the smallest difference in biovolume between evolving and non-evolving strains (Collins & Bell, 2004, 2005; Low-Décarie *et al.*, 2013). A range of evolutionary responses to increased pCO_2 concentrations have been reported in different studies. For example, one experimental study found that a fitness optimum was reached by the marine phytoplankton *Emiliania huxleyi* within 500 generations of growth at high pCO_2 concentrations (Lohbeck *et al.*, 2013), another found that populations growing in competition had lower fitness levels compared to populations of the same species growing alone (Collins, 2010) and a third concluded that plasticity was a good predictor of a species' evolutionary potential (Schaum & Collins, 2014). This diversity of evolutionary responses indicates that (1) different species may have very different evolutionary potentials, which is consistent with our finding that, if allowed to evolve, the generalist outperforms the CO_2 specialist, and species far from their EEE have a stronger potential for evolution compared to species close to their EEE (2) that an array of environmental factors such as resource concentrations and biological factors such as competition can affect evolutionary potential, consistent with our results, and (3) that there are a variety of evolutionary trade-offs involved in adaptation to increasing atmospheric CO_2, not all of which could be considered in this study.

In our model, we defined a trade-off between affinity and the maximum uptake rate, which was a simple way to constrain evolution. In reality, our simple trade-off does not always hold (Spijkerman, Maberly & Coesel, 2005), nor is it the only trade-off at play. For example, if investment in a high bicarbonate uptake rate comes at the cost of a lower CO_2 uptake rate (Ji *et al.*, 2020), then the CO_2 specialist will have a deeper U-shaped isocline (and hence a lower $[CO_2]^*$; see Figure 3.3) in the absence of bicarbonate than the generalist species. Hence, evolution will favour the CO_2 specialist in environments with low bicarbonate concentrations. Trade-offs with traits beyond carbon uptake could also be considered. For well-studied species such as *Chlamydomonas reinhardtii*, it is possible to construct a model where correlations between many traits, which can be viewed as potential trade-offs, are taken into account to find several optimal configurations of trait values (Walworth *et al.*, 2021). By including However, even with alternative trade-off formulations, there are two possible strategies for a population to evolve to reach higher equilibrium biovolumes in the context of changing pCO_2. (1) Optimize uptake kinetics (e.g., by increasing affinity), which, according to our simulations, is particularly beneficial for certain species in competitive scenarios, or when a population finds itself in an environment where it is very far from its EEE (e.g., the generalist species at extremely low HCO_3^-). (2) Decrease the minimum internal storage of carbon (e.g., Q_C). This strategy is likely to be limited in scope, especially for carbon, which forms the bulk of algal biomass and cannot be substituted by N or P. Nevertheless, alternative trade-off formulations could change the way in which traits respond to increasing atmospheric pCO_2 and the resulting competitive outcomes (Figure A3.1.2).

In conclusion, we found that our simple model showed that evolution can alter the competitive outcome among populations competing for carbon supplied from the atmosphere. Specifically, we found that the generalist was a superior competitor when evolved to adapt to carbon limitation because it had more evolutionary potential, in part because it was able to evolve to different conditions on two fronts: CO_2 and HCO_3^- uptake, whereas the CO_2 specialist was limited to a single evolving trait. Finally, we found that evolution was effective at increasing phytoplankton biomass in response to increasing atmospheric CO_2 in cases where the potential for adaptation was high, such as the generalist growing at very low HCO_3^- concentrations, or by taking advantage of independent nutrient and carbon co-limitation. Further research aimed at understanding the evolutionary responses to increasing atmospheric CO_2 should focus not only on fitness in terms of growth rate, but on an array of traits, including resource affinity and maximum uptake rates of CO_2, HCO_3^-, and other, potentially co-limiting resources to gain more complete understanding of the limits, trade-offs, and evolutionary potentials of different species.

3.7 Acknowledgements

We thank Étienne Low-Décarie, Irene Gregory-Eaves, and Frédéric Guichard for helpful comments and discussion about earlier versions of the manuscript. We thank Julien Cotte for providing a large part of the C++ code used for the model.

3.8 Funding

This work was supported by an NSERC Discovery Grant to GFF [RGPIN-2020-04780]. EK was supported through the GRIL-ÉcoLac NSERC CREATE program.

3.9 References

Adamec L. (2010). Ecophysiological look at plant carnivory. pp. 455–489. Springer Netherlands.

Aksnes D.L. & Egge J.K. (1991). A theoretical model for nutrient uptake in phytoplankton. *Marine Ecology Progress Series* **70**, 65–72

Bach L.T., Lohbeck K.T., Reusch T.B.H. & Riebesell U. (2018). Rapid evolution of highly variable competitive abilities in a key phytoplankton species. *Nature Ecology & Evolution* **2**, 611–613. https://doi.org/10.1038/s41559-018-0474-x

Bernhardt J.R., Kratina P., Pereira A.L., Tamminen M., Thomas M.K. & Narwani A. (2020). The evolution of competitive ability for essential resources. *Philosophical Transactions of the Royal Society B: Biological Sciences* **375**, 20190247. https://doi.org/10.1098/rstb.2019.0247

Chesson P. (2000). Mechanisms of maintenance of species diversity. *Annual Review of Ecology and Systematics* **31**, 343–366. https://doi.org/10.1146/annurev.ecolsys.31.1.343

Cole J.J., Caraco N.F., Kling G.W. & Kratz T.K. (1994). Carbon dioxide supersaturation in the surface waters of lakes. *Science* **265**, 1568

Cole J.J. & Prairie Y.T. (2009). Dissolved CO_2. Oxford: Elsevier.

Collins S. (2010). Competition limits adaptation and productivity in a photosynthetic alga at elevated CO_2. *Proceedings of the Royal Society B: Biological Sciences* **278**, 247–255. https://doi.org/10.1098/rspb.2010.1173

Collins S. & Bell G. (2005). Evolution of natural algal populations at elevated CO_2. *Ecology Letters* **9**, 129–135. https://doi.org/10.1111/j.1461-0248.2005.00854.x

Collins S. & Bell G. (2004). Phenotypic consequences of 1,000 generations of selection at elevated CO_2 in a green alga. *Nature* **431**, 566–569. https://doi.org/10.1038/nature02945

Denelle P., Violle C., Consortium D. & Munoz F. (2020). Generalist plants are more competitive and more functionally similar to each other than specialist plants: Insights from network analyses. *Journal of Biogeography* **47**, 1922–1933. https://doi.org/10.1111/jbi.13848

Dlugokencky E. & Tans P. (2021). NOAA/GML (www.esrl.noaa.gov/gmd/ccgg/trends/)

Dykhuizen D.E. (1990). Experimental Studies of Natural Selection in Bacteria. *Annual Review of Ecology and Systematics* **21**, 373–398. https://doi.org/10.1146/annurev.es.21.110190.002105

Fussmann G.F. & Gonzalez A. (2013). Evolutionary rescue can maintain an oscillating community undergoing environmental change. *Interface focus* **3**, 20130036–20130036. https://doi.org/10.1098/rsfs.2013.0036

Giordano M., Beardall J. & Raven J.A. (2005). CO_2 concentrating mechanisms in algae: Mechanisms, environmental modulation, and evolution. *Annual Review of Plant Biology* **56**, 99–131. https://doi.org/10.1146/annurev.arplant.56.032604.144052

Grant P.R. (1999). *Ecology and evolution of darwin's finches*. Princeton University Press.

Gresham D., Desai M.M., Tucker C.M., Jenq H.T., Pai D.A., Ward A., *et al.* (2008). The Repertoire and Dynamics of Evolutionary Adaptations to Controlled Nutrient-Limited Environments in Yeast. *PLoS Genetics* **4**, e1000303. https://doi.org/10.1371/journal.pgen.1000303

Hendry A.P. (2016). *Eco-evolutionary dynamics:* Princeton University Press.

Hereford J. (2009). A Quantitative Survey of Local Adaptation and Fitness Trade-Offs. *The American Naturalist* **173**, 579–588. https://doi.org/10.1086/597611

Hutchinson G.E. (1961). The Paradox of the Plankton. *The American Naturalist* **95**, 137–145. https://doi.org/10.1086/282171

Iversen L.L., Winkel A., Baastrup-Spohr L., Hinke A.B., Alahuhta J., Baattrup-Pedersen A., *et al.* (2019). Catchment properties and the photosynthetic trait composition of freshwater plant communities. *Science* **366**, 878–881. https://doi.org/10.1126/science.aay5945

Ji X., Verspagen J.M.H., Van de Waal D.B., Rost B. & Huisman J. (2020). Phenotypic plasticity of carbon fixation stimulates cyanobacterial blooms at elevated CO_2. *Science Advances* **6**, eaax2926. https://doi.org/10.1126/sciadv.aax2926

Lande R. (1976). Natural selection and random genetic drift in phenotypic evolution. *Evolution* **30**, 314–334. https://doi.org/10.2307/2407703

Leimu R. & Fischer M. (2008). A Meta-Analysis of Local Adaptation in Plants. *PLoS ONE* **3**, e4010. https://doi.org/10.1371/journal.pone.0004010

Lindberg R.T. & Collins S. (2020). Qualityquantity trade-offs drive functional trait evolution in a model microalgal 'climate change winner'. *Ecology Letters* **23**, 780–790. https://doi.org/10.1111/ele.13478

Lohbeck K.T., Riebesell U., Collins S. & Reusch T.B.H. (2013). Functional genetic divergence in high CO_2 adapted *Emiliania huxleyi* populations. *Evolution* **67**, 1892–1900. https://doi.org/10.1111/j.1558-5646.2012.01812.x

Low-Décarie E., Jewell M.D., Fussmann G.F. & Bell G. (2013). Long-term culture at elevated atmospheric CO_2 fails to evoke specific adaptation in seven freshwater phytoplankton species. *Proceedings of the Royal Society B: Biological Sciences* **280**. https://doi.org/10.1098/rspb.2012.2598

Maberly S.C., Ball L.A., Raven J.A. & Sültemeyer D. (2009). Inorganic carbon acquisition by chrysophytes. *Journal of Phycology* **45**, 1052–1061. https://doi.org/10.1111/j.1529-8817.2009.00734.x

Maberly S.C. & Gontero B. (2017). Ecological imperatives for aquatic CO_2-concentrating mechanisms. *Journal of Experimental Botany* **68**, 3797–3814. https://doi.org/10.1093/jxb/erx201

Padfield D., Yvon-Durocher G., Buckling A., Jennings S. & Yvon-Durocher G. (2016). Rapid evolution of metabolic traits explains thermal adaptation in phytoplankton. *Ecology Letters* **19**, 133–142. https://doi.org/10.1111/ele.12545

Price G.D., Badger M.R., Woodger F.J. & Long B.M. (2007). Advances in understanding the cyanobacterial CO_2-concentrating-mechanism (CCM): functional components, Ci transporters, diversity, genetic regulation and prospects for engineering into plants. *Journal of Experimental Botany* **59**, 1441–1461. https://doi.org/10.1093/jxb/erm112

Rael R.C., Vincent T.L. & Cushing J.M. (2011). Competitive outcomes changed by evolution. *Journal of Biological Dynamics* **5**, 227–252. https://doi.org/10.1080/17513758.2010.487160

Raven J.A., Ball L.A., Beardall J., Giordano M. & Maberly S.C. (2005). Algae lacking carbon-concentrating mechanisms. *Canadian Journal of Botany* **83**, 879–890. https://doi.org/10.1139/b05-074

Sandrini G., Ji X., Verspagen J.M.H., Tann R.P., Slot P.C., Luimstra V.M., *et al.* (2016). Rapid adaptation of harmful cyanobacteria to rising CO_2. *Proceedings of the National Academy of Sciences* **113**, 9315–9320. https://doi.org/10.1073/pnas.1602435113

Sandrini G., Matthijs H.C.P., Verspagen J.M.H., Muyzer G. & Huisman J. (2013). Genetic diversity of inorganic carbon uptake systems causes variation in CO_2 response of the cyanobacterium Microcystis. *The ISME Journal* **8**, 589–600. https://doi.org/10.1038/ismej.2013.179

Schaum C.E. & Collins S. (2014). Plasticity predicts evolution in a marine alga. *Proceedings of the Royal Society B: Biological Sciences* **281**, 20141486. https://doi.org/10.1098/rspb.2014.1486

Scheinin M., Riebesell U., Rynearson T.A., Lohbeck K.T. & Collins S. (2015). Experimental evolution gone wild. *Journal of The Royal Society Interface* **12**, 20150056. https://doi.org/10.1098/rsif.2015.0056

Simmons R.E. & Altwegg R. (2010). Necks-for-sex or competing browsers? A critique of ideas on the evolution of giraffe. *Journal of Zoology* **282**, 6–12. https://doi.org/10.1111/j.1469-7998.2010.00711.x

Sperfeld E., Raubenheimer D. & Wacker A. (2016). Bridging factorial and gradient concepts of resource co-limitation: Towards a general framework applied to consumers. *Ecology Letters* **19**, 201–215. https://doi.org/10.1111/ele.12554

Spijkerman E., de Castro F. & Gaedke U. (2011). Independent colimitation for carbon dioxide and inorganic phosphorus. *PLOS ONE* **6**, e28219. https://doi.org/10.1371/journal.pone.0028219

Spijkerman E., Maberly S.C. & Coesel P.F. (2005). Carbon acquisition mechanisms by planktonic desmids and their link to ecological distribution. *Canadian Journal of Botany* **83**, 850–858. https://doi.org/10.1139/b05-069

Sriswasdi S., Yang C. & Iwasaki W. (2017). Generalist species drive microbial dispersion and evolution. *Nature Communications* **8**, 1162. https://doi.org/10.1038/s41467-017-01265-1

Tamminen M., Betz A., Pereira A.L., Thali M., Matthews B., Suter M.J.-F., *et al.* (2018). Proteome evolution under non-substitutable resource limitation. *Nature Communications* **9**. https://doi.org/10.1038/s41467-018-07106-z

Tilman D. (1982). *Resource competition and community structure*. Princeton university press.

Tilman D. (1977). Resource competition between plankton algae: An experimental and theoretical approach. *Ecology* **58**, 338–348. https://doi.org/10.2307/1935608

Tilman D. (1980). Resources: A graphical-mechanistic approach to competition and predation. *The American Naturalist* **116**, 362–393

Titus J.E. & Pagano A.M. (2017). Carbon dioxide and submersed macrophytes in lakes: linking functional ecology to community composition. *Ecology* **98**, 3096–3105. https://doi.org/10.1002/ecy.2030

USEPA (US Environmental Protection Agency) (2009). *National lakes assessment: A collaborative survey of the nation's lakes*. USEPA Office of Water Washington.

Vasseur D.A. & Fox J.W. (2011). Adaptive Dynamics of Competition for Nutritionally Complementary Resources: Character Convergence, Displacement, and Parallelism. *The American Naturalist* **178**, 501–514. https://doi.org/10.1086/661896

Verspagen J.M.H., Van de Waal D.B., Finke J.F., Visser P.M., Van Donk E. & Huisman J. (2014). Rising CO_2 Levels Will Intensify Phytoplankton Blooms in Eutrophic and Hypertrophic Lakes. *PLoS ONE* **9**, e104325. https://doi.org/10.1371/journal.pone.0104325

Walworth N.G., Hinners J., Argyle P.A., Leles S.G., Doblin M.A., Collins S., *et al.* (2021). The evolution of trait correlations constrains phenotypic adaptation to high CO_2 in a eukaryotic alga. *Proceedings of the Royal Society B: Biological Sciences* **288**, 20210940. https://doi.org/10.1098/rspb.2021.0940

4 Discussion

Atmospheric CO_2 concentrations continue to rise, potentially affecting ecosystems across the globe, yet few studies (see Introduction) have focused on the effects of rising pCO_2 in freshwaters. I argue that although rising CO_2 tends to have an accessory role in the eco-evolutionary dynamics of phytoplankton communities, it can still impact lake ecosystems and their health around the world. I support this argument on three fronts: CO_2 can be a co-limiting resource (Chapter 1), the combined effects of increasing atmospheric CO_2 with the highly associated increases in temperature (Chapter 2) and the role of evolution in the context of increasing pCO_2 (Chapter 3).

First, Spijkerman *et al.* (2011) provided laboratory evidence of independent co-limitation of *Chlamydomonas acidophila* for CO_2 and inorganic phosphorus. In Chapter 1, I found support for independent co-limitation of semi-natural phytoplankton communities for CO_2 and inorganic phosphorus. Given that control mesocosms had pCO_2=400 ppm, and summer alkalinity in the study systems was 0.48 to 0.66 meq/L, it seems likely that co-limitation between CO_2 and phosphorus (or possibly other resources) would occur under similar conditions, or ones with lower inorganic carbon concentrations (although support from additional studies would be useful). These pCO_2 conditions are typical of eutrophic, and some mesotrophic lakes, which are particularly at risk of degrading ecosystem health, are often located near human settlements, and are therefore likely to negatively impact humans when they deteriorate. Furthermore, in Chapter 2 I found that, relative to mesocosms with pre-industrial levels of pCO_2, mesocosms with enriched pCO_2 had higher phytoplankton biomass on three of ten sampling days. This suggests that contemporary atmospheric CO_2 concentrations may already be contributing to water quality issues in at-risk systems and are likely to be exacerbated if CO_2 emissions do not decrease.

Second, increasing atmospheric CO_2 also causes global increases in temperature, and both factors can affect aquatic communities. Although, in Chapter 2, we did not find that temperature and CO_2 interact in terms of their effects on biomass and community composition, we still find that both factors have independent and potentially additive effects. Temperature affects the metabolic rates of many organisms, an observation that is supported in Chapter 2, where the phytoplankton and zooplankton communities responded, on some sampling dates, to the warming treatment. CO_2, on the other hand, can affect the nutritional quality of phytoplankton, a finding that is supported in Chapter 2, where I found that seston C:N ratios increased with increasing pCO_2. Although we did not find that the nutritional effect translated to the zooplankton community, the slow zooplankton generation times caused by cold November temperatures could be at cause. Thus, although more research is needed about the combined effects of increasing CO_2 and temperature, it is clear that both factors can affect aquatic ecosystems.

Third, phytoplankton species are likely to adapt to changing CO_2 concentrations, which may cause shifts in phytoplankton community composition and increased biomass. A number of studies have found that changing CO_2 can affect the processes of evolutionary selection and adaptation and interact with a number of other factors (see Introduction). In Chapter 3, I showed that species that can adapt carbon kinetics are able to outcompete their non-evolving brethren and potentially other competitors, which can lead to changes in the community composition. However, the manner in which species may adapt remains an open question, making it difficult to predict how communities may respond to changing pCO_2. On the other hand, as I found in chapter 3, the difference between equilibrium biomass of an evolving and non-evolving species is affected by increasing pCO_2, co-limitation and HCO_3^- concentrations. This finding means that phytoplankton species adapt to the changing environment, they may increase their biomass. As a result, species' evolutionary responses may cause further degradation of water quality.

In conclusion, I found that although CO_2 is unlikely to be the main driver of degrading water quality, it can be an exacerbating factor. In particular, the effects of CO_2 on biomass are most prominent when nutrients are added (Chapter 1 & 2), though evolutionary responses may also be important even when other resources are more strongly limiting (Chapter 3). The results are less clear when it comes to the effects of CO_2 on community composition. Although I saw shifts in community composition across all three Chapters, no general treads emerged. Experiments with species-level taxonomic resolution, or molecular sampling may provide greater clarity, but, as it stands, the community composition response to increasing pCO_2 remains unknown, as are the repercussions of these shifts on water quality. Although the evidence from Chapter 3 suggests that the effects of increasing CO_2 could lead to cascading effects, impacting entire food webs, concrete evidence remains lacking in natural freshwater communities. Investigating the role of CO_2 in freshwater ecosystems provides a unique opportunity to gain a deeper understanding of eco-evolutionary dynamics of phytoplankton, and their cascading effects, while contributing to the greater goal of understanding the impacts of climate change on our precious freshwater resources and the world.

4.1 Reference

Spijkerman E., Castro F. de & Gaedke U. (2011). Independent co-limitation for carbon dioxide and inorganic phosphorus. *PLOS ONE* **6**, e28219. https://doi.org/10.1371/journal.pone.0028219

Appendix A1

Figure A1.1: Picture diagram illustrating the method for controlling CO_2 in mesocosms. Not pictured: timer controlling pumps, set to ON every sixth fifteen-minute interval (i.e. bubbling for 15 minutes every 1.5 hours). Furthermore, two solenoid valves were used for redundancy.

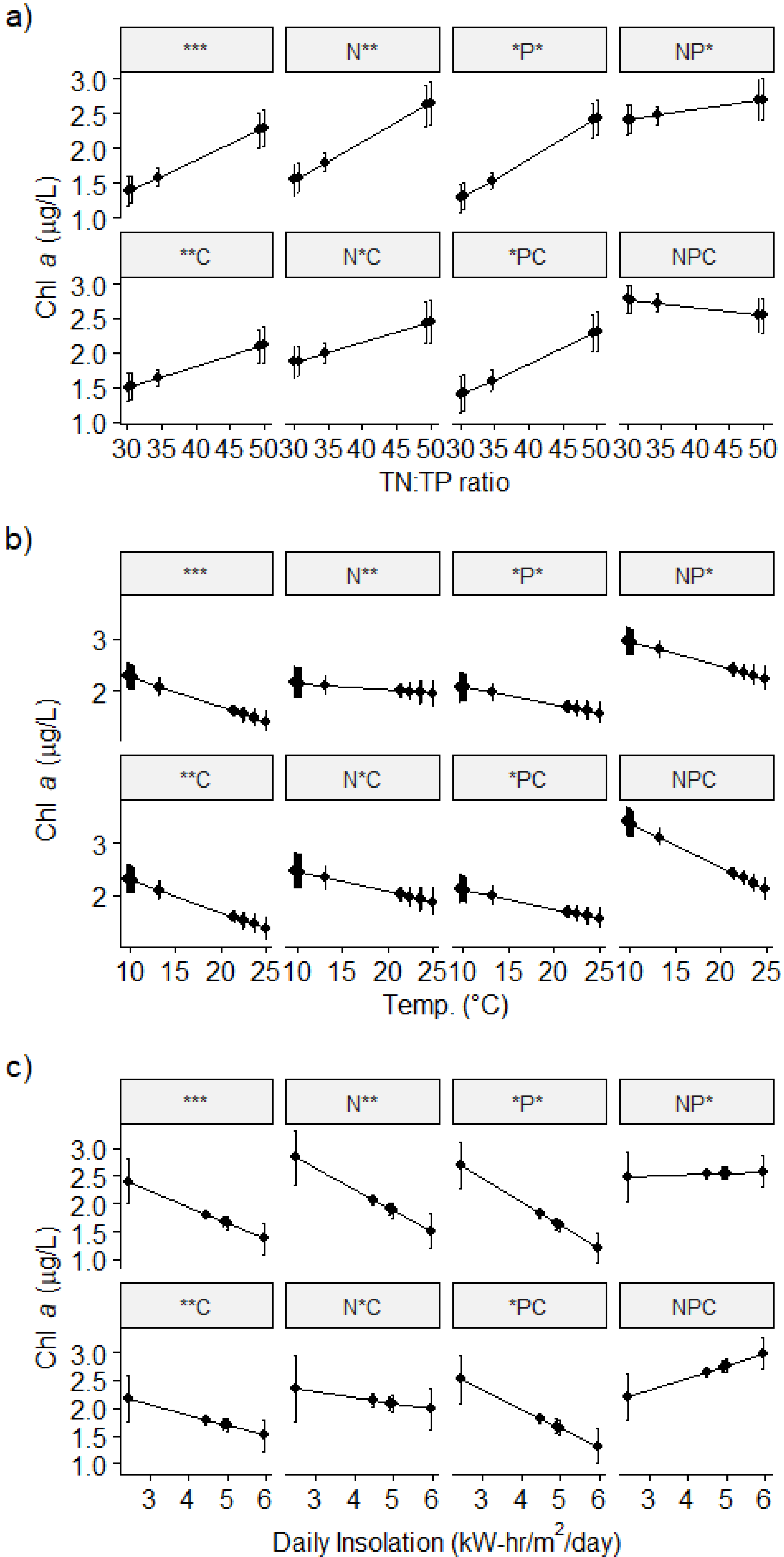

a)
***
N**
P
NP*
**C
N*C
*PC
NPC
3.0
2.5
2.0
1.5
1.0
Chl a (µg/L)
30 35 40 45 50
TN:TP ratio
b)
***
N**
P
NP*
**C
N*C
*PC
NPC
3
2
Chl a (µg/L)
10 15 20 25
Temp. (°C)
c)
***
N**
P
NP*
**C
N*C
*PC
NPC
3.0
2.5
2.0
1.5
1.0
Chl a (µg/L)
3 4 5 6
Daily Insolation (kW-hr/m2/day)

Figure A1.2: Model-estimated marginal means of different experimental treatments (Nitrogen, Phosphorus, and CO_2) as functions of (a) the mean TN:TP ratios in control mesocosms, (b) water temperature in each mesocosm and (c) average daily insolation across the duration of each experiment.

Table A1.1: List of bags that broke over the course of an experiment (or were contaminated, for the case of Mesocosms 7, 14 and 24 in August 2015). The number of days after the start of the experiment that the breakage in the bags were discovered (DaysAfterStart) were recorded in 2015 only. See Figure 1.2 in the main text for explanation of Treatment notation.

Experiment	DaysAfterStart	MesocosmID	Treatment
August 2015	7 days	21	N*C
August 2015	26 days	13	**C
August 2015	8 days	7	*PC
August 2015	8 days	14	*PC
August 2015	8 days	24	*PC
October 2015	3 days	17	N*C
October 2015	9 days	6	N*C
October 2015	13 days	9	N**
April 2016	1 days	2	N*C
April 2016	1 days	4	*P*
April 2016	1 days	5	N**
April 2016	1 days	7	NPC
April 2016	1 days	8	**C
June 2016	1 days	10	NP*
June 2016	1 days	14	N**

Table A2.2: Parameter estimates for model log(Total Chlorophyll a) ~ Nitrogen*Phosphorus*CO2*Experiment.

Term	Estimate	Std. Error	Lower 95%	Upper 95%
Intercept	2.237	0.087	2.063	2.411
NitrogenNo	0.237	0.123	-0.009	0.483
NitrogenYes	1.138	0.138	0.863	1.413
PhosphorusNo	-0.692	0.151	-0.993	-0.391
PhosphorusYes	-0.258	0.138	NA	NA
CO2No	-1.007	0.123	-0.533	0.017
CO2Yes	-0.465	0.123	NA	NA
ExperimentAugust2015	-0.827	0.123	-1.253	-0.761
ExperimentJuly2015	-0.22	0.123	-0.711	-0.219
ExperimentJune2016	0.801	0.205	-1.073	-0.581
ExperimentOctober2015	0.311	0.195	-0.466	0.026
NitrogenNo:PhosphorusNo	0.194	0.205	0.393	1.209

Term	Estimate	Std. Error	Lower 95%	Upper 95%
NitrogenYes:PhosphorusNo	-0.2	0.381	NA	NA
NitrogenNo:PhosphorusYes	0.135	0.185	NA	NA
NitrogenYes:PhosphorusYes	-0.409	0.175	NA	NA
NitrogenNo:CO2No	-0.486	0.185	-0.077	0.7
NitrogenYes:CO2No	-0.276	0.175	NA	NA
NitrogenNo:CO2Yes	-0.088	0.185	NA	NA
NitrogenYes:CO2Yes	0.084	0.175	NA	NA
PhosphorusNo:CO2No	-0.431	0.185	-0.214	0.602
PhosphorusYes:CO2No	-0.171	0.205	NA	NA
PhosphorusNo:CO2Yes	0.352	0.195	NA	NA
PhosphorusYes:CO2Yes	0.141	0.195	NA	NA
NitrogenNo:ExperimentAugust2015	0.3	0.231	-0.958	0.558
NitrogenYes:ExperimentAugust2015	0.02	0.185	-0.234	0.504
NitrogenNo:ExperimentJuly2015	0.09	0.185	-0.757	-0.061
NitrogenYes:ExperimentJuly2015	0.087	0.195	-0.855	-0.117
NitrogenNo:ExperimentJune2016	0.139	0.185	-0.624	0.071
NitrogenYes:ExperimentJune2016	-0.151	0.283	-0.457	0.28

Term	Estimate	Std. Error	Lower 95%	Upper 95%
NitrogenNo:ExperimentOctober2015	0.132	0.262	-0.264	0.432
NitrogenYes:ExperimentOctober2015	-0.555	0.269	-0.8	-0.062
PhosphorusNo:ExperimentAugust2015	-0.31	0.269	-0.579	0.237
PhosphorusYes:ExperimentAugust2015	-0.506	0.296	NA	NA
PhosphorusNo:ExperimentJuly2015	-0.213	0.276	-0.037	0.74
PhosphorusYes:ExperimentJuly2015	-0.101	0.262	NA	NA
PhosphorusNo:ExperimentJune2016	-0.158	0.269	-0.248	0.53
PhosphorusYes:ExperimentJune2016	-0.158	0.262	NA	NA
PhosphorusNo:ExperimentOctober2015	-0.039	0.276	-0.16	0.76
PhosphorusYes:ExperimentOctober2015	-0.136	0.269	NA	NA
CO2No:ExperimentAugust2015	-0.354	0.283	-0.349	0.389
CO2Yes:ExperimentAugust2015	0.023	0.303	NA	NA
CO2No:ExperimentJuly2015	0.076	0.376	-0.279	0.459
CO2Yes:ExperimentJuly2015	0.269	0.386	NA	NA
CO2No:ExperimentJune2016	-0.034	0.4	-0.302	0.476
CO2Yes:ExperimentApril:2016	2.237	0.087	NA	NA
CO2No:ExperimentJune:2016	0.237	0.123	-0.23	0.508

Term	Estimate	Std. Error	Lower 95%	Upper 95%
CO2Yes:ExperimentOctober2015	1.138	0.138	NA	NA
NitrogenNo:PhosphorusNo:CO2No	-0.692	0.151	-0.714	0.413
NitrogenYes:PhosphorusNo:CO2No	-0.258	0.138	NA	NA
NitrogenNo:PhosphorusYes:CO2No	-1.007	0.123	NA	NA
NitrogenYes:PhosphorusYes:CO2No	-0.465	0.123	NA	NA
NitrogenNo:PhosphorusNo:CO2Yes	-0.827	0.123	NA	NA
NitrogenYes:PhosphorusNo:CO2Yes	-0.22	0.123	NA	NA
NitrogenNo:PhosphorusYes:CO2Yes	0.801	0.205	NA	NA
NitrogenYes:PhosphorusYes:CO2Yes	0.311	0.195	NA	NA
NitrogenNo:PhosphorusNo:ExperimentAugust2015	0.194	0.205	-0.389	0.654
NitrogenYes:PhosphorusNo:ExperimentAugust2015	-0.2	0.381	NA	NA
NitrogenNo:PhosphorusYes:ExperimentAugust2015	0.135	0.185	NA	NA
NitrogenYes:PhosphorusYes:ExperimentAugust2015	-0.409	0.175	NA	NA
NitrogenNo:PhosphorusNo:ExperimentJuly2015	-0.486	0.185	-1.091	-0.019
NitrogenYes:PhosphorusNo:ExperimentJuly2015	-0.276	0.175	NA	NA
NitrogenNo:PhosphorusYes:ExperimentJuly2015	-0.088	0.185	NA	NA
NitrogenYes:PhosphorusYes:ExperimentJuly2015	0.084	0.175	NA	NA

Term	Estimate	Std. Error	Lower 95%	Upper 95%
NitrogenNo:PhosphorusNo:ExperimentJune2016	-0.431	0.185	-0.846	0.226
NitrogenYes:PhosphorusNo:ExperimentJune2016	-0.171	0.205	NA	NA
NitrogenNo:PhosphorusYes:ExperimentJune2016	0.352	0.195	NA	NA
NitrogenYes:PhosphorusYes:ExperimentJune2016	0.141	0.195	NA	NA
NitrogenNo:PhosphorusNo:ExperimentOctober2015	0.3	0.231	-1.096	0.084
NitrogenYes:PhosphorusNo:ExperimentOctober2015	0.02	0.185	NA	NA
NitrogenNo:PhosphorusYes:ExperimentOctober2015	0.09	0.185	NA	NA
NitrogenYes:PhosphorusYes:ExperimentOctober2015	0.087	0.195	NA	NA
NitrogenNo:CO2No:ExperimentAugust2015	0.139	0.185	-0.763	0.337
NitrogenYes:CO2No:ExperimentAugust2015	-0.151	0.283	NA	NA
NitrogenNo:CO2Yes:ExperimentAugust2015	0.132	0.262	NA	NA
NitrogenYes:CO2Yes:ExperimentAugust2015	-0.555	0.269	NA	NA
NitrogenNo:CO2No:ExperimentJuly2015	-0.31	0.269	-0.622	0.421
NitrogenYes:CO2No:ExperimentJuly2015	-0.506	0.296	NA	NA
NitrogenNo:CO2Yes:ExperimentJuly2015	-0.213	0.276	NA	NA
NitrogenYes:CO2Yes:ExperimentJuly2015	-0.101	0.262	NA	NA
NitrogenNo:CO2No:ExperimentJune2016	-0.158	0.269	-0.694	0.378

Term	Estimate	Std. Error	Lower 95%	Upper 95%
NitrogenYes:CO2No:ExperimentJune2016	-0.158	0.262	NA	NA
NitrogenNo:CO2Yes:ExperimentJune2016	-0.039	0.276	NA	NA
NitrogenYes:CO2Yes:ExperimentJune2016	-0.136	0.269	NA	NA
NitrogenNo:CO2No:ExperimentOctober2015	-0.354	0.283	-0.68	0.363
NitrogenYes:CO2No:ExperimentOctober2015	0.023	0.303	NA	NA
NitrogenNo:CO2Yes:ExperimentOctober2015	0.076	0.376	NA	NA
NitrogenYes:CO2Yes:ExperimentOctober2015	0.269	0.386	NA	NA
PhosphorusNo:CO2No:ExperimentAugust2015	-0.034	0.4	-0.589	0.511
PhosphorusYes:CO2No:ExperimentAugust2015	2.237	0.087	NA	NA
PhosphorusNo:CO2Yes:ExperimentAugust2015	0.237	0.123	NA	NA
PhosphorusYes:CO2Yes:ExperimentAugust2015	1.138	0.138	NA	NA
PhosphorusNo:CO2No:ExperimentJuly2015	-0.692	0.151	-0.672	0.4
PhosphorusYes:CO2No:ExperimentJuly2015	-0.258	0.138	NA	NA
PhosphorusNo:CO2Yes:ExperimentJuly2015	-1.007	0.123	NA	NA
PhosphorusYes:CO2Yes:ExperimentJuly2015	-0.465	0.123	NA	NA
PhosphorusNo:CO2No:ExperimentJune2016	-0.827	0.123	-0.918	0.209
PhosphorusYes:CO2No:ExperimentJune2016	-0.22	0.123	NA	NA

Term	Estimate	Std. Error	Lower 95%	Upper 95%
PhosphorusNo:CO2Yes:ExperimentJune2016	0.801	0.205	NA	NA
PhosphorusYes:CO2Yes:ExperimentJune2016	0.311	0.195	NA	NA
PhosphorusNo:CO2No:ExperimentOctober2015	0.194	0.205	-0.579	0.625
PhosphorusYes:CO2No:ExperimentOctober2015	-0.2	0.381	NA	NA
PhosphorusNo:CO2Yes:ExperimentOctober2015	0.135	0.185	NA	NA
PhosphorusYes:CO2Yes:ExperimentOctober2015	-0.409	0.175	NA	NA
NitrogenNo:PhosphorusNo:CO2No:ExperimentAugust2015	-0.486	0.185	NA	NA
NitrogenYes:PhosphorusNo:CO2No:ExperimentAugust2015	-0.276	0.175	NA	NA
NitrogenNo:PhosphorusYes:CO2No:ExperimentAugust2015	-0.088	0.185	NA	NA
NitrogenYes:PhosphorusYes:CO2No:ExperimentAugust2015	0.084	0.175	NA	NA
NitrogenNo:PhosphorusNo:CO2Yes:ExperimentAugust2015	-0.431	0.185	NA	NA
NitrogenYes:PhosphorusNo:CO2Yes:ExperimentAugust2015	-0.171	0.205	NA	NA
NitrogenNo:PhosphorusYes:CO2Yes:ExperimentAugust2015	0.352	0.195	NA	NA
NitrogenYes:PhosphorusYes:CO2Yes:ExperimentAugust2015	0.141	0.195	NA	NA
NitrogenNo:PhosphorusNo:CO2No:ExperimentJuly2015	0.3	0.231	-0.671	0.824
NitrogenYes:PhosphorusNo:CO2No:ExperimentJuly2015	0.02	0.185	NA	NA
NitrogenNo:PhosphorusYes:CO2No:ExperimentJuly2015	0.09	0.185	NA	NA

Term	Estimate	Std. Error	Lower 95%	Upper 95%
NitrogenYes:PhosphorusYes:CO2No:ExperimentJuly2015	0.087	0.195	NA	NA
NitrogenNo:PhosphorusNo:CO2Yes:ExperimentJuly2015	0.139	0.185	NA	NA
NitrogenYes:PhosphorusNo:CO2Yes:ExperimentJuly2015	-0.151	0.283	NA	NA
NitrogenNo:PhosphorusYes:CO2Yes:ExperimentJuly2015	0.132	0.262	NA	NA
NitrogenYes:PhosphorusYes:CO2Yes:ExperimentJuly2015	-0.555	0.269	NA	NA
NitrogenNo:PhosphorusNo:CO2No:ExperimentJune2016	-0.31	0.269	-0.499	1.037
NitrogenYes:PhosphorusNo:CO2No:ExperimentJune2016	-0.506	0.296	NA	NA
NitrogenNo:PhosphorusYes:CO2No:ExperimentJune2016	-0.213	0.276	NA	NA
NitrogenYes:PhosphorusYes:CO2No:ExperimentJune2016	-0.101	0.262	NA	NA
NitrogenNo:PhosphorusNo:CO2Yes:ExperimentJune2016	-0.158	0.269	NA	NA
NitrogenYes:PhosphorusNo:CO2Yes:ExperimentJune2016	-0.158	0.262	NA	NA
NitrogenNo:PhosphorusYes:CO2Yes:ExperimentJune2016	-0.039	0.276	NA	NA
NitrogenYes:PhosphorusYes:CO2Yes:ExperimentJune2016	-0.136	0.269	NA	NA
NitrogenNo:PhosphorusNo:CO2No:ExperimentOctober2015	-0.354	0.283	-0.831	0.762
NitrogenYes:PhosphorusNo:CO2No:ExperimentOctober2015	0.023	0.303	NA	NA
NitrogenNo:PhosphorusYes:CO2No:ExperimentOctober2015	0.076	0.376	NA	NA
NitrogenYes:PhosphorusYes:CO2No:ExperimentOctober2015	0.269	0.386	NA	NA

Term	Estimate	Std. Error	Lower 95%	Upper 95%
NitrogenNo:PhosphorusNo:CO2Yes:ExperimentOctober2015	-0.034	0.4	NA	NA
NitrogenYes:PhosphorusNo:CO2Yes:ExperimentOctober2015	2.237	0.087	NA	NA
NitrogenNo:PhosphorusYes:CO2Yes:ExperimentOctober2015	0.237	0.123	NA	NA
NitrogenYes:PhosphorusYes:CO2Yes:ExperimentOctober2015	1.138	0.138	NA	NA

Table A2.3: Parameter estimates for model Chlorophytes ~ Nitrogen*Phosphorus*CO2*Experiment.

Term	Estimate	Std. Error	Lower 95%	Upper 95%
Intercept	4.133	0.405	3.328	4.939
NitrogenNo	1.225	0.572	0.086	2.365
NitrogenYes	7.826	0.64	6.552	9.1
PhosphorusNo	-6.025	0.701	-7.421	-4.63
PhosphorusYes	-2.607	0.64	NA	NA
CO2No	-2.63	0.572	-3.881	-1.333
CO2Yes	-2.208	0.572	NA	NA
ExperimentAugust2015	-1.232	0.572	-3.77	-1.491
ExperimentJuly2015	-1.827	0.572	-3.348	-1.069
ExperimentJune2016	6.41	0.949	-2.372	-0.093
ExperimentOctober2015	2.919	0.905	-2.966	-0.687

Term	Estimate	Std. Error	Lower 95%	Upper 95%
NitrogenNo:PhosphorusNo	2.423	0.949	4.52	8.299
NitrogenYes:PhosphorusNo	-2.328	1.764	NA	NA
NitrogenNo:PhosphorusYes	-3.543	0.858	NA	NA
NitrogenYes:PhosphorusYes	-0.197	0.809	NA	NA
NitrogenNo:CO2No	-3.769	0.858	1.118	4.721
NitrogenYes:CO2No	-1.721	0.809	NA	NA
NitrogenNo:CO2Yes	-3.359	0.858	NA	NA
NitrogenYes:CO2Yes	0.223	0.809	NA	NA
PhosphorusNo:CO2No	-6.108	0.858	0.534	4.313
PhosphorusYes:CO2No	3.249	0.949	NA	NA
PhosphorusNo:CO2Yes	5.905	0.905	NA	NA
PhosphorusYes:CO2Yes	2.094	0.905	NA	NA
NitrogenNo:ExperimentAugust2015	4.872	1.071	-5.84	1.184
NitrogenYes:ExperimentAugust2015	1.181	0.858	-5.252	-1.833
NitrogenNo:ExperimentJuly2015	1.295	0.858	-1.808	1.415
NitrogenYes:ExperimentJuly2015	0.712	0.905	-5.478	-2.059
NitrogenNo:ExperimentJune2016	1.672	0.858	-3.332	-0.11

Term	Estimate	Std. Error	Lower 95%	Upper 95%
NitrogenYes:ExperimentJune2016	-2.524	1.311	-5.068	-1.65
NitrogenNo:ExperimentOctober2015	-1.979	1.214	-1.388	1.835
NitrogenYes:ExperimentOctober2015	-6.775	1.247	-7.817	-4.399
PhosphorusNo:ExperimentAugust2015	-2.792	1.247	1.36	5.139
PhosphorusYes:ExperimentAugust2015	-6.082	1.372	NA	NA
PhosphorusNo:ExperimentJuly2015	-0.213	1.28	4.103	7.706
PhosphorusYes:ExperimentJuly2015	-1.774	1.214	NA	NA
PhosphorusNo:ExperimentJune2016	-1.126	1.247	0.293	3.896
PhosphorusYes:ExperimentJune2016	-2.432	1.214	NA	NA
PhosphorusNo:ExperimentOctober2015	-1.416	1.28	2.741	7.004
PhosphorusYes:ExperimentOctober2015	-2.848	1.247	NA	NA
CO2No:ExperimentAugust2015	-1.34	1.311	-0.528	2.89
CO2Yes:ExperimentAugust2015	-1.948	1.402	NA	NA
CO2No:ExperimentJuly2015	3.277	1.74	-0.414	3.004
CO2Yes:ExperimentJuly2015	1.495	1.787	NA	NA
CO2No:ExperimentJune2016	2.635	1.854	-1.09	2.513
CO2Yes:ExperimentApril:2016	4.133	0.405	NA	NA

Term	Estimate	Std. Error	Lower 95%	Upper 95%
CO2No:ExperimentJune:2016	1.225	0.572	-0.037	3.381
CO2Yes:ExperimentOctober2015	7.826	0.64	NA	NA
NitrogenNo:PhosphorusNo:CO2No	-6.025	0.701	-5.134	0.087
NitrogenYes:PhosphorusNo:CO2No	-2.607	0.64	NA	NA
NitrogenNo:PhosphorusYes:CO2No	-2.63	0.572	NA	NA
NitrogenYes:PhosphorusYes:CO2No	-2.208	0.572	NA	NA
NitrogenNo:PhosphorusNo:CO2Yes	-1.232	0.572	NA	NA
NitrogenYes:PhosphorusNo:CO2Yes	-1.827	0.572	NA	NA
NitrogenNo:PhosphorusYes:CO2Yes	6.41	0.949	NA	NA
NitrogenYes:PhosphorusYes:CO2Yes	2.919	0.905	NA	NA
NitrogenNo:PhosphorusNo:ExperimentAugust2015	2.423	0.949	-4.396	0.438
NitrogenYes:PhosphorusNo:ExperimentAugust2015	-2.328	1.764	NA	NA
NitrogenNo:PhosphorusYes:ExperimentAugust2015	-3.543	0.858	NA	NA
NitrogenYes:PhosphorusYes:ExperimentAugust2015	-0.197	0.809	NA	NA
NitrogenNo:PhosphorusNo:ExperimentJuly2015	-3.769	0.858	-9.258	-4.292
NitrogenYes:PhosphorusNo:ExperimentJuly2015	-1.721	0.809	NA	NA
NitrogenNo:PhosphorusYes:ExperimentJuly2015	-3.359	0.858	NA	NA

Term	Estimate	Std. Error	Lower 95%	Upper 95%
NitrogenYes:PhosphorusYes:ExperimentJuly2015	0.223	0.809	NA	NA
NitrogenNo:PhosphorusNo:ExperimentJune2016	-6.108	0.858	-5.275	-0.309
NitrogenYes:PhosphorusNo:ExperimentJune2016	3.249	0.949	NA	NA
NitrogenNo:PhosphorusYes:ExperimentJune2016	5.905	0.905	NA	NA
NitrogenYes:PhosphorusYes:ExperimentJune2016	2.094	0.905	NA	NA
NitrogenNo:PhosphorusNo:ExperimentOctober2015	4.872	1.071	-8.814	-3.35
NitrogenYes:PhosphorusNo:ExperimentOctober2015	1.181	0.858	NA	NA
NitrogenNo:PhosphorusYes:ExperimentOctober2015	1.295	0.858	NA	NA
NitrogenYes:PhosphorusYes:ExperimentOctober2015	0.712	0.905	NA	NA
NitrogenNo:CO2No:ExperimentAugust2015	1.672	0.858	-2.761	2.334
NitrogenYes:CO2No:ExperimentAugust2015	-2.524	1.311	NA	NA
NitrogenNo:CO2Yes:ExperimentAugust2015	-1.979	1.214	NA	NA
NitrogenYes:CO2Yes:ExperimentAugust2015	-6.775	1.247	NA	NA
NitrogenNo:CO2No:ExperimentJuly2015	-2.792	1.247	-4.191	0.643
NitrogenYes:CO2No:ExperimentJuly2015	-6.082	1.372	NA	NA
NitrogenNo:CO2Yes:ExperimentJuly2015	-0.213	1.28	NA	NA
NitrogenYes:CO2Yes:ExperimentJuly2015	-1.774	1.214	NA	NA

Term	Estimate	Std. Error	Lower 95%	Upper 95%
NitrogenNo:CO2No:ExperimentJune2016	-1.126	1.247	-3.609	1.358
NitrogenYes:CO2No:ExperimentJune2016	-2.432	1.214	NA	NA
NitrogenNo:CO2Yes:ExperimentJune2016	-1.416	1.28	NA	NA
NitrogenYes:CO2Yes:ExperimentJune2016	-2.848	1.247	NA	NA
NitrogenNo:CO2No:ExperimentOctober2015	-1.34	1.311	-4.849	-0.015
NitrogenYes:CO2No:ExperimentOctober2015	-1.948	1.402	NA	NA
NitrogenNo:CO2Yes:ExperimentOctober2015	3.277	1.74	NA	NA
NitrogenYes:CO2Yes:ExperimentOctober2015	1.495	1.787	NA	NA
PhosphorusNo:CO2No:ExperimentAugust2015	2.635	1.854	-3.964	1.132
PhosphorusYes:CO2No:ExperimentAugust2015	4.133	0.405	NA	NA
PhosphorusNo:CO2Yes:ExperimentAugust2015	1.225	0.572	NA	NA
PhosphorusYes:CO2Yes:ExperimentAugust2015	7.826	0.64	NA	NA
PhosphorusNo:CO2No:ExperimentJuly2015	-6.025	0.701	-5.331	-0.365
PhosphorusYes:CO2No:ExperimentJuly2015	-2.607	0.64	NA	NA
PhosphorusNo:CO2Yes:ExperimentJuly2015	-2.63	0.572	NA	NA
PhosphorusYes:CO2Yes:ExperimentJuly2015	-2.208	0.572	NA	NA
PhosphorusNo:CO2No:ExperimentJune2016	-1.232	0.572	-3.951	1.27

Term	Estimate	Std. Error	Lower 95%	Upper 95%
PhosphorusYes:CO2No:ExperimentJune2016	-1.827	0.572	NA	NA
PhosphorusNo:CO2Yes:ExperimentJune2016	6.41	0.949	NA	NA
PhosphorusYes:CO2Yes:ExperimentJune2016	2.919	0.905	NA	NA
PhosphorusNo:CO2No:ExperimentOctober2015	2.423	0.949	-4.739	0.843
PhosphorusYes:CO2No:ExperimentOctober2015	-2.328	1.764	NA	NA
PhosphorusNo:CO2Yes:ExperimentOctober2015	-3.543	0.858	NA	NA
PhosphorusYes:CO2Yes:ExperimentOctober2015	-0.197	0.809	NA	NA
NitrogenNo:PhosphorusNo:CO2No:ExperimentAugust2015	-3.769	0.858	NA	NA
NitrogenYes:PhosphorusNo:CO2No:ExperimentAugust2015	-1.721	0.809	NA	NA
NitrogenNo:PhosphorusYes:CO2No:ExperimentAugust2015	-3.359	0.858	NA	NA
NitrogenYes:PhosphorusYes:CO2No:ExperimentAugust2015	0.223	0.809	NA	NA
NitrogenNo:PhosphorusNo:CO2Yes:ExperimentAugust2015	-6.108	0.858	NA	NA
NitrogenYes:PhosphorusNo:CO2Yes:ExperimentAugust2015	3.249	0.949	NA	NA
NitrogenNo:PhosphorusYes:CO2Yes:ExperimentAugust2015	5.905	0.905	NA	NA
NitrogenYes:PhosphorusYes:CO2Yes:ExperimentAugust2015	2.094	0.905	NA	NA
NitrogenNo:PhosphorusNo:CO2No:ExperimentJuly2015	4.872	1.071	-0.188	6.743
NitrogenYes:PhosphorusNo:CO2No:ExperimentJuly2015	1.181	0.858	NA	NA

Term	Estimate	Std. Error	Lower 95%	Upper 95%
NitrogenNo:PhosphorusYes:CO2No:ExperimentJuly2015	1.295	0.858	NA	NA
NitrogenYes:PhosphorusYes:CO2No:ExperimentJuly2015	0.712	0.905	NA	NA
NitrogenNo:PhosphorusNo:CO2Yes:ExperimentJuly2015	1.672	0.858	NA	NA
NitrogenYes:PhosphorusNo:CO2Yes:ExperimentJuly2015	-2.524	1.311	NA	NA
NitrogenNo:PhosphorusYes:CO2Yes:ExperimentJuly2015	-1.979	1.214	NA	NA
NitrogenYes:PhosphorusYes:CO2Yes:ExperimentJuly2015	-6.775	1.247	NA	NA
NitrogenNo:PhosphorusNo:CO2No:ExperimentJune2016	-2.792	1.247	-2.063	5.053
NitrogenYes:PhosphorusNo:CO2No:ExperimentJune2016	-6.082	1.372	NA	NA
NitrogenNo:PhosphorusYes:CO2No:ExperimentJune2016	-0.213	1.28	NA	NA
NitrogenYes:PhosphorusYes:CO2No:ExperimentJune2016	-1.774	1.214	NA	NA
NitrogenNo:PhosphorusNo:CO2Yes:ExperimentJune2016	-1.126	1.247	NA	NA
NitrogenYes:PhosphorusNo:CO2Yes:ExperimentJune2016	-2.432	1.214	NA	NA
NitrogenNo:PhosphorusYes:CO2Yes:ExperimentJune2016	-1.416	1.28	NA	NA
NitrogenYes:PhosphorusYes:CO2Yes:ExperimentJune2016	-2.848	1.247	NA	NA
NitrogenNo:PhosphorusNo:CO2No:ExperimentOctober2015	-1.34	1.311	-1.057	6.327
NitrogenYes:PhosphorusNo:CO2No:ExperimentOctober2015	-1.948	1.402	NA	NA
NitrogenNo:PhosphorusYes:CO2No:ExperimentOctober2015	3.277	1.74	NA	NA

Term	Estimate	Std. Error	Lower 95%	Upper 95%
NitrogenYes:PhosphorusYes:CO2No:ExperimentOctober2015	1.495	1.787	NA	NA
NitrogenNo:PhosphorusNo:CO2Yes:ExperimentOctober2015	2.635	1.854	NA	NA
NitrogenYes:PhosphorusNo:CO2Yes:ExperimentOctober2015	4.133	0.405	NA	NA
NitrogenNo:PhosphorusYes:CO2Yes:ExperimentOctober2015	1.225	0.572	NA	NA
NitrogenYes:PhosphorusYes:CO2Yes:ExperimentOctober2015	7.826	0.64	NA	NA

Appendix A2

A2.1 pH in Experimental Mesocosms

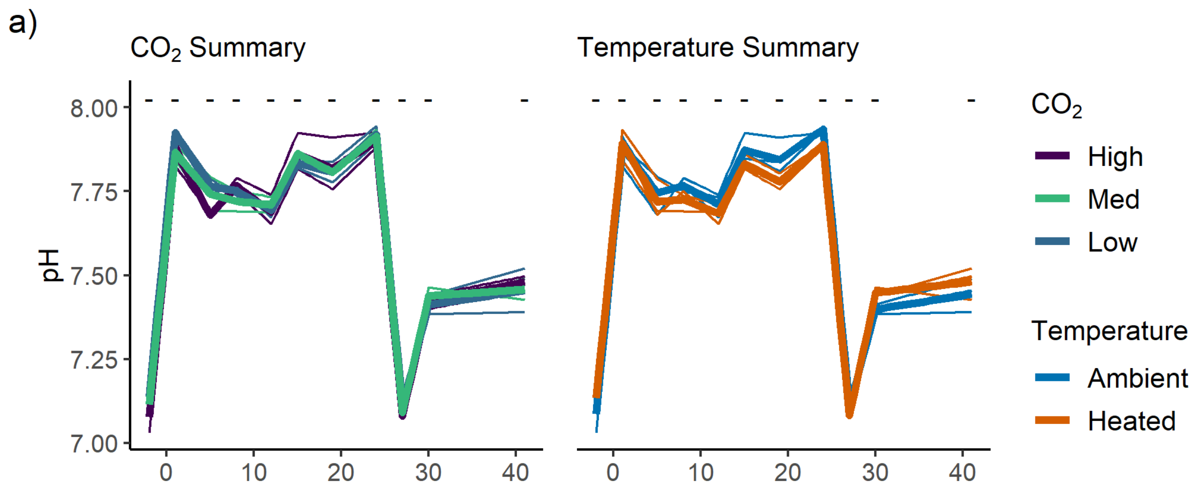

Suppl. Fig. A2.1: Panels and colors as in Figure 2.1, showing the effect of treatments on (a) pH and (b) specific conductance at 25 °C.

A2.2 Lac Hertel

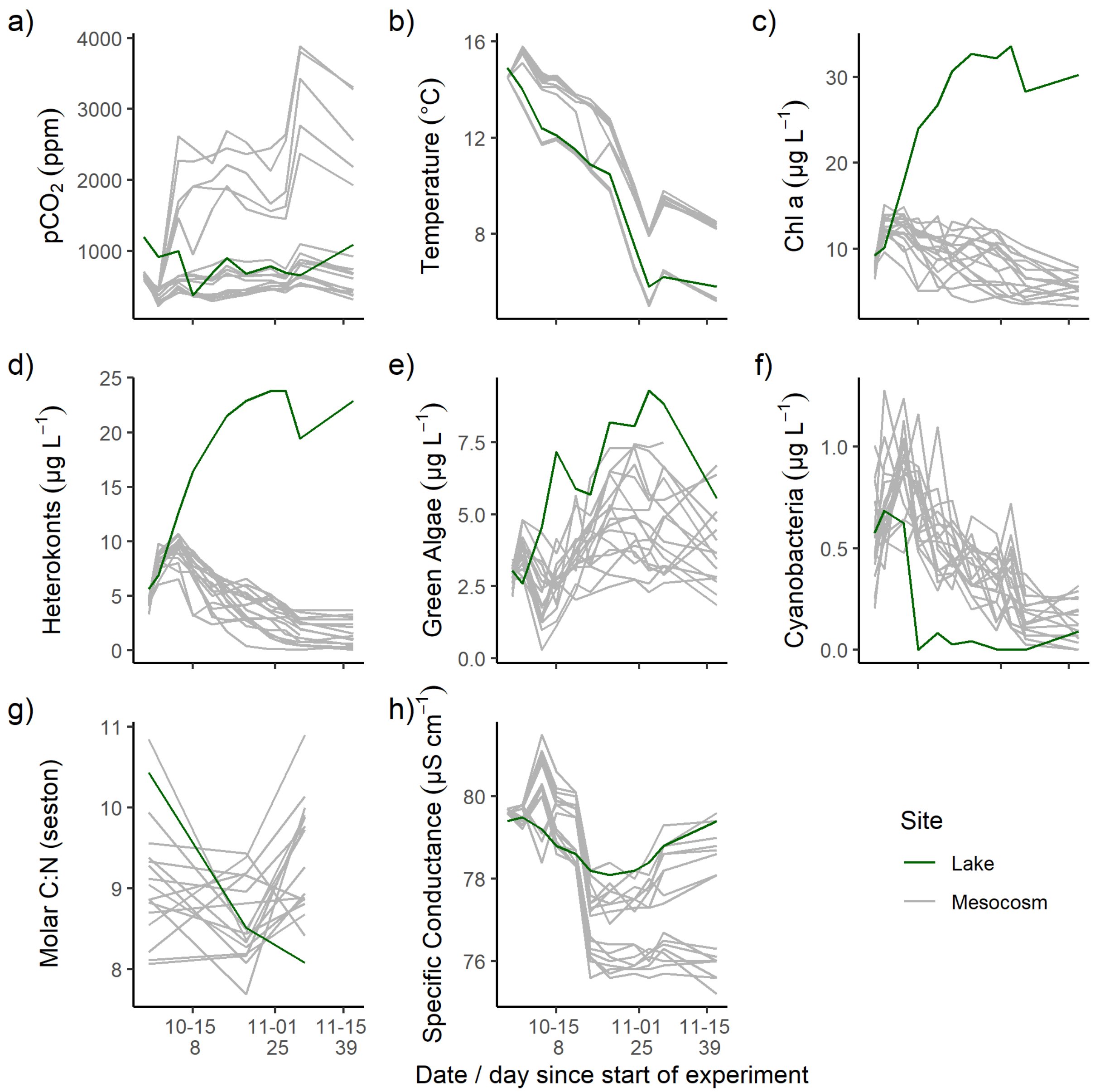

Suppl. Fig. A2.2: Comparison between measurements collected from the lake at a ~30 cm depth, directly off the mesocosm platform (dark green) and the mesocosms (light grey) over the course of the experimental period. a) pCO_2, b) temperature, c) chlorophyll a, d) heterokont biomass, e) green agal biomass, f) cyanobacteria biomass, g) the molar C:N ratio of the seston, and h) specific conductance at 25 °C. Major differences occur at the level of community chlorophyll a and heterokont biomass, likely caused by resource limitation in the mesocosms.

A2.3 Relative Phytoplankton Densities

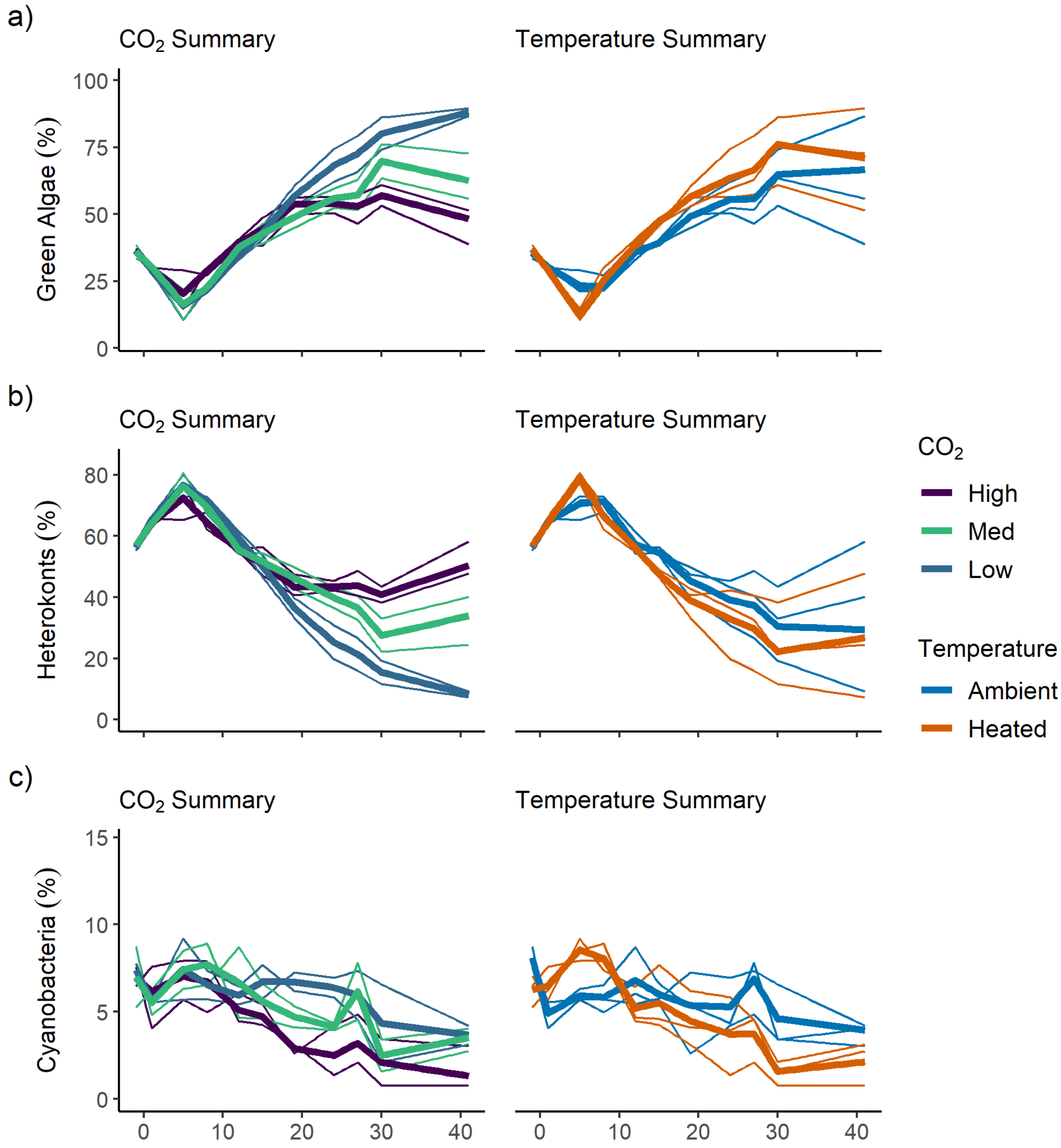

Suppl. Fig. A2.3: Average chlorophyll a contained in (a) green algae, (b) heterokonts, and (c) cyanobacteria, relative to the total chlorophyll a in the system, as measured by the Floroprobe over the course of the experiment. For details about the meaning of the lines and symbols in each panel, see Figure 2.1 caption.

A2.4 Zooplanknton species list

Suppl. Table A2.1: Zooplankton species found across all mesocosms, the lake, and all three sampling dates.

Species
Acanthocyclops vernalis
Alona setulosa
Alona sp.
Alonella excisa
Asplanchna sp.
Bosmina longirostris
Ceriodaphnia dubia
Ceriodaphnia lacustris
Chydorus sphaericus
Conochilus unicornis
Copepodites
Cyclops scutifer
Daphnia ambigua
Diaphanosoma brachyurum
Filinia terminalis
Kellicottia bostoniensis
Keratella cochlearis
Keratella quadrata
Monostyla bulla
Monostyla quadridentata
Nauplius larvae
Platyias quadricornis

Species
Ploesoma truncatum
Polyarthra vulgaris
Semicephalus sp.
Sida crystallina
Trichocerca cylindrica
Tricotia tetractis

A2.5 Model Parameter Estimates and Contrasts

Below are a series of tables which specify the model parameter estimates and contrasts and their statistical significance (calculated using the emmeans R package) for every sampling day of the experiment for chlorophyll, green algae, heterokont, and cyanobacteria biomass (µg/L, as measured by the Fluoroprobe). Differences between all three different CO_2 treatments, and both temperature treatments are shown. Contrasts for the interactive effects are not shown because they were not found to be significant (see Results).

A2.5.1 Chlorophyll *a*

Table A2.5.1.1: Chlorophyll *a* contrasts between temperature treatments for each sampling day.

contrast	Day	estimate	SE	df	t.ratio	p.value
Heated - Ambient	-1	-0.1397	0.9745	48.44	-0.1433	0.8866
Heated - Ambient	1	-1.773	0.9745	48.44	-1.819	0.07507
Heated - Ambient	5	-1.45	0.9745	48.44	-1.488	0.1432
Heated - Ambient	8	-1.62	0.9745	48.44	-1.662	0.103
Heated - Ambient	12	-1.328	0.9745	48.44	-1.362	0.1794
Heated - Ambient	15	0.2865	0.9745	48.44	0.294	0.77
Heated - Ambient	19	0.7204	0.9745	48.44	0.7393	0.4633
Heated - Ambient	24	2.295	0.9745	48.44	2.355	0.02261

contrast	Day	estimate	SE	df	t.ratio	p.value
Heated - Ambient	27	1.955	0.9745	48.44	2.006	0.05049
Heated - Ambient	30	2.769	0.9994	52.02	2.77	0.007746
Heated - Ambient	41	0.9331	1.071	62.24	0.8716	0.3868

Table A2.5.1.2: Chlorophyll *a* contrasts between CO_2 treatments for each sampling day.

contrast	Day	estimate	SE	df	t.ratio	p.value
Med - Low	-1	0.3372	1.147	48.44	0.2941	0.9535
High - Low	-1	0.8479	1.216	48.44	0.6972	0.7663
High - Med	-1	0.5107	1.216	48.44	0.4199	0.9076
Med - Low	1	-0.2611	1.147	48.44	-0.2277	0.9718
High - Low	1	0.07012	1.216	48.44	0.05766	0.9982
High - Med	1	0.3312	1.216	48.44	0.2723	0.96
Med - Low	5	-0.5082	1.147	48.44	-0.4432	0.8976
High - Low	5	0.03483	1.216	48.44	0.02864	0.9995
High - Med	5	0.543	1.216	48.44	0.4465	0.8962
Med - Low	8	-0.7175	1.147	48.44	-0.6257	0.8068
High - Low	8	-0.1438	1.216	48.44	-0.1182	0.9923
High - Med	8	0.5738	1.216	48.44	0.4717	0.8849
Med - Low	12	-0.5123	1.147	48.44	-0.4468	0.896
High - Low	12	-0.2888	1.216	48.44	-0.2375	0.9694
High - Med	12	0.2235	1.216	48.44	0.1838	0.9816
Med - Low	15	-0.347	1.147	48.44	-0.3026	0.9508
High - Low	15	1.589	1.216	48.44	1.307	0.3983
High - Med	15	1.936	1.216	48.44	1.592	0.2587
Med - Low	19	1.781	1.147	48.44	1.553	0.2758
High - Low	19	3.834	1.216	48.44	3.153	0.007683

contrast	Day	estimate	SE	df	t.ratio	p.value
High - Med	19	2.054	1.216	48.44	1.689	0.2198
Med - Low	24	2.162	1.147	48.44	1.885	0.1539
High - Low	24	3.474	1.216	48.44	2.857	0.017
High - Med	24	1.313	1.216	48.44	1.079	0.5313
Med - Low	27	2.411	1.147	48.44	2.103	0.09982
High - Low	27	3.453	1.216	48.44	2.839	0.0178
High - Med	27	1.041	1.216	48.44	0.8563	0.6701
Med - Low	30	2.056	1.147	48.44	1.793	0.1825
High - Low	30	2.538	1.261	53.59	2.013	0.1188
High - Med	30	0.4819	1.261	53.59	0.3822	0.9228
Med - Low	41	-0.8031	1.194	54.22	-0.6726	0.7803
High - Low	41	0.3426	1.346	63.31	0.2546	0.9649
High - Med	41	1.146	1.386	67.82	0.8266	0.6879

Table A2.5.1.3: Chlorophyll *a* paremeter estimates for the random effects model, fit by REML (Chlorophyll *a* ~ CO_2 * Temperature * Day + (1 | Mesocosm)).

Term	Estimate	Std. Error	Lower 95%	Upper 95%
(Intercept)	7.363	1.147	5.536	9.19
CO_2Med	0.649	1.622	-1.935	3.234
CO_2High	1.374	1.813	-1.515	4.264
TemperatureHeated	0.419	1.622	-2.165	3.004
Day1	6.116	1.273	4.108	8.124
Day5	5.688	1.273	3.68	7.696
Day8	4.163	1.273	2.155	6.172
Day12	3.165	1.273	1.157	5.173
Day15	1.685	1.273	-0.323	3.693

Term	Estimate	Std. Error	Lower 95%	Upper 95%
Day19	0.122	1.273	-1.886	2.13
Day24	-0.903	1.273	-2.911	1.105
Day27	-2.289	1.273	-4.297	-0.281
Day30	-3.269	1.273	-5.277	-1.26
Day41	-2.624	1.273	-4.632	-0.616
CO_2Med:TemperatureHeated	-0.624	2.293	-4.279	3.03
CO_2High:TemperatureHeated	-1.053	2.432	-4.929	2.824
CO_2Med:Day1	-0.863	1.8	-3.703	1.977
CO_2High:Day1	-0.992	2.012	-4.168	2.183
CO_2Med:Day5	-0.805	1.8	-3.645	2.035
CO_2High:Day5	-1.147	2.012	-4.323	2.028
CO_2Med:Day8	-1.293	1.8	-4.133	1.547
CO_2High:Day8	-1.238	2.012	-4.414	1.937
CO_2Med:Day12	-1.418	1.8	-4.258	1.422
CO_2High:Day12	-0.96	2.012	-4.135	2.216
CO_2Med:Day15	-2.06	1.8	-4.9	0.78
CO_2High:Day15	0.151	2.012	-3.024	3.326
CO_2Med:Day19	-0.476	1.8	-3.316	2.364
CO_2High:Day19	2.877	2.012	-0.299	6.052
CO_2Med:Day24	-0.258	1.8	-3.098	2.582
CO_2High:Day24	0.668	2.012	-2.507	3.844
CO_2Med:Day27	0.533	1.8	-2.307	3.373
CO_2High:Day27	1.535	2.012	-1.64	4.711
CO_2Med:Day30	0.565	1.8	-2.275	3.405
CO_2High:Day30	0.769	2.012	-2.407	3.944

Term	Estimate	Std. Error	Lower 95%	Upper 95%
CO_2Med:Day41	-0.485	1.8	-3.325	2.355
CO_2High:Day41	-1.221	2.317	-4.876	2.438
TemperatureHeated:Day1	-1.953	1.8	-4.793	0.887
TemperatureHeated:Day5	-1.506	1.8	-4.346	1.334
TemperatureHeated:Day8	-1.803	1.8	-4.643	1.037
TemperatureHeated:Day12	-1.449	1.8	-4.289	1.391
TemperatureHeated:Day15	-0.884	1.8	-3.724	1.956
TemperatureHeated:Day19	-0.493	1.8	-3.333	2.347
TemperatureHeated:Day24	-0.259	1.8	-3.099	2.581
TemperatureHeated:Day27	0.354	1.8	-2.486	3.194
TemperatureHeated:Day30	1.524	1.8	-1.316	4.364
TemperatureHeated:Day41	1.033	1.8	-1.807	3.873
CO_2Med:TemperatureHeated:Day1	0.529	2.545	-3.487	4.546
CO_2High:TemperatureHeated:Day1	0.429	2.7	-3.831	4.689
CO_2Med:TemperatureHeated:Day5	-0.081	2.545	-4.097	3.936
CO_2High:TemperatureHeated:Day5	0.668	2.7	-3.592	4.929
CO_2Med:TemperatureHeated:Day8	0.476	2.545	-3.541	4.492
CO_2High:TemperatureHeated:Day8	0.494	2.7	-3.766	4.754
CO_2Med:TemperatureHeated:Day12	1.137	2.545	-2.879	5.154
CO_2High:TemperatureHeated:Day12	-0.354	2.7	-4.614	3.906
CO_2Med:TemperatureHeated:Day15	2.751	2.545	-1.266	6.767
CO_2High:TemperatureHeated:Day15	1.181	2.7	-3.079	5.441
CO_2Med:TemperatureHeated:Day19	3.839	2.545	-0.177	7.856
CO_2High:TemperatureHeated:Day19	0.22	2.7	-4.04	4.48
CO_2Med:TemperatureHeated:Day24	4.164	2.545	0.148	8.181

Term	Estimate	Std. Error	Lower 95%	Upper 95%
CO_2High:TemperatureHeated:Day24	3.916	2.7	-0.344	8.177
CO_2Med:TemperatureHeated:Day27	3.081	2.545	-0.935	7.098
CO_2High:TemperatureHeated:Day27	2.139	2.7	-2.121	6.399
CO_2Med:TemperatureHeated:Day30	2.309	2.545	-1.707	6.326
CO_2High:TemperatureHeated:Day30	1.844	2.78	-2.544	6.23
CO_2Med:TemperatureHeated:Day41	-1.311	2.63	-5.461	2.842
CO_2High:TemperatureHeated:Day41	1.432	2.934	-3.201	6.06
AIC	664.58			
Sd Mesocosm(Intercept)	1.231			
Residual	1.559			

A2.5.2 Green Algae

Table A2.5.2.1: Green Algae contrasts between temperature treatments for each sampling day.

contrast	Day	estimate	SE	df	t.ratio	p.value
Heated - Ambient	-1	0.03722	0.4512	67.22	0.08249	0.9345
Heated - Ambient	1	-0.6876	0.4512	67.22	-1.524	0.1322
Heated - Ambient	5	-1.709	0.4512	67.22	-3.788	0.0003272
Heated - Ambient	8	-0.1539	0.4512	67.22	-0.3412	0.734
Heated - Ambient	12	-0.366	0.4512	67.22	-0.8111	0.4202
Heated - Ambient	15	0.7646	0.4512	67.22	1.694	0.0948
Heated - Ambient	19	0.86	0.4512	67.22	1.906	0.06095
Heated - Ambient	24	1.933	0.4512	67.22	4.284	5.974e-05
Heated - Ambient	27	1.966	0.4512	67.22	4.357	4.613e-05
Heated - Ambient	30	2.55	0.4647	71.56	5.488	5.82e-07
Heated - Ambient	41	1.368	0.5028	82.83	2.72	0.007945

Table A2.5.2.2: Green Algae contrasts between CO_2 treatments for each sampling day.

contrast	Day	estimate	SE	df	t.ratio	p.value
Med - Low	-1	0.08558	0.531	67.22	0.1612	0.9858
High - Low	-1	0.3217	0.5632	67.22	0.5712	0.8359
High - Med	-1	0.2361	0.5632	67.22	0.4192	0.9078
Med - Low	1	0.086	0.531	67.22	0.162	0.9856
High - Low	1	0.1229	0.5632	67.22	0.2183	0.9741
High - Med	1	0.03692	0.5632	67.22	0.06555	0.9976
Med - Low	5	0.08453	0.531	67.22	0.1592	0.9861
High - Low	5	0.7989	0.5632	67.22	1.419	0.3372
High - Med	5	0.7144	0.5632	67.22	1.268	0.4178
Med - Low	8	-0.08567	0.531	67.22	-0.1613	0.9858
High - Low	8	0.6486	0.5632	67.22	1.152	0.4861
High - Med	8	0.7342	0.5632	67.22	1.304	0.3981
Med - Low	12	0.0915	0.531	67.22	0.1723	0.9838
High - Low	12	0.3837	0.5632	67.22	0.6813	0.7752
High - Med	12	0.2922	0.5632	67.22	0.5188	0.8625
Med - Low	15	-0.1556	0.531	67.22	-0.293	0.9538
High - Low	15	0.7854	0.5632	67.22	1.395	0.3495
High - Med	15	0.941	0.5632	67.22	1.671	0.2239
Med - Low	19	0.5055	0.531	67.22	0.952	0.6095
High - Low	19	1.999	0.5632	67.22	3.549	0.002027
High - Med	19	1.493	0.5632	67.22	2.652	0.02663
Med - Low	24	0.5393	0.531	67.22	1.016	0.5696
High - Low	24	1.095	0.5632	67.22	1.945	0.1342
High - Med	24	0.5559	0.5632	67.22	0.9871	0.5875

contrast	Day	estimate	SE	df	t.ratio	p.value
Med - Low	27	0.7105	0.531	67.22	1.338	0.3793
High - Low	27	0.8428	0.5632	67.22	1.497	0.299
High - Med	27	0.1323	0.5632	67.22	0.235	0.97
Med - Low	30	0.9937	0.531	67.22	1.871	0.1549
High - Low	30	0.2871	0.5872	73.4	0.4889	0.8768
High - Med	30	-0.7066	0.5872	73.4	-1.203	0.4551
Med - Low	41	-1.618	0.5564	74.13	-2.907	0.01318
High - Low	41	-2.214	0.6325	83.92	-3.5	0.002137
High - Med	41	-0.5964	0.654	88.31	-0.9118	0.6343

Table A2.5.2.3: Green Algae paremeter estimates for the random effects model, fit by REML (Green Algae ~ CO_2 * Temperature * Day + (1 | Mesocosm)).

Term	Estimate	Std. Error	Lower 95%	Upper 95%
(Intercept)	2.721	0.531	1.879	3.563
CO_2Med	-0.041	0.751	-1.232	1.15
CO_2High	0.526	0.84	-0.805	1.858
TemperatureHeated	0.089	0.751	-1.102	1.28
Day1	1.313	0.638	0.307	2.32
Day5	0.04	0.638	-0.967	1.046
Day8	-0.259	0.638	-1.266	0.747
Day12	0.752	0.638	-0.254	1.759
Day15	0.931	0.638	-0.075	1.938
Day19	1.223	0.638	0.217	2.23
Day24	1.253	0.638	0.246	2.259
Day27	0.604	0.638	-0.402	1.611
Day30	0.299	0.638	-0.707	1.306

Term	Estimate	Std. Error	Lower 95%	Upper 95%
Day41	1.411	0.638	0.405	2.418
CO_2Med:TemperatureHeated	0.254	1.062	-1.431	1.938
CO_2High:TemperatureHeated	-0.409	1.126	-2.196	1.377
CO_2Med:Day1	0.102	0.902	-1.321	1.526
CO_2High:Day1	-0.371	1.008	-1.963	1.22
CO_2Med:Day5	0.15	0.902	-1.274	1.573
CO_2High:Day5	0.582	1.008	-1.01	2.173
CO_2Med:Day8	-0.096	0.902	-1.52	1.327
CO_2High:Day8	0.196	1.008	-1.395	1.788
CO_2Med:Day12	0.22	0.902	-1.203	1.644
CO_2High:Day12	0.229	1.008	-1.362	1.821
CO_2Med:Day15	-0.66	0.902	-2.083	0.764
CO_2High:Day15	-0.105	1.008	-1.696	1.487
CO_2Med:Day19	-0.492	0.902	-1.916	0.931
CO_2High:Day19	1.399	1.008	-0.192	2.991
CO_2Med:Day24	-0.479	0.902	-1.903	0.944
CO_2High:Day24	-0.19	1.008	-1.781	1.402
CO_2Med:Day27	-0.109	0.902	-1.533	1.314
CO_2High:Day27	-0.135	1.008	-1.726	1.457
CO_2Med:Day30	0.311	0.902	-1.113	1.734
CO_2High:Day30	-0.234	1.008	-1.825	1.357
CO_2Med:Day41	-1.324	0.902	-2.747	0.1
CO_2High:Day41	-2.881	1.16	-4.712	-1.047
TemperatureHeated:Day1	-0.772	0.902	-2.196	0.651
TemperatureHeated:Day5	-1.576	0.902	-3	-0.153

Term	Estimate	Std. Error	Lower 95%	Upper 95%
TemperatureHeated:Day8	-0.228	0.902	-1.652	1.195
TemperatureHeated:Day12	-0.149	0.902	-1.572	1.275
TemperatureHeated:Day15	0.069	0.902	-1.354	1.493
TemperatureHeated:Day19	0.029	0.902	-1.394	1.453
TemperatureHeated:Day24	0.632	0.902	-0.792	2.055
TemperatureHeated:Day27	1.002	0.902	-0.421	2.426
TemperatureHeated:Day30	1.982	0.902	0.558	3.405
TemperatureHeated:Day41	1.353	0.902	-0.07	2.777
CO_2Med:TemperatureHeated:Day1	-0.204	1.276	-2.216	1.809
CO_2High:TemperatureHeated:Day1	0.345	1.353	-1.79	2.481
CO_2Med:TemperatureHeated:Day5	-0.301	1.276	-2.314	1.712
CO_2High:TemperatureHeated:Day5	-0.209	1.353	-2.344	1.926
CO_2Med:TemperatureHeated:Day8	-0.15	1.276	-2.162	1.863
CO_2High:TemperatureHeated:Day8	0.261	1.353	-1.874	2.397
CO_2Med:TemperatureHeated:Day12	-0.429	1.276	-2.441	1.584
CO_2High:TemperatureHeated:Day12	-0.335	1.353	-2.47	1.8
CO_2Med:TemperatureHeated:Day15	0.837	1.276	-1.176	2.85
CO_2High:TemperatureHeated:Day15	1.137	1.353	-0.998	3.272
CO_2Med:TemperatureHeated:Day19	1.825	1.276	-0.188	3.838
CO_2High:TemperatureHeated:Day19	0.556	1.353	-1.579	2.691
CO_2Med:TemperatureHeated:Day24	1.866	1.276	-0.147	3.879
CO_2High:TemperatureHeated:Day24	1.927	1.353	-0.208	4.062
CO_2Med:TemperatureHeated:Day27	1.469	1.276	-0.544	3.482
CO_2High:TemperatureHeated:Day27	1.312	1.353	-0.823	3.447
CO_2Med:TemperatureHeated:Day30	1.195	1.276	-0.818	3.208

Term	Estimate	Std. Error	Lower 95%	Upper 95%
CO_2High:TemperatureHeated:Day30	0.399	1.393	-1.8	2.597
CO_2Med:TemperatureHeated:Day41	-0.759	1.318	-2.838	1.321
CO_2High:TemperatureHeated:Day41	0.691	1.47	-1.631	3.009
AIC	497.13			
Sd Mesocosm(Intercept)	0.485			
Residual	0.781			

A2.5.3 Heterokonts

Table A2.5.3.1: Heterokonts contrasts between temperature treatments for each sampling day.

contrast	Day	estimate	SE	df	t.ratio	p.value
Heated - Ambient	-1	-0.03556	0.6205	41.65	-0.0573	0.9546
Heated - Ambient	1	-1.187	0.6205	41.65	-1.913	0.06265
Heated - Ambient	5	0.05824	0.6205	41.65	0.09386	0.9257
Heated - Ambient	8	-1.541	0.6205	41.65	-2.484	0.01711
Heated - Ambient	12	-0.7213	0.6205	41.65	-1.162	0.2517
Heated - Ambient	15	-0.4171	0.6205	41.65	-0.6722	0.5052
Heated - Ambient	19	-0.1343	0.6205	41.65	-0.2164	0.8297
Heated - Ambient	24	0.4274	0.6205	41.65	0.6889	0.4947
Heated - Ambient	27	0.06533	0.6205	41.65	0.1053	0.9166
Heated - Ambient	30	0.3139	0.6351	44.73	0.4943	0.6235
Heated - Ambient	41	-0.3902	0.677	53.78	-0.5764	0.5667

Table A2.5.3.2: Heterokonts contrasts between CO_2 treatments for each sampling day.

contrast	Day	estimate	SE	df	t.ratio	p.value
Med - Low	-1	0.2399	0.7301	41.65	0.3286	0.9423
High - Low	-1	0.4771	0.7744	41.65	0.6161	0.8122

contrast	Day	estimate	SE	df	t.ratio	p.value
High - Med	-1	0.2372	0.7744	41.65	0.3063	0.9497
Med - Low	1	-0.3119	0.7301	41.65	-0.4272	0.9045
High - Low	1	-0.06142	0.7744	41.65	-0.07931	0.9965
High - Med	1	0.2505	0.7744	41.65	0.3234	0.944
Med - Low	5	-0.5181	0.7301	41.65	-0.7097	0.7592
High - Low	5	-0.6742	0.7744	41.65	-0.8707	0.6616
High - Med	5	-0.1561	0.7744	41.65	-0.2016	0.9779
Med - Low	8	-0.6452	0.7301	41.65	-0.8837	0.6535
High - Low	8	-0.7523	0.7744	41.65	-0.9715	0.5987
High - Med	8	-0.1072	0.7744	41.65	-0.1384	0.9895
Med - Low	12	-0.6359	0.7301	41.65	-0.871	0.6614
High - Low	12	-0.6201	0.7744	41.65	-0.8007	0.7047
High - Med	12	0.01583	0.7744	41.65	0.02045	0.9998
Med - Low	15	-0.1037	0.7301	41.65	-0.142	0.9889
High - Low	15	0.8389	0.7744	41.65	1.083	0.5296
High - Med	15	0.9426	0.7744	41.65	1.217	0.4499
Med - Low	19	1.347	0.7301	41.65	1.844	0.1679
High - Low	19	1.984	0.7744	41.65	2.562	0.03683
High - Med	19	0.6374	0.7744	41.65	0.8231	0.6909
Med - Low	24	1.673	0.7301	41.65	2.291	0.06816
High - Low	24	2.509	0.7744	41.65	3.24	0.006508
High - Med	24	0.8363	0.7744	41.65	1.08	0.5316
Med - Low	27	1.601	0.7301	41.65	2.192	0.08428
High - Low	27	2.64	0.7744	41.65	3.409	0.004077
High - Med	27	1.039	0.7744	41.65	1.342	0.3804

contrast	Day	estimate	SE	df	t.ratio	p.value
Med - Low	30	1.112	0.7301	41.65	1.524	0.2905
High - Low	30	2.3	0.8006	46.1	2.873	0.01654
High - Med	30	1.188	0.8006	46.1	1.484	0.3078
Med - Low	41	0.8054	0.7578	46.65	1.063	0.5417
High - Low	41	2.617	0.8505	54.75	3.077	0.009014
High - Med	41	1.811	0.8744	58.9	2.072	0.1046

Table A2.5.3.3: Heterokonts paremeter estimates for the random effects model, fit by REML (Heterokonts ~ CO_2 * Temperature * Day + (1 | Mesocosm)).

Term	Estimate	Std. Error	Lower 95%	Upper 95%
(Intercept)	4.095	0.73	2.929	5.262
CO_2Med	0.539	1.033	-1.111	2.189
CO_2High	0.727	1.154	-1.117	2.572
TemperatureHeated	0.331	1.033	-1.319	1.98
Day1	4.598	0.777	3.372	5.823
Day5	5.451	0.777	4.225	6.677
Day8	4.308	0.777	3.082	5.534
Day12	2.393	0.777	1.167	3.619
Day15	0.796	0.777	-0.43	2.022
Day19	-1.096	0.777	-2.322	0.129
Day24	-2.064	0.777	-3.29	-0.838
Day27	-2.711	0.777	-3.936	-1.485
Day30	-3.293	0.777	-4.518	-2.067
Day41	-3.653	0.777	-4.879	-2.427
CO_2Med:TemperatureHeated	-0.599	1.46	-2.931	1.734
CO_2High:TemperatureHeated	-0.5	1.549	-2.975	1.974

Term	Estimate	Std. Error	Lower 95%	Upper 95%
CO_2Med:Day1	-0.705	1.099	-2.439	1.028
CO_2High:Day1	-0.304	1.228	-2.242	1.634
CO_2Med:Day5	-0.872	1.099	-2.605	0.862
CO_2High:Day5	-1.611	1.228	-3.549	0.328
CO_2Med:Day8	-1.095	1.099	-2.828	0.639
CO_2High:Day8	-1.233	1.228	-3.171	0.706
CO_2Med:Day12	-1.752	1.099	-3.486	-0.019
CO_2High:Day12	-1.149	1.228	-3.087	0.79
CO_2Med:Day15	-1.233	1.099	-2.966	0.501
CO_2High:Day15	0.296	1.228	-1.642	2.234
CO_2Med:Day19	0.347	1.099	-1.386	2.081
CO_2High:Day19	1.832	1.228	-0.106	3.77
CO_2Med:Day24	0.549	1.099	-1.184	2.283
CO_2High:Day24	1.065	1.228	-0.873	3.004
CO_2Med:Day27	0.759	1.099	-0.974	2.493
CO_2High:Day27	1.771	1.228	-0.167	3.709
CO_2Med:Day30	0.52	1.099	-1.214	2.253
CO_2High:Day30	1.183	1.228	-0.755	3.121
CO_2Med:Day41	0.962	1.099	-0.771	2.696
CO_2High:Day41	1.794	1.415	-0.438	4.027
TemperatureHeated:Day1	-1.097	1.099	-2.831	0.637
TemperatureHeated:Day5	-0.288	1.099	-2.022	1.445
TemperatureHeated:Day8	-1.647	1.099	-3.381	0.086
TemperatureHeated:Day12	-1.304	1.099	-3.038	0.429
TemperatureHeated:Day15	-1.018	1.099	-2.752	0.716

Term	Estimate	Std. Error	Lower 95%	Upper 95%
TemperatureHeated:Day19	-0.388	1.099	-2.122	1.346
TemperatureHeated:Day24	-0.77	1.099	-2.504	0.963
TemperatureHeated:Day27	-0.561	1.099	-2.295	1.172
TemperatureHeated:Day30	-0.313	1.099	-2.046	1.421
TemperatureHeated:Day41	-0.321	1.099	-2.054	1.413
CO_2Med:TemperatureHeated:Day1	0.307	1.554	-2.145	2.758
CO_2High:TemperatureHeated:Day1	-0.47	1.648	-3.07	2.131
CO_2Med:TemperatureHeated:Day5	0.228	1.554	-2.224	2.679
CO_2High:TemperatureHeated:Day5	0.918	1.648	-1.682	3.519
CO_2Med:TemperatureHeated:Day8	0.42	1.554	-2.032	2.871
CO_2High:TemperatureHeated:Day8	0.006	1.648	-2.594	2.606
CO_2Med:TemperatureHeated:Day12	1.753	1.554	-0.699	4.204
CO_2High:TemperatureHeated:Day12	0.103	1.648	-2.498	2.703
CO_2Med:TemperatureHeated:Day15	1.778	1.554	-0.674	4.229
CO_2High:TemperatureHeated:Day15	0.132	1.648	-2.469	2.732
CO_2Med:TemperatureHeated:Day19	1.519	1.554	-0.933	3.97
CO_2High:TemperatureHeated:Day19	-0.651	1.648	-3.251	1.949
CO_2Med:TemperatureHeated:Day24	1.767	1.554	-0.685	4.218
CO_2High:TemperatureHeated:Day24	1.933	1.648	-0.667	4.533
CO_2Med:TemperatureHeated:Day27	1.203	1.554	-1.248	3.655
CO_2High:TemperatureHeated:Day27	0.784	1.648	-1.817	3.384
CO_2Med:TemperatureHeated:Day30	0.705	1.554	-1.746	3.157
CO_2High:TemperatureHeated:Day30	1.281	1.697	-1.397	3.959
CO_2Med:TemperatureHeated:Day41	-0.794	1.606	-3.327	1.742
CO_2High:TemperatureHeated:Day41	0.692	1.791	-2.135	3.518

Term	Estimate	Std. Error	Lower 95%	Upper 95%
AIC	550.08			
Sd Mesocosm(Intercept)	0.833			
Residual	0.951			

A2.5.4 Cyanobacteria

Table A2.5.4.1: Cyanobacteria contrasts between temperature treatments for each sampling day.

contrast	Day	estimate	SE	df	t.ratio	p.value
Heated - Ambient	-1	-0.143	0.08033	116.3	-1.78	0.07766
Heated - Ambient	1	0.1027	0.08033	116.3	1.279	0.2035
Heated - Ambient	5	0.2011	0.08033	116.3	2.503	0.0137
Heated - Ambient	8	0.07533	0.08033	116.3	0.9378	0.3503
Heated - Ambient	12	-0.2309	0.08033	116.3	-2.875	0.004807
Heated - Ambient	15	-0.06025	0.08033	116.3	-0.75	0.4548
Heated - Ambient	19	-0.005389	0.08033	116.3	-0.06708	0.9466
Heated - Ambient	24	-0.06528	0.08033	116.3	-0.8126	0.4181
Heated - Ambient	27	-0.07778	0.08033	116.3	-0.9682	0.3349
Heated - Ambient	30	-0.1013	0.0834	116.7	-1.215	0.2269
Heated - Ambient	41	-0.0576	0.09201	117.4	-0.626	0.5325

Table A2.5.4.2: Cyanobacteria contrasts between CO_2 treatments for each sampling day.

contrast	Day	estimate	SE	df	t.ratio	p.value
Med - Low	-1	0.01283	0.09452	116.3	0.1358	0.9899
High - Low	-1	0.05092	0.1003	116.3	0.5079	0.8677
High - Med	-1	0.03808	0.1003	116.3	0.3799	0.9236
Med - Low	1	-0.03533	0.09452	116.3	-0.3738	0.9259
High - Low	1	0.008417	0.1003	116.3	0.08395	0.9961

contrast	Day	estimate	SE	df	t.ratio	p.value
High - Med	1	0.04375	0.1003	116.3	0.4364	0.9005
Med - Low	5	-0.07522	0.09452	116.3	-0.7958	0.7064
High - Low	5	-0.09033	0.1003	116.3	-0.901	0.6408
High - Med	5	-0.01511	0.1003	116.3	-0.1507	0.9876
Med - Low	8	0.01467	0.09452	116.3	0.1552	0.9868
High - Low	8	-0.03867	0.1003	116.3	-0.3857	0.9213
High - Med	8	-0.05333	0.1003	116.3	-0.532	0.8558
Med - Low	12	0.01717	0.09452	116.3	0.1816	0.982
High - Low	12	-0.05308	0.1003	116.3	-0.5295	0.8571
High - Med	12	-0.07025	0.1003	116.3	-0.7007	0.7636
Med - Low	15	-0.08688	0.09452	116.3	-0.9191	0.6293
High - Low	15	-0.03463	0.1003	116.3	-0.3454	0.9364
High - Med	15	0.05225	0.1003	116.3	0.5212	0.8612
Med - Low	19	-0.072	0.09452	116.3	-0.7617	0.7272
High - Low	19	-0.1484	0.1003	116.3	-1.48	0.3041
High - Med	19	-0.07642	0.1003	116.3	-0.7622	0.7269
Med - Low	24	-0.05017	0.09452	116.3	-0.5307	0.8564
High - Low	24	-0.1301	0.1003	116.3	-1.297	0.3995
High - Med	24	-0.07992	0.1003	116.3	-0.7971	0.7055
Med - Low	27	0.1007	0.09452	116.3	1.065	0.5377
High - Low	27	-0.02817	0.1003	116.3	-0.2809	0.9574
High - Med	27	-0.1288	0.1003	116.3	-1.285	0.4065
Med - Low	30	-0.04883	0.09452	116.3	-0.5166	0.8634
High - Low	30	-0.05664	0.1058	116.9	-0.5356	0.854
High - Med	30	-0.007809	0.1058	116.9	-0.07384	0.997

contrast	Day	estimate	SE	df	t.ratio	p.value
Med - Low	41	0.002591	0.1003	116.9	0.02582	0.9996
High - Low	41	-0.05018	0.116	117.5	-0.4327	0.9021
High - Med	41	-0.05277	0.1208	117.7	-0.437	0.9002

Table A2.5.4.3: Cyanobacteria paremeter estimates for the random effects model, fit by REML (Cyanobacteria ~ CO_2 * Temperature * Day + (1 | Mesocosm)).

Term	Estimate	Std. Error	Lower 95%	Upper 95%
(Intercept)	0.546	0.095	0.397	0.695
CO_2Med	0.153	0.134	-0.058	0.364
CO_2High	0.123	0.149	-0.113	0.358
TemperatureHeated	-0.002	0.134	-0.213	0.209
Day1	0.204	0.131	-0.003	0.411
Day5	0.196	0.131	-0.011	0.403
Day8	0.114	0.131	-0.093	0.321
Day12	0.021	0.131	-0.186	0.228
Day15	-0.044	0.131	-0.251	0.163
Day19	-0.005	0.131	-0.212	0.202
Day24	-0.093	0.131	-0.3	0.114
Day27	-0.182	0.131	-0.389	0.025
Day30	-0.274	0.131	-0.481	-0.067
Day41	-0.381	0.131	-0.588	-0.174
CO_2Med:TemperatureHeated	-0.28	0.189	-0.578	0.018
CO_2High:TemperatureHeated	-0.144	0.201	-0.46	0.173
CO_2Med:Day1	-0.26	0.185	-0.553	0.032
CO_2High:Day1	-0.318	0.207	-0.645	0.009
CO_2Med:Day5	-0.084	0.185	-0.376	0.209

Term	Estimate	Std. Error	Lower 95%	Upper 95%
CO_2High:Day5	-0.119	0.207	-0.447	0.208
CO_2Med:Day8	-0.102	0.185	-0.394	0.191
CO_2High:Day8	-0.202	0.207	-0.529	0.125
CO_2Med:Day12	0.082	0.185	-0.211	0.374
CO_2High:Day12	-0.043	0.207	-0.37	0.284
CO_2Med:Day15	-0.167	0.185	-0.459	0.126
CO_2High:Day15	-0.041	0.207	-0.368	0.287
CO_2Med:Day19	-0.332	0.185	-0.624	-0.039
CO_2High:Day19	-0.357	0.207	-0.684	-0.03
CO_2Med:Day24	-0.328	0.185	-0.62	-0.035
CO_2High:Day24	-0.207	0.207	-0.534	0.12
CO_2Med:Day27	-0.118	0.185	-0.41	0.175
CO_2High:Day27	-0.101	0.207	-0.428	0.226
CO_2Med:Day30	-0.269	0.185	-0.561	0.024
CO_2High:Day30	-0.183	0.207	-0.51	0.145
CO_2Med:Day41	-0.126	0.185	-0.419	0.166
CO_2High:Day41	-0.114	0.237	-0.488	0.26
TemperatureHeated:Day1	-0.079	0.185	-0.372	0.213
TemperatureHeated:Day5	0.361	0.185	0.069	0.654
TemperatureHeated:Day8	0.074	0.185	-0.218	0.367
TemperatureHeated:Day12	0.004	0.185	-0.288	0.297
TemperatureHeated:Day15	0.068	0.185	-0.224	0.361
TemperatureHeated:Day19	-0.132	0.185	-0.424	0.161
TemperatureHeated:Day24	-0.116	0.185	-0.408	0.177
TemperatureHeated:Day27	-0.087	0.185	-0.379	0.206

Term	Estimate	Std. Error	Lower 95%	Upper 95%
TemperatureHeated:Day30	-0.147	0.185	-0.439	0.146
TemperatureHeated:Day41	-0.001	0.185	-0.293	0.292
CO_2Med:TemperatureHeated:Day1	0.424	0.262	0.01	0.838
CO_2High:TemperatureHeated:Day1	0.551	0.278	0.112	0.99
CO_2Med:TemperatureHeated:Day5	-0.008	0.262	-0.422	0.405
CO_2High:TemperatureHeated:Day5	-0.044	0.278	-0.483	0.395
CO_2Med:TemperatureHeated:Day8	0.207	0.262	-0.207	0.621
CO_2High:TemperatureHeated:Day8	0.225	0.278	-0.214	0.664
CO_2Med:TemperatureHeated:Day12	-0.155	0.262	-0.569	0.259
CO_2High:TemperatureHeated:Day12	-0.122	0.278	-0.561	0.317
CO_2Med:TemperatureHeated:Day15	0.134	0.262	-0.28	0.547
CO_2High:TemperatureHeated:Day15	-0.09	0.278	-0.529	0.349
CO_2Med:TemperatureHeated:Day19	0.493	0.262	0.079	0.907
CO_2High:TemperatureHeated:Day19	0.315	0.278	-0.124	0.754
CO_2Med:TemperatureHeated:Day24	0.529	0.262	0.115	0.943
CO_2High:TemperatureHeated:Day24	0.052	0.278	-0.387	0.491
CO_2Med:TemperatureHeated:Day27	0.411	0.262	-0.003	0.825
CO_2High:TemperatureHeated:Day27	0.044	0.278	-0.395	0.483
CO_2Med:TemperatureHeated:Day30	0.414	0.262	0	0.828
CO_2High:TemperatureHeated:Day30	0.15	0.286	-0.301	0.601
CO_2Med:TemperatureHeated:Day41	0.232	0.27	-0.195	0.659
CO_2High:TemperatureHeated:Day41	0.026	0.301	-0.449	0.501
AIC	109.66			
Sd Mesocosm(Intercept)	0.032			
Residual	0.161			

Appendix A3

A3.1 Supplemental Figures

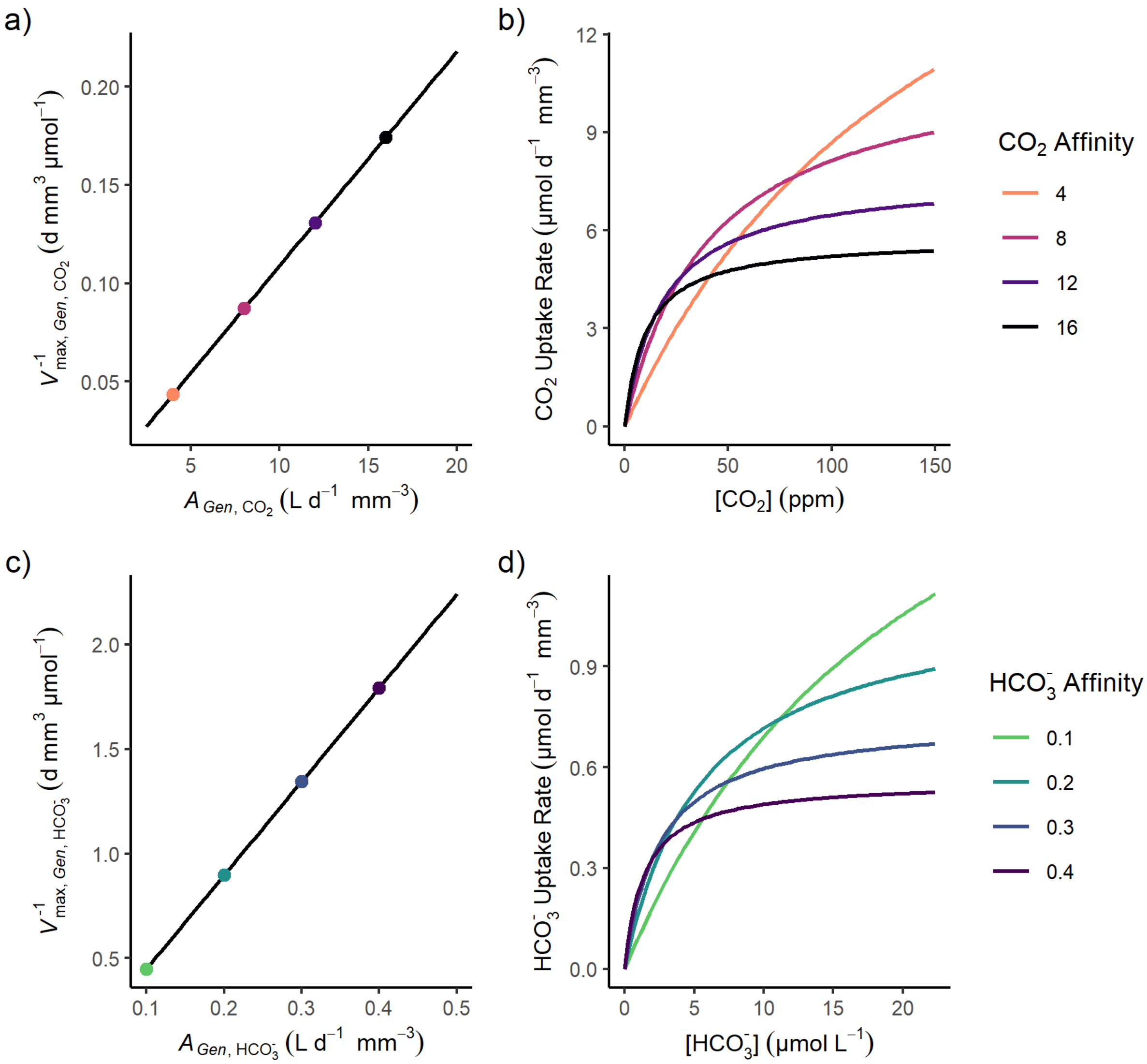

Figure A3.1.1: This figure represents the trade-offs involved in CO_2 (a,b) and HCO_3^- (c,d) of the generalist species. (a,c) The trade-off between the inverse of the maximum resource uptake rate (x-axis) and affinity (y-axis). Certain affinities are highlighted with coloured points (see colour legends in b and d). (b,d) Resource uptake rates (y-axis) across a range of resource concentrations (x-axis) for each of the affinity values highlighted in a) or c) (colour legend). The equations are parameterized for CO_2 and HCO_3^- uptake of the generalist species (Tables A3.2.2), though the same principles apply for all species. In this case, $\boldsymbol{p_{Gen,\mathrm{CO_2}} = p_{Gen,\mathrm{HCO_3^-}} = 1}$; $\boldsymbol{c_{Gen,\mathrm{CO_2}} = 1.09 \cdot 10^4\ \mathrm{d^2\ mm^6\ L^{-1}\ mol^{-1}}}$; $\boldsymbol{c_{Gen,\mathrm{HCO_3^-}} = 4.48 \cdot 10^6\ \mathrm{d^2\ mm^6\ L^{-1}\ mol^{-1}}}$.

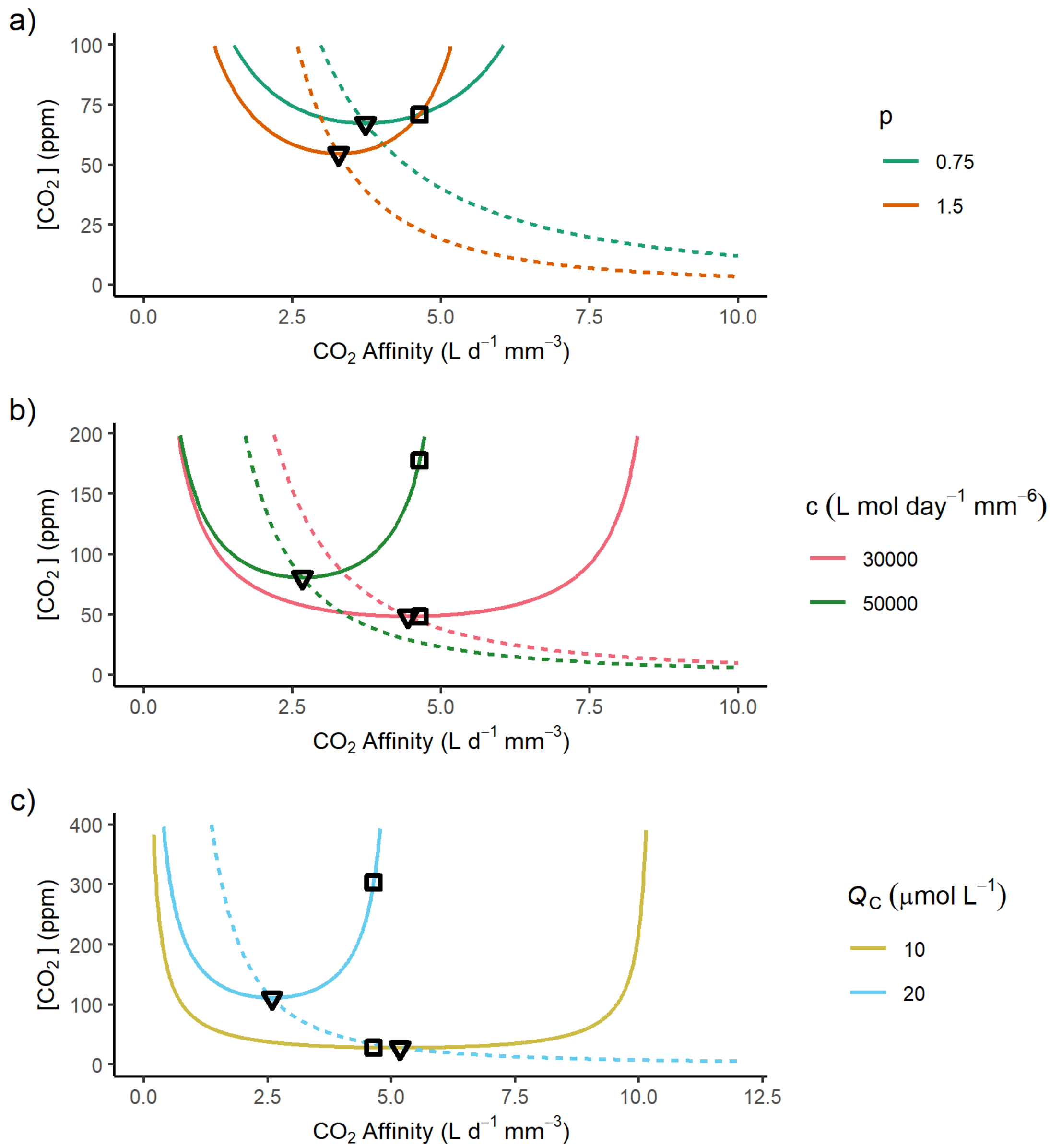

Figure A3.1.2: Here we present the effects of three species-specific variables–p (a), c (b), and Q_C (c)–on the ecological and evolutionary equilibrium dynamics for the CO_2 specialist (note that the result is analogous for the generalist). See Figure 3.3a for a description of the different plot elements. In summary, full lines define the ecological isocline ($dX/dt = 0$), dotted lines the evolutionary isoclines ($dA/dt = 0$), whereas the square and triangle represent the equilibria of a non-evolving and an evolving strain respectively. Overall, this graph shows that assumptions and errors in parameter estimates can have significant effects on equilibrium values and potentially even competitive outcomes.

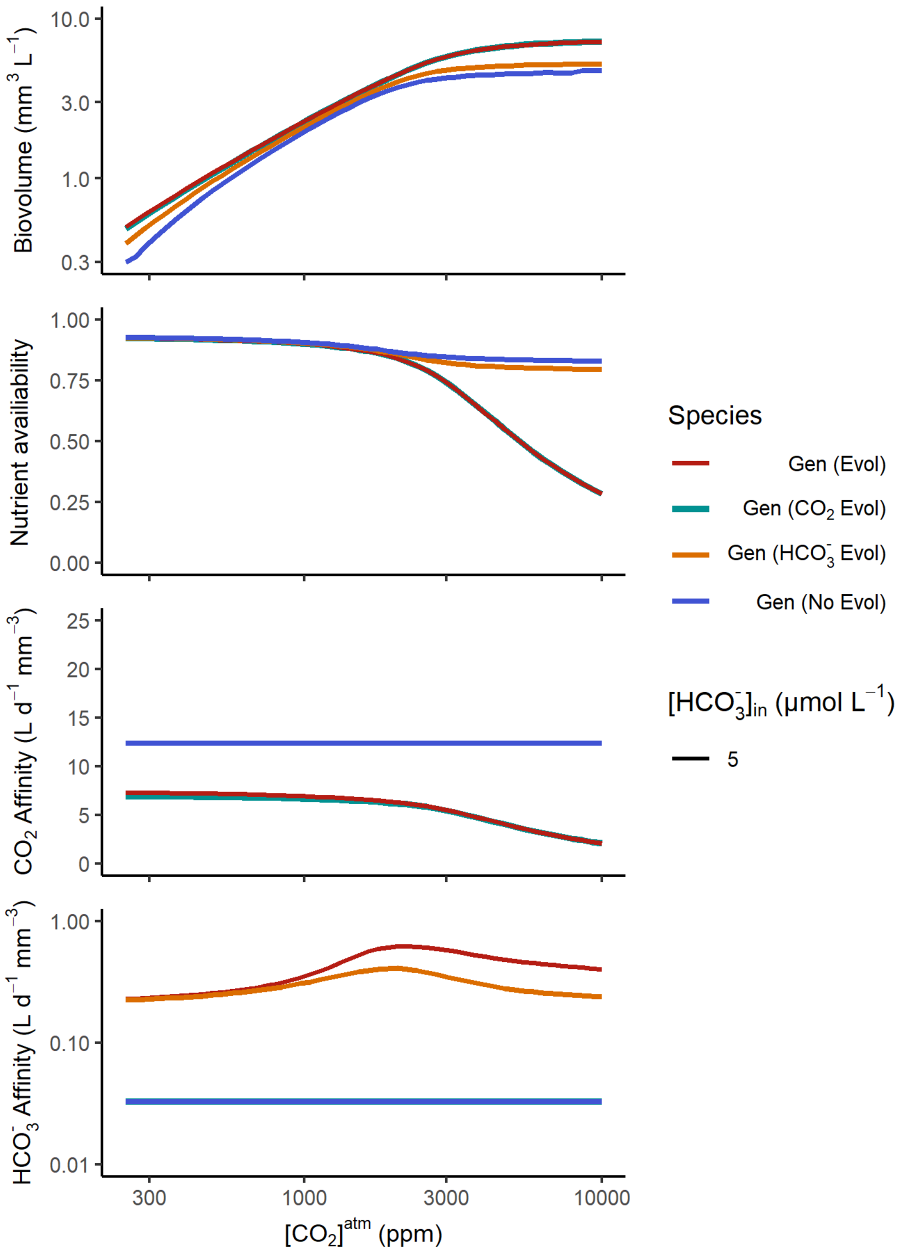

Figure A3.1.3: See Figure 3.6 caption. Here, we focus on the generalist species at a starting bicarbonate concentration of 5 µmol L^{-1}. We show the equilibrium landscape for four strains, with different potentials for evolution: no evolution (blue), only HCO_3^- affinity evolves (orange), only CO_2 affinity evolves (turquoise), and both, CO_2 and HCO_3^- affinities evolve (red).

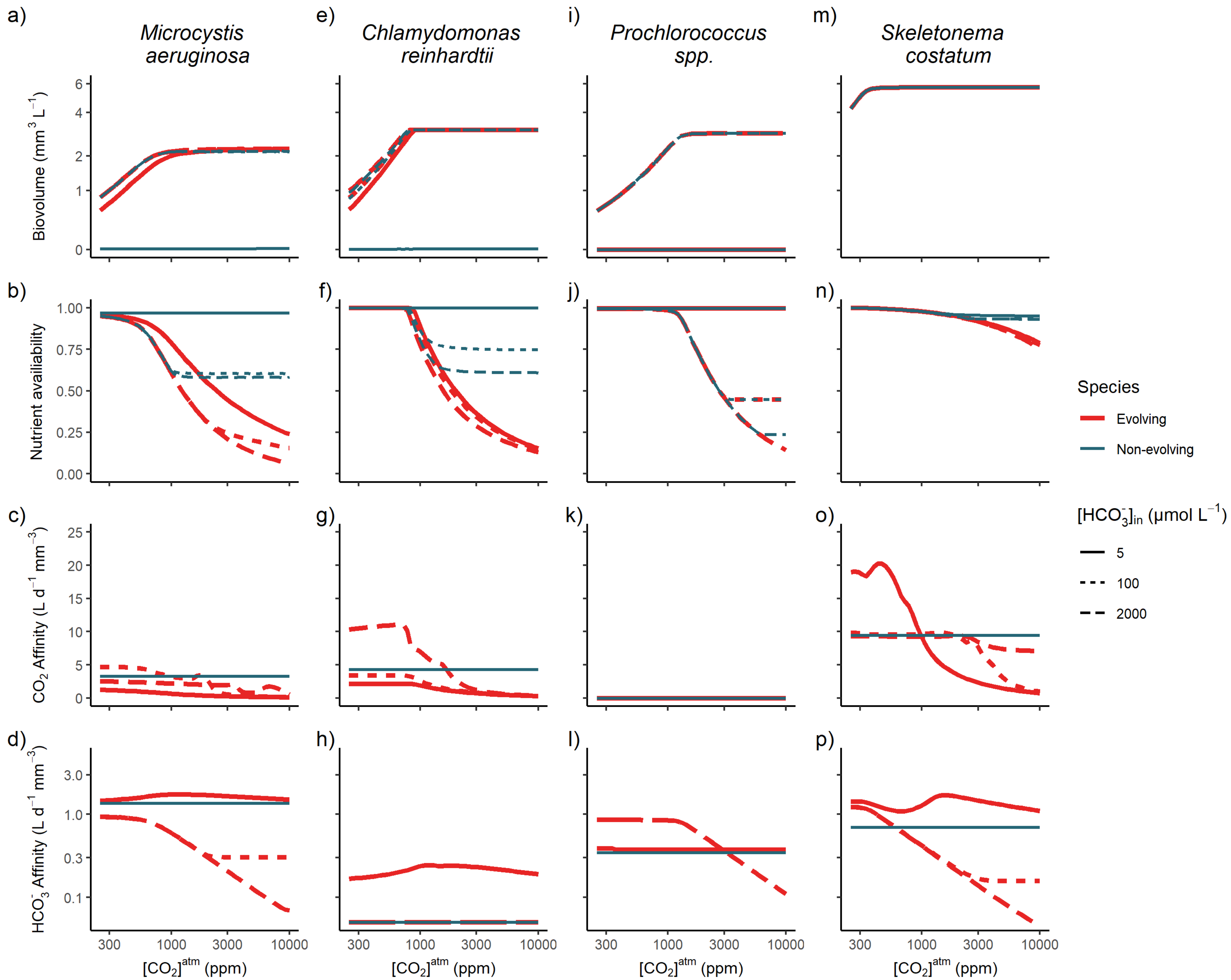

Figure A3.1.4: See caption for Figure 3.6 in main text. The simulations were run until equilibrium was reached, up to a maximum of 20000 days. Additionally, three of the four populations without the ability to evolve were unable to grow at starting HCO_3^- concentrations of 5 µmol L^{-1} (a,e,i,m). In order to bring more focus to carbon limitation, we increased the nutrient supply from the default of 20 µmol L^{-1} (used for *Microcystsi aeruginosa* (a,b,c,d) and the generalist and CO_2 specialist (Figure 3.6; main text)) up to 40 µmol L^{-1} for *Chlamydomonas reinhardtii* (e,f,g,h), and up to 100 µmol L^{-1} for *Prochlorococcus spp.* (i,j,k,l) and for *Skeletonema costatum* (m,n,o,p). Also note that *Prochlorococcus spp.* is an HCO_3^- specialist, which is why the CO_2 affinity is set to zero (k).

A3.2 Supplemental Tables

Table A3.2.1: System-specific variables used in the simulations, representative of a shallow lake with an input stream. The temperature and salinity are set to be representative of an average US lake in summer, according to the 2007 National Lake Assessment dataset [1] and are used to convert CO_2 concentrations (in mol L^{-1}) to partial pressures (in ppm).

Symbol	Value	Unit	Description
I_{in}	400	μmol m^{-2} s^{-1}	Input light intensity
z_m	5	m	Depth
k_{bg}	$1.3 \cdot 10^{-6}$	m^2 μmol^{-1}	Light extinction coefficient of the water
T	24	°C	Water Temperature
s	0.36	g L^{-1}	Salinity
g	$2.78 \cdot 10^{-5}$	m s^{-1}	Velocity of CO_2 exchange
D	0.001	d^{-1}	Dilution rate
S	20	μmol L^{-1}	Nutrient supply concentration
$[CO_2]^{\mathrm{atm}}$	250-10000	ppm	Atmospheric CO_2 concentration
$[HCO_3^-]_{\mathrm{in}}$	5[1], 100[2], 2000[3]	μmol L^{-1}	Initial HCO_3^- concentration

[1] A value which is close to the minimum HCO_3^- values observed in lakes and the one we use to demonstrate an example of competitive reversal (Table A3.2.2; Results).
[2] A relatively low, but more common concentration that may be found in a soft-water lake.
[3] An average HCO_3^- concentration across freshwater and marine systems [1].

Table A3.2.2: Species-specific variables, their initial values, and parameter values used in the model simulations. Note that variables $A_{i,j}$ and $V_{\max,i,j}$ are related (Eq. 3.3; Figure 3.1).

Type	Symbol	Generalist (*Cosmarium abbreviatum*)	CO_2 Specialist (*Closterium acutum*)	*Microcystis aeruginosa*	*Chlamydomonas reinhardtii*	*Prochlorococcus*	*Skeletonema costatum*	Unit	Description
Variable	X_i	0.1	0.1	0.1	0.1	0.1	0.1	$mm^3\ L^{-1}$	Biovolume
Variable	$A_{CO_2,i}$	12.4[2–4]	4.64[2,4–7]	3.3[4,8]	4.3[4,9,10]	–[4,11]	9.49[4,12,13]	$L\ mm^{-3}\ d^{-1}$	Starting CO_2 affinity (i.e., the slope of the CO_2 uptake curve when [CO_2] = 0 ppm).
Variable	$A_{HCO_3^-,i}$	0.0327[2–4]	–[2,4–7]	1.36[4,8]	0.0403[4,9,10]	0.347[4,11]	0.697[4,12,13]	$L\ mm^{-3}\ d^{-1}$	Starting HCO_3^- affinity (as for CO_2 affinity).
Variable	$V_{\max,CO_2,i}$	12.5[2–4]	12[2,4–7]	2.76[4,8]	14.9[4,9,10]	–[4,11]	14.8[4,12,13]	$\mu mol\ mm^{-3}\ d^{-1}$	Starting maximum CO_2 uptake rate
Variable	$V_{\max,HCO_3^-,i}$	11.5[2–4]	0[2,4–7]	14.2[4,8]	12.1[4,9,10]	119[4,11]	13.6[4,12,13]	$\mu mol\ mm^{-3}\ d^{-1}$	Starting maximum HCO_3^- uptake rate
Parameter	m_i	0.25	0.25	0.3[14]	0.25	0.32[15]	0.25[15]	d^{-1}	Mortality
Parameter	$Q_{C,i}$	25[3]	15[5,6]	15.7[8]	16.8[5,10]	22.7[16]	3.92[17]	$\mu mol\ mm^{-3}$	Cellular carbon quota
Parameter	$p_{CO_2,i}$	1	1	1	1	1	1	–	Curvature of the trade-off between the CO_2 affinity and maximum uptake rate.
Parameter	$p_{HCO_3^-,i}$	1	1	1	1	1	1	–	Curvature of the trade-off between the HCO_3^- affinity and maximum uptake rate.
Parameter	$c_{CO_2,i}$	0.0109	0.0387	0.229	0.0601	–	0.0278	$d^2\ mm^6\ L^{-1}\ \mu mol^{-1}$	Trade-off constant for CO_2. Note that units depend on p_{CO_2}.
Parameter	$c_{HCO_3^-,i}$	4.48	–	0.108	7.9	0.0797	0.411	$d^2\ mm^6\ L^{-1}\ \mu mol^{-1}$	Trade-off constant for CO_2. Note that units depend on p_{CO_2}.
Parameter	$\varepsilon_{CO_2,i}$	10^{-6}	10^{-6}	10^{-6}	10^{-6}	10^{-6}	10^{-6}	$L^2\ mm^{-6}\ d^{-2}$	Rate of evolution of CO_2 uptake (0 = no evolution)
Parameter	$\varepsilon_{HCO_3^-,i}$	10^{-8}	10^{-8}	10^{-8}	10^{-8}	10^{-8}	10^{-8}	$L^2\ mm^{-6}\ d^{-2}$	Rate of evolution of HCO_3^- uptake (0 = no evolution)
Parameter	h_i	8[3]	20[14]	18[14]	90[18]	63[11]	92.4[19]	$\mu mol\ m^{-2}\ s^{-1}$	Half-saturation constant for light (photons)

Type	Symbol	Generalist (*Cosmarium abbreviatum*)	CO_2 Specialist (*Closterium acutum*)	*Microcystis aeruginosa*	*Chlamydomonas reinhardtii*	*Prochlorococcus*	*Skeletonema costatum*	Unit	Description
Parameter	P_i	0.594	0.464	0.479	0.26	0.305	0.256	–	Photosynthetic efficiency in the light climate of the system (0 = no production; 1 = maximum production).
Parameter	$v_{\max,i,\mathrm{P}}/A_{i,\mathrm{P}}$	1.54[20]	1.54[20,21]	0.645[22]	0.0071[23]	0.75[24]	0.63[25,26]	$\mu mol\ L^{-1}$	Half-saturation constant for nutrient (P).
Parameter	$Q_{i,\mathrm{P}}$	0.0108[20]	0.0108[20,21]	0.0294[22,27]	0.078[23,28]	0.214[11,24]	0.14[25,26,29]	$\mu mol\ mm^{-3}$	Cellular nutrient (P) quota.

References

1. USEPA (US Environmental Protection Agency). 2009 *National lakes assessment: A collaborative survey of the nation's lakes*. USEPA Office of Water Washington.

2. Spijkerman E, Maberly SC, Coesel PF. 2005 Carbon acquisition mechanisms by planktonic desmids and their link to ecological distribution. *Canadian Journal of Botany* **83**, 850–858. (doi:10.1139/b05-069)

3. Coesel PFM, Wardenaar K. 1994 Light-limited growth and photosynthetic characteristics of two planktonic desmid species. *Freshwater Biology* **31**, 221–226. (doi:10.1111/j.1365-2427.1994.tb00856.x)

4. See Supplemental Text A3.1: Light limitation to see how we account for a fixed degree of light limitation in this parameter.

5. Verity PG, Robertson CY, Tronzo CR, Andrews MG, Nelson JR, Sieracki ME. 1992 Relationships between cell volume and the carbon and nitrogen content of marine photosynthetic nanoplankton. *Limnology and Oceanography* **37**, 1434–1446. (doi:10.4319/lo.1992.37.7.1434)

6. Vonk JA, Bijkerk R, Noordhuis R, Geest HG van der. 2019 Verrijkte dataset taxonomische samenstelling van de microalgengemeenschap in het IJsselmeer en markermeer 1994-2015. (doi:10.5281/ZENODO.3473250)

7. Yacobi YZ, Zohary T. 2009 Carbon:chlorophyll a ratio, assimilation numbers and turnover times of Lake Kinneret phytoplankton. *Hydrobiologia* **639**, 185–196. (doi:10.1007/s10750-009-0023-3)

8. Ji X, Verspagen JMH, Van de Waal DB, Rost B, Huisman J. 2020 Phenotypic plasticity of carbon fixation stimulates cyanobacterial blooms at elevated CO_2. *Science Advances* **6**, eaax2926. (doi:10.1126/sciadv.aax2926)

9. Amoroso G, SuÏtemeyer D, Thyssen C, Fock HP. 1998 Uptake of HCO_3^- and CO_2 in Cells and Chloroplasts from the Microalgae *Chlamydomonas reinhardtii* and *Dunaliella tertiolecta*. *Plant Physiology* **116**, 193–201. (doi:10.1104/pp.116.1.193)

10. Ban S, Lin W, Luo Z, Luo J. 2019 Improving hydrogen production of *Chlamydomonas reinhardtii* by reducing chlorophyll content via atmospheric and room temperature plasma. *Bioresource Technology* **275**, 425–429. (doi:10.1016/j.biortech.2018.12.062)

11. Hopkinson BM, Young JN, Tansik AL, Binder BJ. 2014 The Minimal CO_2-Concentrating Mechanism of *Prochlorococcus spp.* MED4 Is Effective and Efficient. *Plant Physiology* **166**, 2205–2217. (doi:10.1104/pp.114.247049)

12. Rost B, Riebesell U, Burkhardt S, Sültemeyer D. 2003 Carbon acquisition of bloom-forming marine phytoplankton. *Limnology and Oceanography* **48**, 55–67. (doi:10.4319/lo.2003.48.1.0055)

13. Riper DM, Owens TG, Falkowski PG. 1979 Chlorophyll turnover in *skeletonema costatum*, a marine plankton diatom. *Plant Physiology* **64**, 49–54.

14. Coesel PFM. 1993 Poor physiological adaptation to alkaline culture conditions in *Closterium acutum* var. *variabile*, a planktonic desmid from eutrophic waters. *European Journal of Phycology* **28**, 53–57. (doi:10.1080/09670269300650081)

15. Worden AZ, Binder BJ. 2003 Application of dilution experiments for measuring growth and mortality rates among *prochlorococcus* and *synechococcus* populations in oligotrophic environments. *Aquatic Microbial Ecology* **30**, 159–174.

16. Cailliau C, Claustre H, Vidussi F, Marie D, Vaulot D. 1996 Carbon biomass, and gross growth rates as estimated from 14C pigment labelling, during photoacclimation in *Prochlorococcus* CCMP 1378. *Marine Ecology Progress Series* **145**, 209–221. (doi:10.3354/meps145209)

17. Harrison PJ, Conway HL, Holmes RW, Davis CO. 1977 Marine diatoms grown in chemostats under silicate or ammonium limitation. III. Cellular chemical composition and morphology of *Chaetoceros debilis*, *Skeletonema costatum*, and *Thalassiosira gravida*. *Marine Biology* **43**, 19–31. (doi:10.1007/bf00392568)

18. Janssen M, Janssen M, Winter M de, Tramper J, Mur LR, Snel J, Wijffels RH. 2000 Efficiency of light utilization of *Chlamydomonas reinhardtii* under medium-duration light/dark cycles. *Journal of Biotechnology* **78**, 123–137. (doi:10.1016/s0168-1656(99)00233-3)

19. Oh S-J, Kang I-S, Yoon Y-H, Yang H-S. 2008 Optical characteristic on the growth of centric diatom, *skeletonema costatum* (grev.) Cleve isolated from jinhae bay in korea. *Korean Journal of Environmental Biology* **26**, 57–65.

20. Spijkerman E, Coesel PFM. 1996 Phosphorus uptake and growth kinetics of two planktonic desmid species. *European Journal of Phycology* **31**, 53–60. (doi:10.1080/09670269600651191)

21. Species-specfic values were not found. Instead, we used the value for *cosmarium abbreviatum*, a species of the same family.

22. Baldia SF, Evangelista AD, Aralar EV, Santiago AE. 2007 Nitrogen and phosphorus utilization in the cyanobacterium *Microcystis aeruginosa* isolated from Laguna de Bay, Philippines. *Journal of Applied Phycology* **19**, 607–613. (doi:10.1007/s10811-007-9209-0)

23. Grover JP. 1989 Phosphorus-dependent growth kinetics of 11 species of freshwater algae. *Limnology and Oceanography* **34**, 341–348. (doi:10.4319/lo.1989.34.2.0341)

24. Krumhardt KM, Callnan K, Roache-Johnson K, Swett T, Robinson D, Reistetter EN, Saunders JK, Rocap G, Moore LR. 2013 Effects of phosphorus starvation versus limitation on the marine cyanobacterium *Prochlorococcus* MED4 I: uptake physiology. *Environmental Microbiology* **15**, 2114–2128. (doi:10.1111/1462-2920.12079)

25. Ou L, Wang D, Huang B, Hong H, Qi Y, Lu S. 2008 Comparative study of phosphorus strategies of three typical harmful algae in Chinese coastal waters. *Journal of Plankton Research* **30**, 1007–1017. (doi:10.1093/plankt/fbn058)

26. Tarutani K, Yamamoto T. 1994 Phosphate uptake and growth kinetics of *skeletonema costatum* [*bacillariophyceae*] isolated from hiroshima bay [in japan]. *Journal of the Faculty of Applied Biological Science-Hiroshima University (Japan)*

27. Robarts RD, Zohary T. 1984 *Microcystis aeruginosa* and underwater light attenuation in a hypertrophic lake (hartbeespoort dam, south africa). *The Journal of Ecology* **72**, 1001. (doi:10.2307/2259547)

28. Spijkerman E. 2007 Phosphorus acquisition by *Chlamydomonas acidophila* under autotrophic and osmo-mixotrophic growth conditions. *Journal of Experimental Botany* **58**, 4195–4202. (doi:10.1093/jxb/erm276)

29. Conway HL, Harrison PJ. 1977 Marine diatoms grown in chemostats under silicate or ammonium limitation. IV. Transient response of *Chaetoceros debilis*, *Skeletonema costatum*, and *Thalassiosira gravida* to a single addition of the limiting nutrient. *Marine Biology* **43**, 33–43. (doi:10.1007/bf00392569)

Supplemental Text A3.1: Light Limitation

To account for a certain degree of light limitation, we assumed fixed parameter values for incoming light intensity, I_{in}, light extinction coefficient in the water k_{bg}, and lake depth z_m; and the species-specific light half-saturation constant h_i. We neglect the fact that light limitation increases as phytoplankton biovolume in the lake increases. See Tables A3.2.1 & A3.2.2 for parameter values used in our simulations. Fundamentally, the photosynthetic rate ($r_i(I)$) is described by Michaelis-Menten kinetics and is a function of the maximum photosynthetic rate ($r_{\max,i}$), h_i, and the light intensity (I; Eqn. A3.1).

$$r_i(I) = \frac{r_{\max,i}\, I}{h_i + I} \qquad (A3.1)$$

However, the light intensity decreases exponentially with depth (z) in the water ($I(z)$) and, following Lambert-Beer's Law, depends on I_{in} and a background turbidity factor (K_{bg}; Eqn. A3.2).

$$I(z) = I_{\text{in}}\, exp\left(-K_{\text{bg}}\, z\right) \qquad (A3.2)$$

At the maximum depth (z_m), the light intensity is $I_{\text{out}} = I(z_m)$. We can integrate over the photosynthetic rates at all the depths to calculate the total photosynthetic rate in the media (P_i) by assuming that the phytoplankton are equally distributed in the water column and that there is no self-shading (Huisman & Weissing 1994; Eqn. A3.3). Because we are interested in the degree of limitation, and not the precise photosynthetic output, we assume that $r_{\max,i} = 1$. As a result, the P_i is unitless and has a range of 0 to 1, with 0 meaning no photosynthesis, and 1 meaning maximum photosynthesis. For each species, we transformed the maximum CO_2 and HCO_3^- uptake rates found in the literature by multiplying them by P_i in order to obtain a more realistic $V_{\max,i,j}$ (Tables A3.2.1 & A3.2.2).

$$P_i \; = \; \frac{1}{z_m}\int_{z=0}^{z_m} p_i\left(I(z)\right)dz \; = \left(\frac{1}{\ln(I_{\text{in}}/I_{\text{out}})}\right)\ln\left(\frac{h_i + I_{\text{in}}}{h_i + I_{\text{out}}}\right) \qquad (A3.3)$$

Reference

Huisman, J. and Weissing, F.J., 1994 Light-limited growth and competition for light in well-mixed aquatic environments: an elementary model. *Ecology* **75**, 507-520. (doi:10.2307/1939554)

Supplemental Text A3.2: Coexistence Point and Boundary Carbon Depletion Trajectory Calculations

Coexistence Point

To calculate the boundary carbon depletion trajectory, we must first calculate the coexistence point of two species. The coexistence point of two species is the point where the ZNGIs of two species intersect in the $[CO_2]$-$[HCO_3^-]$ plane and can be calculated by equating Eqn. 3.6 (either the CO_2, or HCO_3^- equation can be used; here we select the CO_2 equation) for both species (named, in this case, 1 and 2; Eqn. A3.3). We denote the coexistence concentrations as $[CO_2]^c$ and $[HCO_3^-]^c$.

$$\frac{V_{\max,1,CO_2}\left(m_1\ Q_{C,1} - v_{1,HCO_3^-}\right)}{A_{1,CO_2}\left(V_{\max,1,CO_2} - m_1\ Q_{C,1} + v_{1,HCO_3^-}\right)} = \frac{V_{\max,2,CO_2}\left(m_2\ Q_{C,2} - v_{2,HCO_3^-}\right)}{A_{2,CO_2}\left(V_{\max,2,CO_2} - m_2\ Q_{C,2} + v_{2,HCO_3^-}\right)} \quad (A3.3)$$

This equation can be expressed as a quadratic function and solved using the quadratic formula (Eqn. A3.4), where a, b and c are defined below (Eqn. A3.5, A3.6 and A3.7). Afterwards, $[HCO_3^-]^c$ can be plugged into Eqn. 3.6 to calculate $[CO_2]^c$.

$$a\ ([HCO_3^-]^c)^2 + b\ [HCO_3^-]^c + c = 0 \Leftrightarrow [HCO_3^-] = \frac{-b \pm \sqrt{b^2 - 4ac}}{2a} \quad (A3.4)$$

where

$$\begin{aligned} a = \quad & -\frac{V_{\max,1,CO_2}\ m_1\ Q_{C,1}\ m_2\ Q_{C,2}}{A_{1,CO_2}} + \frac{V_{\max,1,CO_2}\ V_{\max,1,HCO_3^-}\ m_2\ Q_{C,2}}{A_{1,CO_2}} \\ & + \frac{V_{\max,2,CO_2}\ m_1\ Q_{C,1}\ m_2\ Q_{C,2}}{A_{2,CO_2}} - \frac{V_{\max,2,CO_2}\ V_{\max,1,HCO_3^-}\ m_2\ Q_{C,2}}{A_{2,CO_2}} \\ & - \frac{V_{\max,1,CO_2}\ V_{\max,2,CO_2}\ m_2\ Q_{C,2}}{A_{2,CO_2}} + \frac{V_{\max,1,CO_2}\ V_{\max,2,HCO_3^-}\ m_1\ Q_{C,1}}{A_{1,CO_2}} \\ & - \frac{V_{\max,1,CO_2}\ V_{\max,1,HCO_3^-}\ V_{\max,2,HCO_3^-}}{A_{1,CO_2}} - \frac{V_{\max,2,CO_2}\ V_{\max,2,HCO_3^-}\ m_1\ Q_{C,1}}{A_{2,CO_2}} \\ & + \frac{V_{\max,2,CO_2}\ V_{\max,1,HCO_3^-}\ V_{\max,2,HCO_3^-}}{A_{2,CO_2}} + \frac{V_{\max,1,CO_2}\ V_{\max,2,CO_2}\ V_{\max,2,HCO_3^-}}{A_{2,CO_2}} \\ & + \frac{V_{\max,1,CO_2}\ V_{\max,2,CO_2}\ m_1\ Q_{C,1}}{A_{1,CO_2}} - \frac{V_{\max,1,CO_2}\ V_{\max,2,CO_2}\ V_{\max,1,HCO_3^-}}{A_{1,CO_2}} \end{aligned} \quad (A3.5)$$

$$
\begin{aligned}
b = \quad & -\frac{V_{\mathrm{max},1,CO_2}\, V_{\mathrm{max},1,HCO_3^-}\, m_1\, Q_{C,1}\, m_2\, Q_{C,2}}{A_{1,CO_2}\, A_{1,HCO_3^-}} + \frac{V_{\mathrm{max},2,CO_2}\, V_{\mathrm{max},1,HCO_3^-}\, m_1\, Q_{C,1}\, m_2\, Q}{A_{2,CO_2}\, A_{1,HCO_3^-}} \\
& -\frac{V_{\mathrm{max},1,CO_2}\, V_{\mathrm{max},2,CO_2}\, V_{\mathrm{max},1,HCO_3^-}\, m_2\, Q_{C,2}}{A_{2,CO_2}\, A_{1,HCO_3^-}} + \frac{V_{\mathrm{max},1,CO_2}\, V_{\mathrm{max},1,HCO_3^-}\, V_{\mathrm{max},2,HCO_3^-}}{A_{1,CO_2}\, A_{1,HCO_3^-}} \\
& -\frac{V_{\mathrm{max},2,CO_2}\, V_{\mathrm{max},1,HCO_3^-}\, V_{\mathrm{max},2,HCO_3^-}\, m_1\, Q_{C,1}}{A_{2,CO_2}\, A_{1,HCO_3^-}} \\
& +\frac{V_{\mathrm{max},1,CO_2}\, V_{\mathrm{max},2,CO_2}\, V_{\mathrm{max},1,HCO_3^-}\, V_{\mathrm{max},2,HCO_3^-}}{A_{2,CO_2}\, A_{1,HCO_3^-}} - \frac{V_{\mathrm{max},1,CO_2}\, V_{\mathrm{max},2,HCO_3^-}\, m_1\, Q_{C,1}}{A_{1,CO_2}\, A_{2,HCO_3^-}} \\
& +\frac{V_{\mathrm{max},1,CO_2}\, V_{\mathrm{max},1,HCO_3^-}\, V_{\mathrm{max},2,HCO_3^-}\, m_2\, Q_{C,2}}{A_{1,CO_2}\, A_{2,HCO_3^-}} + \frac{V_{\mathrm{max},2,CO_2}\, V_{\mathrm{max},2,HCO_3^-}\, m_1\, Q_{C,1}\, m}{A_{2,CO_2}\, A_{2,HCO_3^-}} \\
& -\frac{V_{\mathrm{max},2,CO_2}\, V_{\mathrm{max},1,HCO_3^-}\, V_{\mathrm{max},2,HCO_3^-}\, m_2\, Q_{C,2}}{A_{2,CO_2}\, A_{2,HCO_3^-}} - \frac{V_{\mathrm{max},1,CO_2}\, V_{\mathrm{max},2,CO_2}\, V_{\mathrm{max},2,HCO_3^-}}{A_{2,CO_2}\, A_{2,HCO_3^-}} \\
& +\frac{V_{\mathrm{max},1,CO_2}\, V_{\mathrm{max},2,CO_2}\, V_{\mathrm{max},1,HCO_3^-}\, m_1\, Q_{C,1}}{A_{1,CO_2}\, A_{1,HCO_3^-}} + \frac{V_{\mathrm{max},1,CO_2}\, V_{\mathrm{max},2,CO_2}\, V_{\mathrm{max},2,HCO_3^-}\, m}{A_{1,CO_2}\, A_{2,HCO_3^-}} \\
& -\frac{V_{\mathrm{max},1,CO_2}\, V_{\mathrm{max},2,CO_2}\, V_{\mathrm{max},1,HCO_3^-}\, V_{\mathrm{max},2,HCO_3^-}}{A_{1,CO_2}\, A_{2,HCO_3^-}}
\end{aligned}
\qquad (A3.6)
$$

$$
\begin{aligned}
c = \quad & -\frac{V_{\mathrm{max},1,CO_2}\, V_{\mathrm{max},1,HCO_3^-}\, V_{\mathrm{max},2,HCO_3^-}\, m_1\, Q_{C,1}\, m_2\, Q_{C,2}}{A_{1,CO_2}\, A_{1,HCO_3^-}\, A_{2,HCO_3^-}} \\
& +\frac{V_{\mathrm{max},2,CO_2}\, V_{\mathrm{max},1,HCO_3^-}\, V_{\mathrm{max},2,HCO_3^-}\, m_1\, Q_{C,1}\, m_2\, Q_{C,2}}{A_{2,CO_2}\, A_{1,HCO_3^-}\, A_{2,HCO_3^-}} \\
& -\frac{V_{\mathrm{max},1,CO_2}\, V_{\mathrm{max},2,CO_2}\, V_{\mathrm{max},1,HCO_3^-}\, V_{\mathrm{max},2,HCO_3^-}\, m_2\, Q_{C,2}}{A_{2,CO_2}\, A_{1,HCO_3^-}\, A_{2,HCO_3^-}} \\
& +\frac{V_{\mathrm{max},1,CO_2}\, V_{\mathrm{max},2,CO_2}\, V_{\mathrm{max},1,HCO_3^-}\, V_{\mathrm{max},2,HCO_3^-}\, m_1\, Q_{C,1}}{A_{1,CO_2}\, A_{1,HCO_3^-}\, A_{2,HCO_3^-}}
\end{aligned}
\qquad (A3.7)
$$

Boundary Carbon Depletion Trajectory

The boundary carbon depletion trajectory leads to the coexistence point and separates the $[\mathrm{CO_2}]^{\mathrm{atm}}$-$[\mathrm{HCO_3^-}]_{\mathrm{in}}$ plane into areas where different species dominate. To simplify the notation, we refer to $[\mathrm{CO_2}]^{\mathrm{atm}}$ as $[\mathrm{CO_2}]$ and to $[\mathrm{HCO_3^-}]_{\mathrm{in}}$ as $[\mathrm{HCO_3^-}]$. Since alkalinity (Alk) remains fixed over time, all points along the boundary carbon depletion trajectory that leads to the coexistence point have the same alkalinity (Alk^c). The alkalinity depends on the concentration of $[\mathrm{HCO_3^-}]$, $[\mathrm{CO_3^{2-}}]$, $[\mathrm{OH^-}]$, and $[\mathrm{H^+}]$ ions and can be calculated as:

$$Alk = [\mathrm{HCO_3^-}] + 2[\mathrm{CO_3^{2-}}] + [\mathrm{OH^-}] - [\mathrm{H^+}] \qquad (A3.8)$$

$[H^+]$, $[OH^-]$ and $[CO_3^{2-}]$ can be calculated from $[CO_2]$ and $[HCO_3^-]$ using temperature and salinity-dependent chemical equilibrium constants K_1, K_2 and K_w (Dickson and Riley 1979; Stumm & Morgan 2013) as follows:

$$[\mathrm{H}^+] = K_1 \frac{[\mathrm{CO}_2]}{[\mathrm{HCO}_3^-]} \qquad (A3.9)$$

$$[\mathrm{OH}^-] = \frac{K_w}{[\mathrm{H}^+]} \qquad (A3.10)$$

$$[\mathrm{CO}_3^{2-}] = \frac{K_2\ [\mathrm{HCO}_3^-]}{[\mathrm{H}^+]} \qquad (A3.11)$$

Using Eqn. A3.9, A3.10 and A3.11, we can re-formulate Eqn. A3.8 in terms of $[CO_2]$ and $[H^+]$:

$$Alk = \frac{K_1\ [\mathrm{CO}_2]}{[\mathrm{H}^+]} + \frac{2\ K_1 K_2\ [\mathrm{CO}_2]}{[\mathrm{H}^+]^2} + \frac{K_w}{[\mathrm{H}^+]} - [\mathrm{H}^+] \qquad (A3.12)$$

We express Eqn. A3.12 as a cubic equation by multiplying both sides by $[H^+]^2$ and re-arranging the terms:

$$[\mathrm{H}^+]^3 + Alk\ [\mathrm{H}^+]^2 - (K_1\ [\mathrm{CO}_2] + K_w)\ [\mathrm{H}^+] - 2\ K_1\ K_2\ [\mathrm{CO}_2] = 0 \qquad (A3.13)$$

For both populations to be viable, $[CO_2]$ must be equal to or greater than $[CO_2]^c$. For each $[CO_2]$ > $[CO_2]^c$, solving Eqn. A3.13 to find the corresponding $[H^+]$ yields one positive real solution (Eqn. A3.14). Subsequently, each $[H^+]$ can be used to calculate the $[HCO_3]$ from the corresponding $[CO_2]$, and the constant K_1 (Eqn. A3.9).

$$
\begin{aligned}
a &= 1 \\
b &= Alk^c \\
c &= -(K_1\,[\mathrm{CO_2}] + K_w) \\
d &= -2\,K_1 K_2\,[\mathrm{CO_2}] \\
f &= \left(\frac{3c}{a} - \frac{b^2}{a^2}\right)/3 \\
g &= \left(\left(\frac{2b^3}{a^3}\right) - \left(\frac{9bc}{a^2}\right) + \left(\frac{27d}{a}\right)\right)/27 \\
h &= \left(\frac{g^2}{4}\right) + \left(\frac{f^3}{27}\right) \\
i &= \sqrt{\left(\frac{g^2}{4} - h\right)} \\
j &= i^{1/3} \\
k &= \arccos\left(-\frac{g}{2i}\right) \\
[H^+] &= 2\,j\,\cos\left(\frac{k}{3}\right) - \left(\frac{b}{3a}\right)
\end{aligned}
\tag{A3.14}
$$

References

Dickson, A. G., & Riley, J. P. (1979). The estimation of acid dissociation constants in seawater media from potentionmetric titrations with strong base. I. The ionic product of water—Kw. *Marine Chemistry*, 7(2), 89-99.

Stumm, W., & Morgan, J. J. (2013). Aquatic chemistry : chemical equilibria and rates in natural waters (3rd ed.). Wiley.

Supplemental Text A3.3: Non-Equilibrium Evolutionary Dynamics

Away from equilibrium conditions, we find that, if the resource concentration is below that of the populations' R^* (dotted lines in Figure A3.3.1), $A_{i,j}$ tends to increase (for each color, $dA/dt > 0$ left of the dotted line in Figure A3.3.1). Note that the increase in $A_{i,j}$ causes the R^* to decrease (compare dotted lines in Figure A3.3.1). In contrast, if the resource concentration is higher than the R^*, $A_{i,j}$ decreases (for each color, $dA/dt > 0$ right of each dotted line in Figure A3.3.1), causing the R^* to increase. Notice that the absolute value of dA/dt reaches much higher values when the resource concentration is higher than the R^* than when it is lower than the R^* (seen most clearly in the curve for $A_{i,j} = 10$ in Figure A3.3.1). This means that populations can adapt to elevated resource concentrations much more rapidly than to low resource concentrations. Additionally, as the $A_{i,j}$ reaches higher values, the curve flattens out (compare curves with increasing $A_{i,j}$ in Figure A3.3.1), meaning that as populations try to adapt to scarce resources by increasing $A_{i,j}$, the rates of adaptation (dA/dt) tend to decrease. Conversely, populations adapting to an abundance of resources can do so at a more rapid pace as the $A_{i,j}$ decreases.

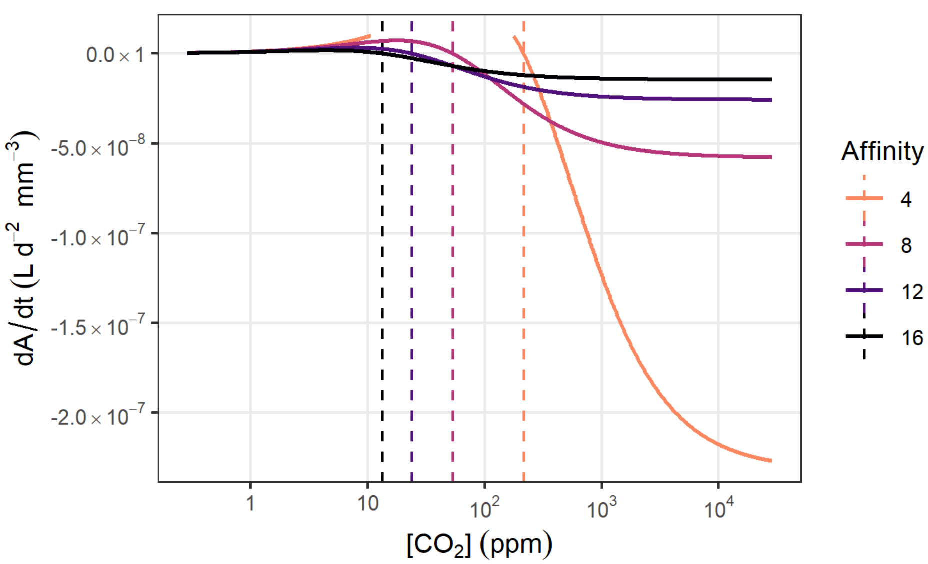

Figure A3.3.1: The change in CO_2 affinity through time (y-axis) depends on the CO_2 concentration (x-axis) and on the CO_2 affinity itself (see colour legend; Eqn. 3.7). The vertical dotted lines represent the populations' R_j^* corresponding to the associated affinity (Eqn. 3.8). Although the equation is parameterised according to the CO_2 uptake of a CO_2 specialist species (Table A3.2.2), the principle is the same for other species and resources.

Supplemental Text A3.4: Simulations with the Generalist

Many patterns observed in the specialist species are shared with the generalist. For example, for either species, the evolving strain reaches higher biovolumes and out-competes the non-evolving strain by changing CO_2 and HCO_3^- affinities. To demonstrate, we analyse the response of the generalist under very low $[HCO_3^-]_{in}$ (5 μmol L^{-1}).

The effect of evolution was more pronounced on all fronts for the case of the generalist species *Cosmarium abbreviatum* without competition. With evolution, the alga's equilibrium biovolume increased to $0.872\ mm^3\ L^{-1}$ compared to $0.649\ mm^3\ L^{-1}$ without evolution. Similarly, the maximum growth rate increased to $0.312\ d^{-1}$ in the evolving strain, compared to $0.27\ d^{-1}$ in the non-evolving one (Figure A3.4.1a,d). With evolution, the CO_2 concentrations are drawn down 49.4 ppm lower than 139 ppm without evolution and HCO_3^- concentrations are drawn down to 3.71 μmol L^{-1} with evolution, compared to 4.13 μmol L^{-1} without evolution (Figure A3.4.1b,e). Without evolution, the resource affinities cannot change (Figure A3.4.1c). With evolution, the resource affinities for both resources reach an EEE, which, for CO_2, is lower than the starting value, but higher than the starting value for HCO_3^- (Figure A3.4.1c,f).

As with the specialist, the evolving strain is able to outcompete the non-evolving strain (Figure A3.4.1g). The evolving strain also controls the final resource concentrations (Figure A3.4.1h) and the affinities behave in essentially the same way as when growing alone (Figure A3.4.1i).

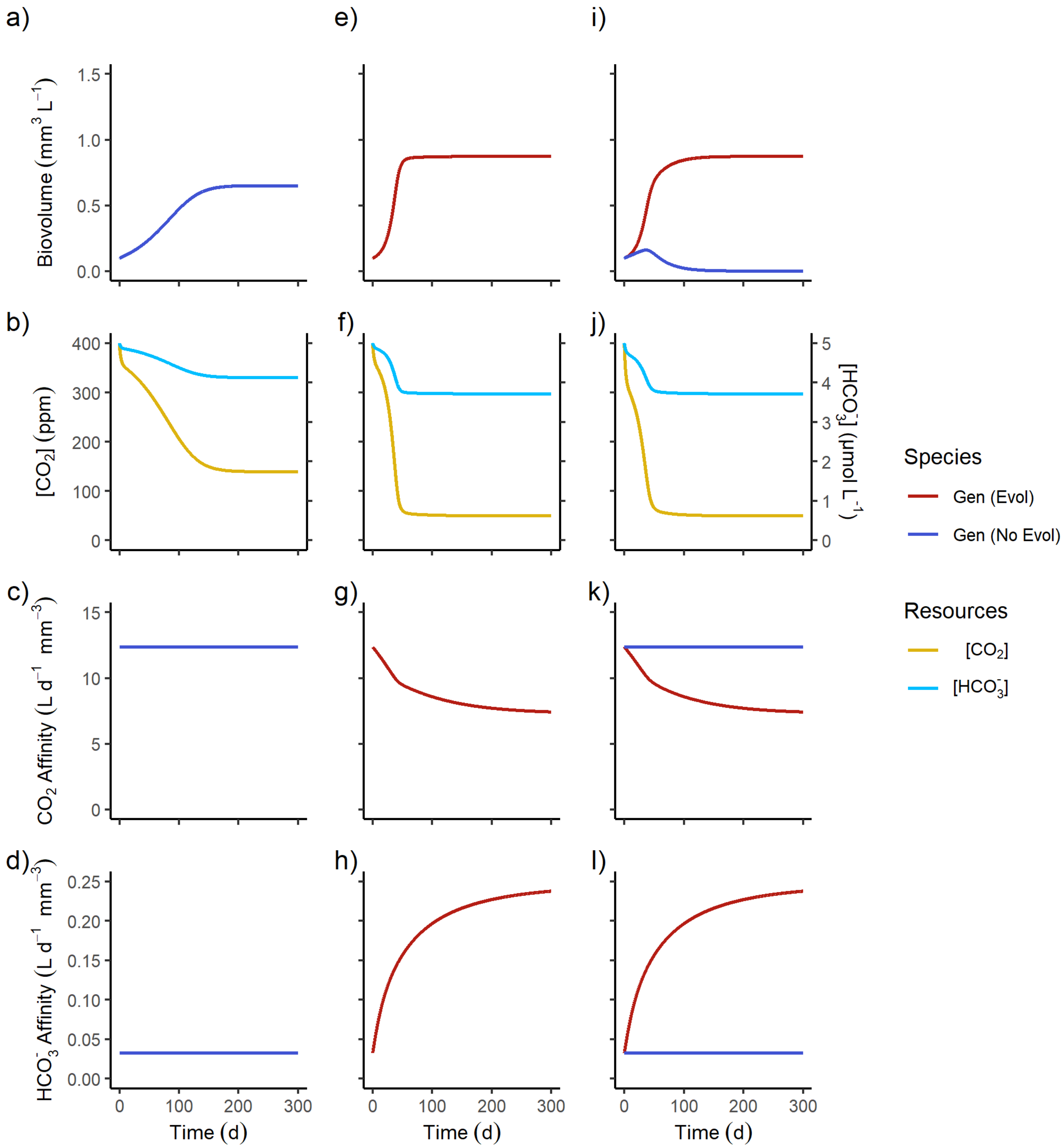

Figure A3.4.1: Simulations featuring a single non-evolving strain of the generalist *Cosmarium abbreviatum* (a-d), a single evolving strain of the same species (e-h), and a competitive scenario between both strains (i-l). We compare the biovolume concentration (a, e, i), the resource concentrations (b, f, j) and each population's affinity for CO_2 (c, g, k) and HCO_3^- (d, h, l).

Supplemental Text A3.5: Nutrient Limitation

To implement nutrient limitation, we introduce nutrient availability ($f_{i,\mathrm{P}}$), such that Eqn. 3.1 becomes Eqn. A3.15.

$$\frac{dX_i}{dt} = \left(\frac{\sum_{j\in C} v_{i,j}}{Q_{C,i}} f_{i,\mathrm{P}} - m_i\right) X_i \qquad i = 1, \ldots, n \tag{A3.15}$$

consequently, Eqn. 3.7 becomes Eqn. A3.16.

$$\frac{dA_{j,i}}{dt} = \frac{\varepsilon_{j,i} \cdot f_{i,\mathrm{P}}}{Q_{C,i}} \left(\frac{[R_j]}{1 + \frac{V_{\max,i,j}}{A_{i,j}}[R_j]} - \frac{V_{\max,i,j}\,(p_{j,i}+1)\,[R_j]^2}{A_{i,j}\left(1 + \frac{V_{\max,i,j}}{A_{i,j}}[R_j]\right)^2} \right) \tag{A3.16}$$

Next, $f_{i,\mathrm{P}}$ is defined by the the nutrient concentration ($[P]$) and the half-saturation constant, defined as the maximum uptake rate ($V_{\max,i,\mathrm{P}}$) over affinity ($A_{i,\mathrm{P}}$; Eqn. A3.17).

$$f_{i,\mathrm{P}} = \frac{[P]}{k_{i,\mathrm{P}} + [P]} \tag{A3.17}$$

Nutrients are supplied at a fixed concentration (S), which is diluted out at a constant rate (D) and taken up by new phytoplankton growth ($\mu_i = \frac{\sum_{j\in C} v_{i,j}}{Q_{C,i}} f_{i,\mathrm{P}}$), depending on the species-specific nutrient quota ($Q_{i,\mathrm{P}}$; Eqn. A3.18). Note that we select a dilution rate that is low enough to have a negligible effect on the carbon input, assuming that water from this inflow is at equilibrium with the atmosphere (Table A3.2.1).

$$\frac{d[P]}{dt} = D(S - [P]) - \sum_{i=1}^{n} X_i\ \mu_i\ Q_{i,\mathrm{P}} \tag{A3.18}$$

To simplify the notation, we define $G_i = \frac{m_i Q_{C,i}}{f_{i,\mathrm{P}}^*}$, where $f_{i,\mathrm{P}}^*$ is the equilibrium phosphate availability. Unfortunately, $f_{i,\mathrm{P}}^*$ is difficult to calculate analytically. However, as the phosphate supply S tends to infinity, $f_{i,\mathrm{P}}^*$ tends to 1. At lower S, $f_{i,\mathrm{P}}^*$ decreases, causing the R^* values to increase.

$$
\begin{aligned}
[\mathrm{CO_2}]_i^* &= \frac{V_{\max,i,\mathrm{CO_2}}\left(G_i - v_{i,\mathrm{HCO_3^-}}\right)}{A_{i,\mathrm{CO_2}}\left(V_{\max,i,\mathrm{CO_2}} - G_i + v_{i,\mathrm{HCO_3^-}}\right)} \\
[\mathrm{HCO_3^-}]_i^* &= \frac{V_{\max,i,\mathrm{HCO_3^-}}\left(G_i - v_{i,\mathrm{CO_2}}\right)}{A_{i,\mathrm{HCO_3^-}}\left(V_{\max,i,\mathrm{HCO_3^-}} - G_i + v_{i,\mathrm{CO_2}}\right)}
\end{aligned}
\qquad (A3.19)
$$

In the introductory figures, we assume, for simplicity, that $f_{i,\mathrm{P}} = 1$ (i.e., no nutrient limitation; Figure 3.2, 3.7 & Figure A3.3.1). For the mathematical simulations, on the other hand, we used parameter values for the kinetics of phosphorus uptake and assimilation (Table A3.2.2), as and some system parameters that may reflect a eutrophic lake (Table A3.2.1). Note that we ignore the buffering capacity of dissolved phosphate.